Tubular Proteinuria and Vitamin D Deficiency in Sickle Cell Disease

by

Megan Laura Gliozzi

BS, University of Pittsburgh, 2014

Submitted to the Graduate Faculty of

Graduate School of Public Health in partial fulfillment

of the requirements for the degree of

Doctor of Philosophy

University of Pittsburgh

2019

UNIVERSITY OF PITTSBURGH

GRADUATE SCHOOL OF PUBLIC HEALTH

This dissertation was presented

by

Megan Laura Gliozzi

It was defended on

May 30, 2019

and approved by

David N. Finegold, MD
Professor, Department of Human Genetics
Graduate School of Public Health, University of Pittsburgh

James R. Johnston, MD
Professor, Department of Medicine
School of Medicine, University of Pittsburgh

Zsolt Urban, PhD
Associate Professor, Department of Human Genetics
Graduate School of Public Health, University of Pittsburgh

Dissertation Advisor:
Ora A. Weisz, PhD
Professor, Department of Medicine and Cell Biology
School of Medicine, University of Pittsburgh

Ora A. Weisz, PhD

Tubular Proteinuria and Vitamin D Deficiency in Sickle Cell Disease

Megan Laura Gliozzi, PhD

University of Pittsburgh, 2019

Abstract

Kidney disease is a significant complication of sickle cell disease (SCD) with great public health concern, causing over 18% of total patient mortality. Proximal tubule (PT) dysfunction, including tubular proteinuria, is a common early symptom of kidney disease in SCD patients and can lead to chronic kidney disease. Although not well understood, PT dysfunction in SCD is thought to be caused by exposure to higher cell-free hemoglobin (Hb) concentrations from increased red blood cell hemolysis. Hb is filtered by the glomerulus to enter the tubule lumen, where it is reabsorbed by PT cells upon binding to multiligand receptors megalin and cubilin. Megalin and cubilin bind to numerous proteins in the kidney filtrate, including albumin, vitamin D binding protein (DBP), and retinol binding protein (RBP), and are important for maintaining vitamin homeostasis and a protein-free urine.

To better understand PT dysfunction at the cellular level, we treated PT cells with physiologic levels of Hb estimated in SCD and measured protein endocytosis and toxicity/oxidative stress. We found that Hb inhibited albumin, DBP, and RBP uptake by PT cells to variable degrees. Hb inhibition occurred in the absence of a cytotoxic response and appeared to be due to direct competition for megalin/cubilin binding. These results suggest that binding competition between Hb and normally filtered proteins may be the primary cause of tubular proteinuria in SCD patients. Additionally, Hb inhibition appeared to be selective for highly alpha

helical proteins. Understanding the selectivity of Hb binding competition could help to identify biomarkers and therapeutic compounds to detect and treat tubular proteinuria in SCD patients prior to the onset of kidney disease.

Inhibition of DBP uptake by PT cells could contribute to vitamin D deficiency commonly observed in SCD patients. We also found prolonged Hb exposure created an increased cytotoxic response and alteration of vitamin D hydroxylase expression in PT cells, indicating Hb-induced toxicity may affect vitamin D metabolism. Finally, we observed selective changes in protein reabsorption by PT cells with variation of active vitamin D availability, suggesting further possible complications in protein reabsorption and vitamin D homeostasis in SCD patients with low vitamin D status.

Table of Contents

List of Tables

List of Figures

Preface

I would like to express my deepest appreciation and sincerest gratitude to the faculty, staff, and students in the Human Genetics Department and Renal-Electrolyte Division. Your willingness to collaborate and share your expertise has significantly enriched my academic progression as well as my development as a scientist. I'd also like to thank all the faculty and students I've met during my Clinical and Translational Science TL1 fellowship for helping me understand the importance and application of translational research. I'd like to especially thank Dr. Samuel Poloyac for his willingness to provide any possible guidance or help I needed during my fellowship.

I'm extremely fortunate to have two outstanding women as mentors during my time at Pitt, Dr. Susanne Gollin and Dr. Ora Weisz. It was during my undergraduate research under the advisement of Dr. Gollin where I truly became enamored by genetics research. Dr. Gollin continuously pushed me to think outside the box and to never settle in my aspirations. In fact, if it were not for her push in my applying to Pitt's Human Genetics PhD program, I may not be in here writing and defending my PhD dissertation.

From the start of my graduate studies in her lab, Dr. Weisz has served as an exemplary role model of a woman in science and an extraordinary mentor. She has supported my scientific and professional development while unremittingly pushing me outside my comfort zone to help me achieve my goals. Dr. Weisz has always made time to talk whenever I've needed advice and she has taught me to expand my expectations of my success. I would not be nearly as successful as I am today without the support, guidance, and encouragement that I've received from her.

I'd also like to thank past and present Weisz lab members for teaching me so much and making my work environment beyond enjoyable for the past five years. I'd like to especially thank

Youssef Rbaibi, Dr. Venkatesan Raghavan, and Dr. Anatália Labilloy for my onboarding in the lab, Dr. Catherine Baty and Dr. Kimberly Long for their remarkable advice and help, and Katherine Shipman and William Moorhead for their friendship and comradery.

Many thanks to my additional collaborators without whom I would have struggled to put together the work outlined in this dissertation. This includes Dr. Amandeep Kaur, Dr. Jesús Tejero, Dr. Dario Vitturi, and Dr. Thomas Nolin. I'd also like to give a special thanks to Dr. David Finegold, Dr. James Johnston, and Dr. Zsolt Urban for your guidance and support as my dissertation committee members.

I would be remiss if I did not thank my incredible friends and family for their support throughout the years leading up to this day. To my parents Michael and Mary Beth Eshbach, I am eternally grateful for your love and unwavering support. Since as long as I can remember they have always encouraged me to reach for the stars and have never let me feel as though there was something I couldn't do. It's their support that has allowed me to succeed in the pursuit of my ambitions. Finally, words cannot express how grateful I am for the support of my wonderful husband, Michael Gliozzi. From the day I met you, you have never been intimidated or unsupportive of my scientific aspirations and have been my rock throughout this entire process. I cannot wait to see what our next chapter holds!

1.0 Introduction

1.1 Public Health Significance

Sickle cell disease (SCD) is the most common hereditary hemoglobinopathy and one of the most common monogenic diseases, affecting approximately 300,000 newborns annually [1, 2] and 100,000 individuals in the United States [3]. The number of individuals affected by SCD in the United States is predicted to rise as advances in medicine and patient treatment have led to a drastic increase in SCD patient lifespan. Over the past 40 years alone the median SCD patient life expectancy has risen from 14.3 years (1970s) to 61 years (2014) [4, 5]. Unfortunately, as patients are living longer, they are developing more severe secondary organ damage that is proving to require an entirely new therapeutic approach.

One of the most common and severe secondary complications of SCD is sickle cell nephropathy (SCN). In fact, kidney-related injury and disease account for 16-18% of total SCD patient mortality and renal failure ranks within the top three most common primary causes of death in patients [6-8]. The prevalence of SCN is also predicted to rise in the coming years due to disproportionate advances in treatment of SCD and SCN. Diagnosis, prevention, and treatment of early kidney disease are lacking and kidney injury in patients can quickly progress to chronic kidney disease (CKD), in which the median age of onset is 37 years old [9]. CKD is present in approximately 11.6% of SCD patients, making it the most common SCN manifestation [9]. Unfortunately, treatment options once a patient progresses into CKD and/or renal failure are limited to renal replacement therapy. Thus, there is an immense need for improved kidney-specific treatment and prevention of kidney disease progression in SCD patients.

Symptoms of SCN can manifest as early as infancy in SCD patients. One of the earliest observed SCN symptoms in patients is development of tubular proteinuria, indicating dysfunction of the proximal tubule (PT) segment of the nephron [10-12]. While PT dysfunction and tubular proteinuria have not yet been linked to progression of kidney disease in SCN, both have been linked to kidney inflammation and fibrosis in other diseases and can eventually lead to glomerular dysfunction, frank proteinuria, and end-stage renal failure (ESRD) [13, 14].

Additionally, PT dysfunction can prevent normal uptake of several vitamin carriers that bind to megalin and cubilin, including vitamin D binding protein (DBP) and retinol binding protein (RBP) [15]. Failure to reabsorb these carrier proteins can lead to vitamin deficiencies. This is particularly true for vitamin D as the PT is the primary site for vitamin D reclamation and activation [16]. There is a high prevalence of vitamin D deficiency in SCD patients [17, 18], which may be due in part to PT dysfunction. Additionally, vitamin D deficiency is reportedly correlated with increased inflammation and vaso-occlusive crises in SCD patients [19]. Together, this suggests early PT dysfunction could hinder the critical maintenance of vitamin D status in SCD patients to further contribute to disease pathogenesis.

1.2 Sickle Cell Disease

SCD was first characterized in 1910 upon the observation of “sickle-shaped” red blood cells (RBCs) in a blood sample [20]. It is most prevalent in areas plagued by malaria due to the protective effect of the sickle cell trait against infection. However, the distribution of SCD has spread outside these areas due to global migration in the last two centuries [21, 22]. SCD is caused by mutation of the hemoglobin β-globin subunit gene, *HBB*. While many disease-causing variants

have been reported, the classic and most well-studied variant, hemoglobin S (HbS), is caused by a single nucleic acid change (c.17T>A), leading to an amino acid change (p.Glu6Val) early in the β-globin protein. The HbS mutation changes the structural integrity of hemoglobin (Hb) to promote polymerization in RBCs, forcing the affected cells into a rigid, sickled shape that increases the likelihood of vasculature blockage and RBC hemolysis.

1.2.1 Sickle cell disease genetics

The most prevalent form of SCD is sickle cell anemia, which is caused by the inheritance of two HbS variants [23]. Although all reported SCD genotypes contain at least one copy of the HbS variant, many other pathogenic *HBB* variants exist. Other variants include different single and dual point mutations and large deletions within the *HBB* gene. Appendix A Table 2, modified from reference [1], provides a comprehensive list of genotypes previously reported to cause SCD characterized by their associated disease severity.

Most SCD cases outside of sickle cell anemia are caused by hemoglobin SC disease, which is characterized by the coinheritance of the HbS and hemoglobin C (HbC) variants [24]. The third most common form of SCD occurs through coinheritance of the HbS variant and β-thalassemia alleles [1]. Rather than altering Hb's structural conformation, β-thalassemia alleles decrease production of the affected *HBB* gene and are characterized by the reduction in protein expression (for more information on β-thalassemia see reference [25]). All other SCD cases caused by various mutations are quite rare and thus not well studied.

1.2.2 Hemoglobin

Expressed exclusively in RBCs (immature reticulocytes and mature erythrocytes), Hb is the primary circulating oxygen carrier protein in the body. Within RBCs, Hb functions as a heterotetramer comprised of two symmetric heterodimer pairs and one heme molecule per monomer [26]. Hb dimers are created by the association of one polypeptide chain from the α-globin gene cluster (α and ζ genes; chromosome 16) and another from the β-globin gene cluster (β, γ, ε genes; chromosome 11) [27]. These gene clusters have evolved to create a temporal expression pattern throughout development, shifting gene expression from 5' to 3' during the progression from fetus to adult (Fig. 1) [27, 28].

The most commonly expressed Hb formation in adults is hemoglobin A (HbA), which consists of two αβ heterodimers [26, 27]. However, the principally expressed Hb formation in fetal development is hemoglobin F (HbF), comprised of two αγ heterodimers. HbF is expressed during fetal development to facilitate oxygen flow from mother to fetus as it has a stronger affinity for oxygen than HbA [27]. After birth, γ-globin genes are downregulated and the β-globin gene is upregulated (Fig. 1), shifting Hb tetramer expression from HbF to HbA within the first year of life [29]. Because of this shift in expression after birth, SCD patients are commonly asymptomatic until around 8-10 weeks of age [30]. Although significant progress has been made recently to elucidate the regulation of the expressional shift from γ-globin to β-globin [31], the exact mechanism is still not completely understood.

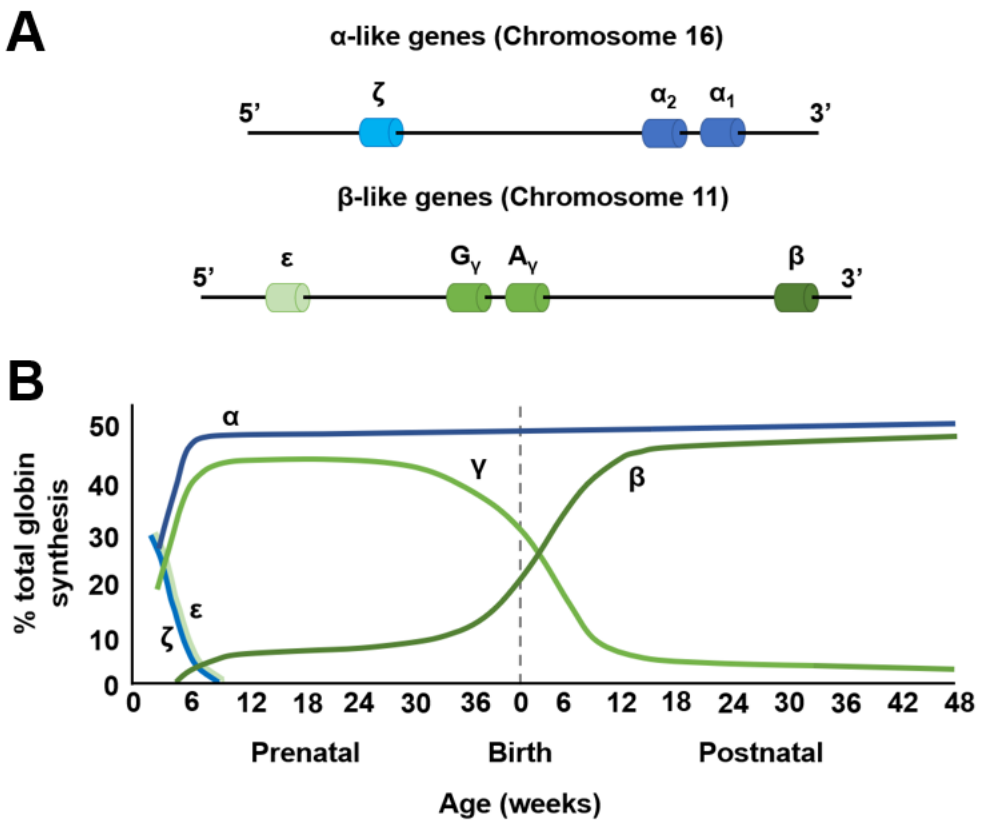

Figure 1. Globin gene location and temporal expression during development.

Hb monomer globin gene clusters are spatially arranged on chromosomes (α-like on Chr.16 and β-like on Chr.11) 5' to 3' (A) to mirror expression changes during development and adulthood (B). ζ-globin and ε-globin genes are first expressed in the fetal yolk sac, para-aortic region, and liver. Around six weeks after conception, these genes are downregulated and the α-globin (α_1 and α_2) and γ-globin (Aγ and Gγ) genes are upregulated, giving rise to a predominant hemoglobin F (HbF) expression. Downregulation of γ-globin genes and upregulation of β-globin begins at birth [27]. At approximately 8-10 weeks postnatal, the majority of Hb tetramers are hemoglobin A (HbA) type [30].

Adult Hb αβ tetramers are spatially arranged so that α-globin monomers bind to β-globin monomers via two distinct interfaces with differing binding affinities, denoted as $\alpha_1\beta_1$ and $\alpha_1\beta_2$. Initially, αβ dimers form through extremely high affinity binding at the $\alpha_1\beta_1$ interface. These dimers then interact with each other through a lower affinity $\alpha_1\beta_2$ interface, forming tetramers [32]. The $\alpha_1\beta_2$ interface is destabilized upon oxygen molecule (O_2) binding at the heme group of one subunit to create a conformational change within the tetramer, facilitating additional O_2 binding at

other heme sites. This cooperative binding of O_2 is considered positive allosteric regulation as each bound O_2 enhances O_2 binding at other sites within the tetramer [32]. Alternatively, allosteric regulation of O_2 binding by other molecules can promote O_2 release when tissue oxygenation is needed. For example, metabolic tissues with high O_2 demands produce large amounts of carbon dioxide (CO_2) which is taken up and metabolized by erythrocytes, producing carbonic acid and one hydrogen atom (H^+) per reaction. H^+ allosterically interacts with Hb, a process referred to as the Bohr effect, to stimulate O_2 release and delivery to the tissue [33]. Additionally, 2,3-diphosphoglycerate (2,3-DPG), a by-product of glycolysis, can allosterically regulate Hb to facilitate O_2 release, ensuring efficient O_2 delivery to metabolically active tissues [34].

In order to bind O_2, the iron within the heme group of each subunit must be in its reduced ferrous (Fe^{2+}) state. This form of Hb is referred to as oxyhemoglobin (oxyHb) and is the primary circulating form of Hb. Because O_2 has a higher redox potential than iron, oxyHb can occasionally autoxidize to form superoxide and methemoglobin (metHb), the form of Hb containing oxidized ferric (Fe^{3+}) iron. Normally metHb levels amount to less than 2% of all circulating Hb. Genetic mutations in Hb that increase its propensity to autoxidize, including HbS, and exposure to certain oxidizing drugs and toxins can unnaturally increase metHb levels in the body [32, 35]. MetHb is unable to bind O_2 and is more unstable than oxyHb. MetHb instability leads to an increased risk of heme loss and reactive oxygen species (ROS) production [32, 36]. Because of this, there are mechanisms within erythrocytes, such as enzymatic conversion of metHb by metHb reductase, to ensure that most Hb tetramers are maintained in the oxyHb conformation [32, 37]. In addition to O_2, Hb is capable of interacting with CO_2, carbon monoxide, and nitric oxide (NO) [27].

1.2.3 Pathophysiology

HbS protein misfolding in RBCs alters the general binding dynamics of Hb tetramers and lowers O_2 binding affinity. In its deoxygenated state, mutant Hb polymerizes to form long chains, forcing affected RBCs into the characteristic sickled shape and reducing their flexibility. This reduced flexibility impairs RBC rheology, or flow, through the blood [38, 39]. RBCs can aggregate within the vascular system to further impede blood flow and create vaso-occlusive crises in patients [39].

In addition to RBC shape, lipid and membrane dynamics are altered via direct and indirect responses to Hb polymerization and corresponding oxidative stress. Many ion channels and membrane proteins along the RBC membrane become dysfunctional from recurring cycles of HbS polymerization, resulting in cellular dehydration and loss of membrane to form circulating microparticles [38, 40]. Large loss of RBC membrane over time allows for significant rearrangement of membrane lipid composition, particularly allowing phosphatidylserine localization to extend from inner to outer membrane. Exposed phosphatidylserine on circulating RBCs increases cellular interactions with other RBCs, white blood cells, and platelets. This can cause activation of endothelial cells and coagulation pathways [41]. Endothelial cell activation, in turn, increases inflammation by producing pro-inflammatory markers, such as interleukin-6 (IL-6), and tumor necrosis factor alpha (TNF-α) [38, 42]. Altogether, these mechanisms increase the likelihood of further vaso-occlusion.

Vaso-occlusion and sickled RBC instability lead to a significant increase in hemolysis. In fact, the average erythrocyte lifespan in SCD patients is significantly shorter than in healthy individuals [43, 44]. While hemolysis is thought to primarily occur outside of the vasculature (mediated by macrophage phagocytosis in the spleen), approximately one-third of all hemolysis

occurs intravascularly during the resolution of vaso-occlusion [45]. Increased hemolysis generates higher concentrations of cell-free Hb and heme in the plasma (estimated concentrations are listed in Appendix A Table 3), which can lead to increased oxidative stress. Both Hb and heme can create superoxide, ROS, and other oxidative species to induce cellular toxicity as well as vasoconstriction [44]. Additionally, cell-free Hb scavenges NO to reduce potential vasodilatory response, further worsening blood flow and increasing risk of vaso-occlusion [46]. Although there are carrier proteins to sequester cell-free Hb in the serum, such as haptoglobin (Hpt) and hemopexin, the expression of these carriers are eventually depleted in many SCD patients [47, 48].

Recurring vaso-occlusive crises, accompanied by increased oxidative stress and inflammation, function to create clinical manifestations of disease in both the vascular system and essentially every organ system of the body (see Appendix A Table 4 for a comprehensive list of common SCD complications). SCD patients are generally immunocompromised as much of the disease pathology involves the chronic abuse of the body's immune system and splenic function. Because of this, infection has historically been a great concern for patient health and a major cause of mortality in patients during infancy [30, 49]. However, with the implementation of SCD newborn screening and improved patient treatment, many SCD patients live well into adulthood, especially in developed countries like the US. Consequently, with the increase in patients reaching adulthood, there is a significant rise in irreversible secondary organ damage and chronic disease.

1.2.4 Sickle cell nephropathy

SCN is one of the most common secondary complications in SCD and patients exhibit a wide range of renal disease manifestations throughout all stages of life. The severity of SCN should not be overlooked as kidney-related injury and disease account for 16-18% of SCD patient

mortality [6]. Complications contributing to SCN arise from both vaso-occlusion/hemolysis within the kidney microvasculature and oxidative stress/toxicity related to increased cellular exposure to free Hb and heme.

Vaso-occlusion occurs most frequently in the vasa recta of the medulla because of its naturally hypoxic environment. Recurring cycles of vaso-occlusion create episodes of ischemia that can either result in infarction or resolution and reperfusion of the tissue. Blood flow infarction as well as repeated ischemia-reperfusion events can lead to increased oxidative stress, tissue dysfunction, and necrosis [6, 50]. Common disease phenotypes linked to this pathology are papillary necrosis, hyposthenuria, and hematuria [51-53]. Additionally, renal hyperperfusion and hyperfiltration are indirectly connected to these vaso-occlusive events. Although increased vaso-occlusion impedes blood flow in the microvasculature of the renal medulla, hyperperfusion and hyperfiltration predominate whole kidney dynamics. This phenomenon, referred to as the perfusion paradox [54], is thought to be caused in part by a vasodilatory effect of increased prostaglandin and heme oxygenase-1 (HO-1) expression in response to ischemia and oxidative stress [6].

Glomerular hyperfiltration commonly occurs early in SCD patients before signs of glomerular impairment are evident. Hyperfiltration increases the load of protein and solutes delivered to the nephron. To compensate, the PT increases its resorptive and metabolic functions to maintain glomerulotubular balance. However, the sustainability of this PT hyperfunction is difficult and a significant proportion of young SCD patients (~15%) develop tubular proteinuria, which is urinary loss of proteins normally filtered by the glomerulus and reabsorbed by the PT [10-12]. These patients frequently lack noticeable glomerular damage at diagnosis of tubular proteinuria, suggesting that PT dysfunction occurs early in the progression of their kidney disease.

PT hypermetabolism and increased oxygen consumption can cause oxidative stress and dysfunction in the PT and surrounding interstitial tissue [55]. Early PT dysfunction may also occur as a result of increased exposure to free Hb as PT cells are exceptionally sensitive to heme toxicity [56-58]. Free Hb is readily filtered by the glomerulus (fractional filtration coefficient of 0.03) and delivered to the PT, where it can be taken up through binding to multiligand receptors megalin and cubilin [59, 60]. For more information on PT protein resorption and megalin/cubilin binding see sections on PT function below.

Glomerular health and function diminish with age due to the pressure of hyperfiltration and targeted injury. Hb and heme generate toxic effects in podocytes to impair their function in maintaining the filtration barrier [61]. Additionally, increased levels of endothelin-1, a vasoconstrictive signaling peptide, interact with podocytes via the endothelin type A (ETA) receptor to further induce injury [62]. As podocyte injury accumulates, glomerular filtration becomes leakier. This allows more ions and protein to enter the tubule, further overwhelming PT resorptive capacity. The development of frank proteinuria and albuminuria commonly develop in patients as glomerular filtration deteriorates. With continued renal damage and loss of function, patients can develop CKD and renal failure. While it is likely that continued renal vascular insult, tubular/glomerular dysfunction, and tubulointerstitial damage contribute together to the development of CKD, the exact mechanism remains unclear.

1.2.5 Disease management and treatment

Although the cause of SCD has been known for approximately 70 years, treatment of the disease and its severe complications has proven difficult. The first recommended treatment for a secondary complication of SCD was the use of prophylactic penicillin in children to prevent life-

threatening infection. Penicillin prophylaxis dramatically increased childhood survival rates as its use alone has been shown to reduce pneumococcal bacterial infection by 84% in SCD patients [63]. Because of the significant increase in childhood SCD survival rate using prophylactic penicillin, there has been a great effort to institute universal newborn screening programs for SCD. Screening was established across all US states in 2007 [64]. Prevention of infection is critical in many SCD patients as elective splenectomy is common to treat mass acute sequestration and anemia, forcing patients to be further immunocompromised [1].

Currently, there are only two FDA approved drugs to treat SCD: hydroxyurea and Endari®. Hydroxyurea, also known as hydroxycarbamide, is a chemotherapeutic drug that increases levels of HbF in SCD patients and thus decreases HbS levels to reduce RBC sickling. Hydroxyurea treatment has been approved for use in both children and adults and is associated with decreased risks of frequent vaso-occlusive crises, acute chest syndrome, and stroke [38, 65]. However, it does have limitations in efficacy as increased HbF sustainability varies among patients and patient adherence can be poor due to challenges in cost and perceptions of toxicity [66, 67]. Endari® is an oral formulation of L-glutamine that functions to increase NADH levels, providing more cellular antioxidant activity. Although more studies are needed to determine the long term effects of Endari®, it has been shown to decrease frequency of vaso-occlusive crises in patients when used alone or in combination with hydroxyurea treatment [68, 69].

Recurring blood transfusions aid in the prevention of vaso-occlusive crises as donor RBCs dilute sickled patient cells. Blood transfusions are also useful in treating anemia and preventing stroke in SCD patients. However, chronic transfusions can lead to delayed secondary complications, including erythrocyte alloimmunization, increased hemolysis, and iron deposition [1, 2]. Additionally, steroids are used to decrease inflammation and analgesics, including

nonsteroidal anti-inflammatory drugs (NSAIDs) and opioids, are used in an attempt to decrease chronic pain. However, continued analgesic use should be used with caution as patient dependence and analgesic-induced nephropathy can develop [9].

Hematopoietic stem cell transplantation has been demonstrated to be curative in a limited number of patients. However, this treatment is extremely costly and is currently limited to patients with a healthy sibling donor, making it an unlikely option for many [1, 70]. To overcome the need for a proper donor candidate, researchers are exploring gene therapy and genome editing techniques to alter SCD patient cells. Clinical trials are currently underway using gene therapy, including the addition of an anti-sickling *HBB* gene variant and the deletion of the *BCL11A* gene (partly responsible for repression of γ-globin expression). Additionally, researchers are looking into using genome editing techniques to induce γ-globin expression or correct SCD mutation in the patient's genome [71, 72]. While time will only tell if these genetic techniques will provide patients with a more permanent treatment of their disease, one known certainty is that gene therapy would still be costly, making patient access a continued concern. However, if this form of therapy would prove to be curative the price may outweigh the cost of lifelong treatment and burden of disease.

1.2.5.1 Treatment of sickle cell nephropathy

In addition to prevention of vaso-occlusive crises in SCD patients, targeted treatments for SCN have recently emerged. Angiotensin-converting enzyme (ACE) inhibitors and angiotensin receptor type II blockers (ARBs) are used to block angiotensin II signaling, which increases efferent arteriole dilation and lowers local blood pressure. Preliminary data has shown ACE inhibitors and ARBs reduce the frequency of proteinuria in patients [9, 73]. However, adequately powered studies are needed to further assess the benefit and determine a recommendation of when

to use this treatment. Use of alkalizing agents such as sodium bicarbonate and acetazolamide to neutralize acidity in the medulla can increase O_2 binding and prevent RBC sickling and hemolysis within the kidney [74]. Studies in a SCD mouse model have shown promise in using endothelin-1 receptor inhibitors to reduce vaso-occlusion and associated kidney damage [75-77]. However, clinical trials are needed to test efficacy in humans.

Once kidney damage has progressed to CKD or ESRD, patients are placed on renal replacement therapy, involving hemodialysis and/or kidney transplant. Although SCD is an independent risk factor of death in patients receiving new kidneys, patients may have more trouble receiving transplants in comparison to age- and race-matched individuals without SCD [78]. Additionally, hemodialysis can be very difficult and ineffective for SCD patients as mortality rates are 26% higher in comparison to SCD patients pre-dialysis and 2.8 times higher than dialysis patients without SCD [79, 80].

1.3 Receptor-Mediated Endocytosis in the Proximal Tubule

Sections within 1.3 are reprinted with minor edits from Annual Review of Physiology, vol. 79 (1), Megan L. Eshbach and Ora A. Weisz, Receptor-mediated endocytosis in the proximal tubule, 425-488, Copyright (2017) with permission from Annual Reviews.

Epithelial cells that form the PT play an essential role in the retrieval of ions and proteins that escape the glomerular filtration barrier. Cells in the proximal convoluted tubule (which includes the S1 and S2 segments) express high levels of the multiligand receptors megalin and cubilin, which mediate the efficient uptake of low molecular weight (LMW) proteins and other ligands from the filtrate. The apical endocytic pathway in PT cells is uniquely specialized to

accommodate the high capacity needs of these cells and is acutely and chronically regulated in response to changes in ligand exposure. Yet despite the critical role of endocytosis in PT function, we know little about how the apical endocytic pathway is organized and regulated in these cells. Numerous genetic, acute, and chronic diseases impair the endocytic uptake of filtered ligands by PT cells, resulting in tubular proteinuria (aka LMW proteinuria). Megalin and cubilin bind to numerous vitamin carrier proteins, and defective uptake of these proteins leads to vitamin deficiencies. In many instances, kidney function deteriorates progressively in patients with tubular proteinuria. However, it remains unclear whether tubular proteinuria is a marker of PT damage or a direct cause of further damage [81]. A better understanding of the PT apical endocytic pathway and the consequences of its dysfunction may thus identify new interventional targets to prevent or limit kidney disease.

1.3.1 Multiligand receptors of the proximal tubule

The multiligand receptors megalin and cubilin coordinate the uptake of most filtered proteins and many other small bioactive molecules from the glomerular ultrafiltrate (Fig. 2).

Megalin (also called gp330 or *LRP2*) is a member of the low-density lipoprotein receptor (LDLR) family of proteins that was originally identified by Kerjaschki & Farquhar as a major pathogenic antigen in Heymann nephritis in 1982 [82] and found to be equivalent to brushin, a ~600 kDa PT brush border protein previously described by the Muramatsu group [83]. Within the kidney, megalin is expressed primarily at the apical surface and in apical endocytic compartments of epithelial cells that comprise the S1 segment of the PT, with decreasing expression in the S2 and S3 segments of the PT. Megalin is also expressed in podocytes, and antigenic responses to megalin in these cells is a primary cause of Heymann nephritis in rats [84].

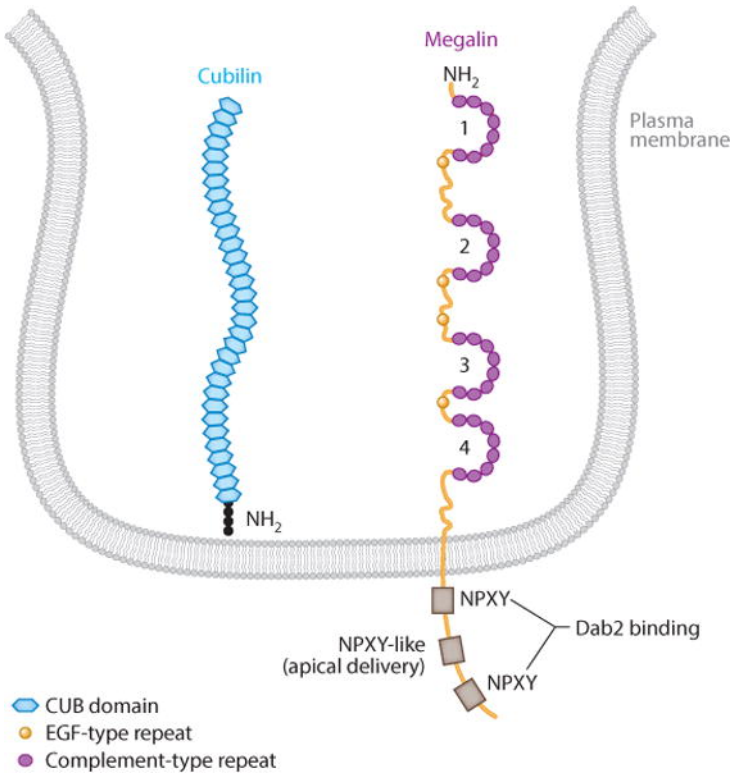

Figure 2. Multiligand receptors in the proximal tubule.

Megalin and cubilin regulate the uptake of low molecular weight proteins from the glomerular filtrate. The cytoplasmic tail of megalin contains two NPXY motifs that bind to the Dab2 clathrin adaptor protein as well as a related NQNY sequence implicated in apical delivery. Megalin/cubilin ligands that are filtered through the glomerular barrier are listed in Appendix A Table 5. Abbreviations: CUB, complement C1r/C1s, Uegf, Bmp1; Dab2, Disabled-2 protein; EGF, epidermal growth factor.

The sequences of rat and human megalin were reported in 1994 and 1996, respectively [85, 86]. Rat megalin contains 4660 amino acids and is a type I transmembrane protein with a large lumenal domain that contains 36 LDLR ligand binding complement type repeat motifs clustered into four domains. These domains are interspersed with epidermal growth factor (EGF)-type repeats and beta propeller spacers characterized by YWTD motifs that mediate ligand dissociation in acidified compartments (see reference [87] for an excellent review on the structure and function of LDLR family member domains). The cytoplasmic tails of all LDL receptor family members are divergent other than the presence of two NPXY motifs that mediate endocytosis; in addition,

megalin contains an additional NPXY-like motif VENQNY that may be important for apical delivery of the protein [88]. Similar to other members of the LDLR family, megalin also contains an RXRR motif that can be cleaved by furin and related proteases. Cleavage at this site could explain the soluble form observed associated with cells and secreted into the urine [89]. Megalin was also demonstrated to undergo regulated intramembrane proteolytic cleavage [90]; however, the physiological significance of this is unclear [91, 92].

Folding and biosynthetic trafficking of megalin are facilitated by its interaction with the chaperone receptor-associated protein (RAP) that is localized primarily to the endoplasmic reticulum. RAP also accompanies megalin to the plasma membrane [93, 94] and dissociates from the receptor in acidified compartments [95]. RAP also interacts with the LDLR-related protein LRP. It was proposed that binding to RAP prevents premature interaction of megalin with ligands along the biosynthetic pathway [94].

Early studies aimed at identifying the function of megalin demonstrated that it interacts with several proteins that also bind to LRP, including ApoE and lipoprotein lipase. Since then, interaction of megalin with an increasing number of filtered ligands has been reported [96]. An essential role for megalin in the uptake of filtered proteins was cemented in 1996 by the demonstration that mice lacking megalin exhibit tubular proteinuria [97] and by the observation that RAP competes with albumin for uptake in microperfused tubules [98].

Whereas megalin can bind to many ligands independently, it may require a coreceptor for some interactions. Cubilin is a 460 kDa receptor expressed abundantly in the PT that interacts with megalin and increases the multiligand binding capability of the complex. Cubilin was originally identified as the receptor for intrinsic factor-vitamin B12 complex in the intestine [99] and was subsequently shown to be identical to a previously described antigen that localized to coated pits

in the rat PT [100, 101]. The receptor was cloned from rat yolk sac in 1998 and named cubilin based on the presence of 27 tandem CUB (complement C1r/C1s, Uegf, Bmp1) domain repeats that encompass the majority of the protein sequence [102]. Unlike megalin, cubilin has no transmembrane domain and requires megalin for its association with the membrane. Cubilin binds to several of the proteins recognized by megalin, including albumin, Hb, RAP, and Ig light chains. Appendix A Table 5 lists the ligands known to be retrieved by the PT through their interactions with megalin and cubilin. In addition, cubilin may also bind to other proteins that do not bind to megalin, including transferrin, intrinsic factor-vitamin B12 complex, and apoA1. Cubilin-specific ligands were originally identified in the urine of dogs with mutations in cubilin and in patients with Imerslund-Gräsbeck syndrome, who have vitamin B12 malabsorption. However, there may be some species-specific differences in cubilin binding selectivity, as unlike dogs lacking functional cubilin, cubilin knockout mice showed no increase in urinary excretion of transferrin or apoA1 [103, 104].

Cubilin also interacts with amnionless, a 38–50 kDa transmembrane protein that, similar to megalin, contains cytoplasmic NPXY motifs that direct internalization. Amnionless appears to be essential for cubilin transport to the apical surface, as cubilin is retained intracellularly in PT cells of amnionless knockout mice [105]. Mutations in amnionless also cause Imerslund-Gräsbeck syndrome [106]. Cubilin binds simultaneously to megalin and amnionless [107], but whether and how these three proteins interact functionally at the apical membrane of PT cells remain unclear.

More recently, the ubiquitously expressed MHC-related Fc receptor for IgG (FcRN) has also emerged as a potential receptor that participates in IgG and albumin recovery from the ultrafiltrate. This heterodimeric receptor, comprising an MHC class I-like α chain and its obligatory β2-microglobulin subunit, binds independently to IgG and to albumin at acidic pH but

not at neutral pH. FcRN is known to play an important role in salvaging serum IgG and albumin in many nonrenal tissues (reviewed in [108]). The current model in these cells is that these proteins are taken up by pinocytosis and bind to FcRN in acidified compartments. Proteins that bind to FcRN escape the default route to the degradative pathway and are instead recycled to the cell surface where the increase in pH causes them to be released. Consistent with this model, FcRN knockout mice have half the levels of serum albumin as normal mice, apparently due to increased degradation kinetics [109].

FcRN is expressed abundantly in the glomerulus and PT of the kidney. Within the glomerulus, FcRN is expressed at the surface of podocytes and may function to scavenge albumin and immunoglobulins from the basement membrane to limit clogging of the filtration barrier [110]. In contrast, in the PT, FcRN binds to soluble albumin that dissociates from megalin/cubilin in acidified endocytic compartments and delivers it via transcytosis to the basolateral surface for reentry into the plasma [111]. The extent to which this pathway in the PT contributes to the maintenance of serum albumin levels remains controversial. One contested parameter is the amount of albumin that actually reaches the PT (nicely reviewed in [112]). Another key issue that remains to be addressed is the extent to which transcytosis of albumin occurs in the kidney, and how much of this is mediated by FcRN. Tenten et al. [111] attempted to address the role of FcRN-mediated transcytosis of postfiltered albumin by observing the appearance in serum of tagged albumin expressed selectively in podocytes of control and FcRN knockout mice. Although tagged albumin could be detected in the serum, the capacity of this salvage pathway relative to the degradative pathway in PT cells could not be assessed in this study. Of note, earlier studies assessing the fate of radioiodinated albumin in HK-2 human proximal kidney cells, perfused ex vivo rat kidneys, and microperfused rabbit PTs concluded that the majority of internalized albumin

was degraded rather than transcytosed to the basolateral surface [113, 114]. On balance, the evidence to date remains consistent with the idea that PT reclamation of albumin represents a relatively low-level salvage pathway to recover a small amount of filtered protein rather than a high capacity transcytotic pipeline necessary to maintain serum albumin levels.

1.3.2 Clathrin-dependent endocytosis

The apical endocytic pathway in PT cells is highly specialized for robust internalization and is uniquely organized for this function [115]. Moreover, the capacity for apical endocytosis is both acutely and chronically flexible, as described further in later sections. The preference for apically driven endocytosis and the consequent organization of the endocytic pathway is recapitulated to differing extents in primary and immortalized cell culture models of the PT [116-118]. Although in vivo studies have provided a detailed morphological description of the PT endocytic pathway, the lack of an ideal cell culture model system has hampered our ability to understand how endocytosis and recycling are regulated at the molecular level in these cells. To date, our most detailed information about the organization, cellular machinery, and regulation of the apical endocytic pathway in polarized kidney epithelial cells comes from studies conducted in Madin-Darby canine kidney (MDCK) cells, which maintain a limited apical endocytic capacity and are not considered a representative model of the PT (Fig. 3). Many PT cell culture models do exist, however, but most are poorly differentiated and lack the apical microvilli characteristic of the PT brush border. Others exhibit relatively poor megalin expression and/or apical endocytic capacity and may better represent S2 or S3 segments of the PT. At present, the opossum kidney (OK) cell line remains the preferred cell culture model for the S1 segment of the PT, as it most

closely recapitulates PT ion transport functions, expresses megalin, retains a robust apical endocytic capacity, and is well differentiated.

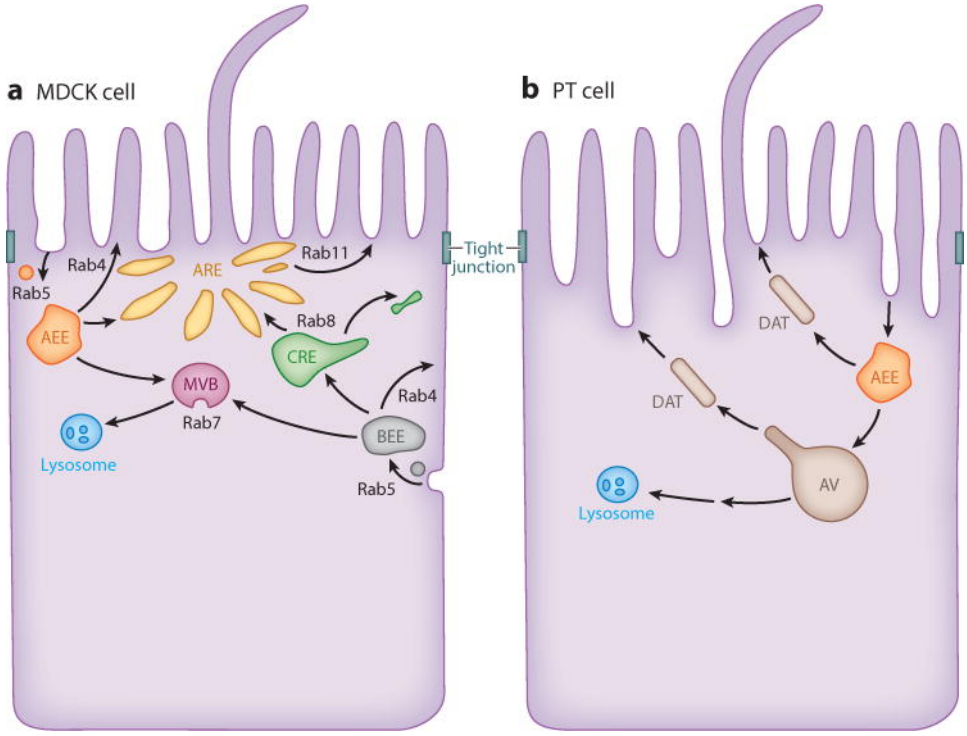

Figure 3. The apical endocytic pathway in MDCK and proximal tubule cells.

(a) Cargo internalized from the apical and basolateral surface of MDCK cells via clathrin-coated pits enters Rab5-positive AEEs and BEEs, respectively. Most proteins return to the plasma membrane from these compartments via a Rab4-dependent fast recycling pathway, but they may also be delivered to Rab11-positive AREs or Rab8-positive CREs. Ligands released from internalized receptors in acidified early endosomes are transported to Rab7-positive MVBs and eventually to lysosomes. (b) In PT cells, apical proteins are internalized in irregular clathrin-coated invaginations into apical early endosomes that fuse to form larger AVs. Recycling of membrane proteins can occur from AEEs or AVs via DATs, whereas soluble components of AVs are delivered to lysosomes. The Rab proteins and other machinery associated with these compartments remain largely unknown. Abbreviations: AEE, apical early endosomes; ARE, apical recycling endosomes; AV, apical vacuole; BEE, basolateral early endosomes; CRE, common recycling endosomes; DAT, dense apical tubules; MDCK, Madin-Darby canine kidney; MVB, multivesicular bodies; PT, proximal tubule.

1.4 Vitamin D Metabolism

Vitamin D metabolism is a highly regulated, multiorgan process (outlined in Appendix A Fig. 18). First, prohormone vitamin D is produced in the skin through conversion from 7-dehydrocholesterol upon ultraviolet irradiation and thermal rearrangement or is absorbed from a diet that includes dairy products and/or fish oils. Vitamin D is then transported to the liver where it is converted to 25-hydroxyvitamin D [25(OH)D], which is the primary circulating vitamin D metabolite by concentration [119]. Although not hormonally active just yet, 25(OH)D serum concentration is used as the most reliable biomarker of vitamin D status because of its normally high concentration and long half-life (approximately 2-3 weeks) [120-122]. Of note, DBP and albumin, the two vitamin D metabolite carriers, are also produced in the liver [123]. Vitamin D metabolites are estimated to be 85-90% bound to DBP, 10-15% bound to albumin, and less than 1% unbound in the serum, suggesting these carrier proteins play a large role in both vitamin D transport and availability. In particular, DBP plays a large role in vitamin D availability as vitamin D metabolite affinity for DBP is much higher than albumin and only metabolites that are unbound or bound to albumin are considered bioavailable [16].

At any given time DBP is primarily bound to 25(OH)D. This is because 25(OH)D is most abundant in the serum and DBP binds 25(OH)D with greater affinity than other vitamin D metabolites [124]. DBP travels to the kidney where it binds to megalin/cubilin receptors to enter PT cells. Once inside PT cells, DBP is degraded in lysosomes, and any associated 25(OH)D is trafficked to mitochondria for activation. The mitochondrial enzyme 25-hydroxyvitamin D-1 alpha hydroxylase (CYP27B1) converts 25(OH)D to its metabolically active form 1,25-dihydroxyvitamin D [1,25$(OH)_2$D] (Fig. 4). After activation, 1,25$(OH)_2$D is released on the basolateral side of PT cells to enter the bloodstream for distribution to target tissues [125].

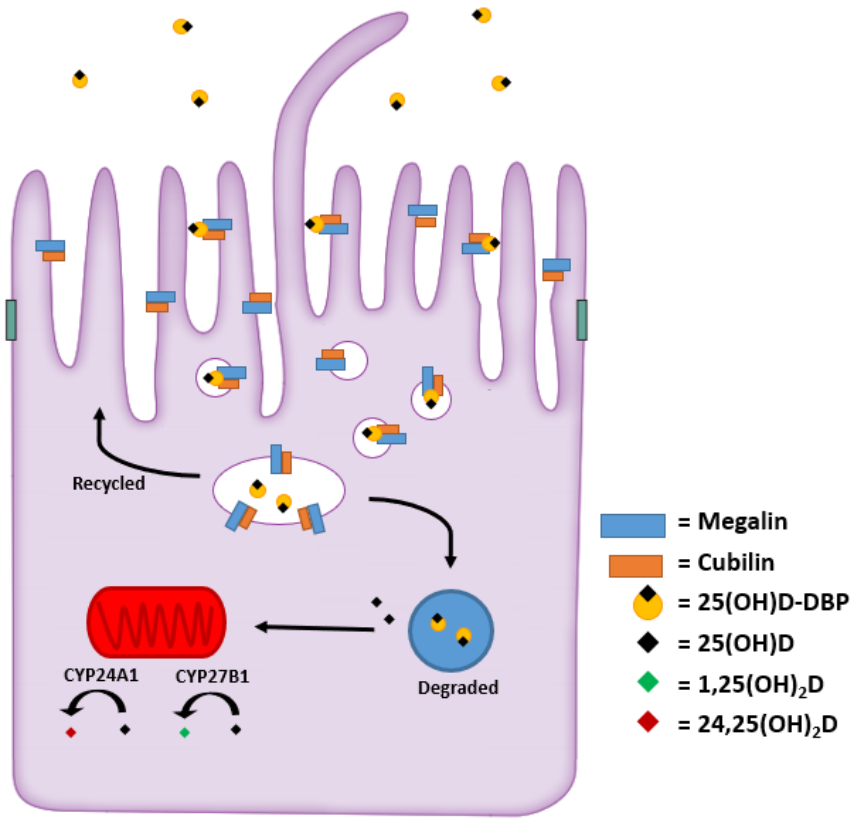

Figure 4. Vitamin D trafficking and metabolism in the proximal tubule cell.

Vitamin D-binding protein (DBP) carrying 25(OH)D binds to megalin and cubilin receptors and enters PT cells via endocytosis. Once inside cells, 25(OH)D-DBP is sorted and trafficked to lysosomes and megalin and cubilin are recycled back to the surface for continued endocytosis. DBP is degraded in lysosomes and 25(OH)D is trafficked to the mitochondria. Mitochondrial vitamin D hydroxylases CYP27B1 and CYP24A1 metabolize 25(OH)D. CYP27B1 converts 25(OH)D to its active form $1,25(OH)_2D$. CYP24A1 converts 25(OH)D to $24,25(OH)_2D$, which is thought to be targeted for degradation. The conversion of 25(OH)D is dependent on concentrations of circulating $1,25(OH)_2D$.

While several extra-renal tissues are reported to express CYP27B1, the PT is the primary site for vitamin D activation [16]. Several disease models have provided compelling data to support the importance of PT-specific vitamin D activation. Anephric patients have extremely low and sometimes undetectable $1,25(OH)_2D$ serum levels [126]. Megalin knockout mice lose DBP in urine and develop vitamin D deficiency and consequent bone disease [97, 127]. Cubilin-deficient

dogs also exhibit lower serum levels of vitamin D [25(OH)D and 1,25$(OH)_2$D] [128]. Patients with Dent disease, caused by a mutation in an antiporter involved in PT endocytosis, have low vitamin D levels and frequently develop bone disease [129].

1.4.1 Vitamin D signaling in the proximal tubule

In target cells of vitamin D signaling, bioavailable 1,25$(OH)_2$D interacts with vitamin D receptor (VDR) in the nucleus to enact transcriptional alteration [119]. VDR binds at vitamin D response elements (VDREs) in DNA to cause enhancement or inhibition of gene transcription depending on VDRE location [130]. While VDR cellular localization has been identified outside of the nucleus, including along the apical brush border of PT cells [131], the function of this VDR pool is widely debated. Additionally, it is still unclear how 1,25$(OH)_2$D enters the nucleus of target cells, especially those not expressing megalin or cubilin, to enact transcriptional regulation [16]. However, PT cells are known to express VDR, both in and outside of the nucleus, and megalin/cubilin receptors, enabling 1,25$(OH)_2$D transport into the cell and nucleus to perform transcriptional regulation. In fact, 1,25$(OH)_2$D signaling in the PT is imperative in the regulation of continued vitamin D metabolism.

Overall, VDR signaling in the PT works as a feedback loop to reduce vitamin D activation. This is accomplished primarily through decreased expression of CYP27B1 and increased expression of another mitochondrial enzyme 1,25-dihydroxyvitamin D 24-hydroxylase (CYP24A1). Decreased CYP27B1 expression reduces 1,25$(OH)_2$D production. Increased CYP24A1 expression expedites 1,25$(OH)_2$D and 25(OH)D breakdown as 24-hydroxylated metabolites, 1,24,25$(OH)_3$D and 24,25$(OH)_2$D are thought to be degradation products [119]. VDR signaling has also been reported to affect expression of PT receptors megalin and cubilin. In PT

cells grown in culture, addition of $1,25(OH)_2D$ increased megalin and decreased cubilin expression [132, 133]. However, it is unknown whether these transcriptional changes ultimately affect PT cell endocytic uptake of DBP and other proteins.

1.4.2 Vitamin D immunomodulation and its effects on inflammation in sickle cell disease

Recent research has begun to emerge demonstrating several immunomodulatory effects of vitamin D signaling, particularly in the suppression of the adaptive immune system. Vitamin D signaling diminishes the adaptive immune response in several ways. It reduces dendritic cell maturation and macrophage antigen presentation [134-137]. Additionally, vitamin D signaling promotes T cell differentiation into T helper cell type 2 (Th2) and regulatory T (Treg) cells rather than T helper cell type 1 (Th1) and T helper cell type 17 (Th17) cells [137-140]. This change in immune cell differentiation reduces inflammation by increasing anti-inflammatory and decreasing pro-inflammatory cytokine expression (Appendix A Fig. 19) [141-143].

Chronic inflammation is very common in SCD and is thought to be partly caused by cytokine dysregulation, resulting in increased pro-inflammatory and decreased anti-inflammatory cytokine expression. Vitamin D signaling also alters the expression of many of these same dysregulated cytokines, including IL-6, IL-10, IL-17, IL-4, and TNF-α [19, 144-146], to suppress an inflammatory response. This suggests an important role for vitamin D in the deterrence of inflammation in SCD. SCD patients are commonly vitamin D deficient and low vitamin D status is reportedly associated with several comorbidities, including vaso-occlusive crisis [18, 147]. Additionally, vitamin D supplementation has already been demonstrated to be useful in the treatment of inflammation in other diseases, including acute congestive cardiac failure and autoimmune cytopenias [148, 149], and has been reported to decrease pro-inflammatory cytokine

expression in SCD patients [19]. However, very few studies have focused on vitamin D supplementation in SCD and there is a need for more comprehensive study to determine the full benefits of supplementation and treatment recommendations.

1.5 Specific Aims

While there has been a great deal of progress in the treatment of acute complications in SCD, treatment of chronic secondary complications, including SCN, is lacking. Patients that develop SCN have minimal treatment options and a very poor prognosis once their disease has progressed to CKD. A common symptom in young SCD patients is tubular proteinuria, which is indicative of PT dysfunction early in the progression of SCN. PT dysfunction may also be a factor in low vitamin D status commonly observed in SCD patients as the PT is the primary site of vitamin D activation. Since the PT is known to be sensitive to heme toxicity and patients exhibit increased levels of cell-free Hb chronically and during hemolytic crisis, PT dysfunction is thought to be associated with increased Hb exposure although the pathophysiology is unclear.

The purpose of this dissertation is to identify any correlation between increased cell-free Hb concentrations and PT dysfunction in the context of SCD. Understanding the mechanism of PT dysfunction and tubular proteinuria development could help to identify early biomarkers and possible therapeutic targets before considerable progression of kidney damage occurs in patients. Additionally, preventing PT dysfunction may have significant contributions in maintaining patient vitamin D levels, which could further improve patient outcomes as vitamin D is shown to negatively regulate inflammation. *I hypothesized that increased Hb levels inhibit PT protein uptake to cause tubular proteinuria. Along with inhibition of DBP uptake, I hypothesized that PT*

cell toxicity from increased Hb exposure prevents proper vitamin D metabolism and signaling to contribute to vitamin D deficiency. I tested my hypotheses in the following specific aims:

1. Characterize the inhibitory role of Hb on protein endocytosis by PT cells.
2. Define the effects of Hb exposure on the metabolism of vitamin D in PT cells.
3. Characterize the effects of decreased vitamin D levels on endocytosis in the PT.

2.0 Materials And Methods

2.1 Cell Culture

All cell culture reagents were from Sigma unless otherwise specified. Opossum kidney (OK) cells (*Didelphis virginiana*, adult female, kidney cortex) were cultured in DMEM/F12 medium with either 10% (all experiments in chapter 3 and uptake experiments in chapter 4) or 5% (non-uptake experiments in chapter 4 and all experiments in chapter 5) FBS (Atlanta Biologicals) and 5 mM GlutaMAX (GIBCO). HK-2 cells (*Homo sapiens*, adult male, cortex/proximal tubules, papilloma immortalized) were cultured in DMEM/F12 with 5 µg/ml insulin, 0.02 µg/ml dexamethasone, 0.01 µg/ml selenium, 5 µg/ml transferrin, 2 mM L-glutamine, and 10% FBS (Atlanta Biologicals). LLC-PK1 cells (*Sus scrofa*, male, kidney epithelium) were cultured in DMEM/F12 medium with 10% FBS (Atlanta Biologicals) and 5 mM GlutaMAX (GIBCO).

2.2 Quantitation and Imaging of Endocytosis

2.2.1 Measurement of a single fluorescently-tagged protein uptake in the presence of unlabeled protein competition

In experiments measuring the uptake of a single protein HK-2 (5×10^5), LLC-PK1 (5×10^5), or OK (4×10^5) cells were plated in duplicate to triplicate samples on 12-mm Transwell (0.4 µm pore) polycarbonate membrane inserts (Corning) in a 12-well plate, with 0.5 ml apical and 1.5

ml basolateral culture medium. The following day, cells were transferred to an orbital shaker set at 74–146 rpm in the incubator and allowed to grow for an additional 3-4 days with daily medium changes. Studies in our lab demonstrate that chronic exposure to orbital shear stress enhances cell differentiation and endocytic capacity [150].

For experiments measuring albumin uptake, cells were incubated with apically added 0.6 µM Alexa Fluor 647-BSA (Thermo Fisher Scientific) and unlabeled Hb or L-NAME (30 min pretreatment) as indicated in DMEM/F12 medium with 25 mM HEPES (GIBCO) for 1 h at 37°C under continuous orbital rotation. For endocytosis studies in Fig. 9B, oxyHb and Hpt (Athens Research and Technology) were added to cells as indicated 30 min prior to addition of albumin. In experiments measuring uptake of Hb uptake, cells were incubated with 2 µM Alexa Fluor 568-conjugated Hb for 1 h at 37°C under orbital shear stress in the presence of unlabeled albumin or oxyHb as specified.

Purified DBP (GC-Globulin; Athens Research & Technology) and RBP (RBP4; Athens Research & Technology) were labeled with Alexa Fluor-647 using the Protein Labeling Kit (Invitrogen) according to the manufacturer's instructions. Cells were incubated with DBP (25nM in OK cells; 500nM in LLC-PK1 cells) or RBP (100nM in OK cells; 500nM in LLC-PK1 cells) for 1 h at 37°C under orbital shear stress alone or in the presence of unlabeled oxyHb as specified.

To quantify the uptake of fluorescent ligands, filters were washed 3-5 times with cold PBS containing Ca^{2+} and Mg^{2+}, solubilized in 300 µl 20 mM MOPS, pH 7.4/0.1% Triton X-100 for 30 min shaking at 4°C, and fluorescence was quantified using the GloMax Multi-Detection System (Promega). Cells on filters used for imaging were washed, fixed in 4% paraformaldehyde, and imaged using a Leica TCS SP5 confocal microscope. Maximum projections of confocal stacks were created in FIJI.

2.2.2 Measurement of two fluorescently-tagged proteins differential uptake

In experiments measuring the dual uptake of two fluorescently-tagged proteins OK (6×10^4) cells were plated in sextuplicate samples on a glass-bottomed, black-welled 96 well plate (PerkinElmer) with 200ul medium. Cells were cultured for two days with daily medium changes. Cells were then incubated with apically added 0.6 µM Alexa Fluor 647-BSA or 25nM Alexa Fluor 647-DBP and Alexa Fluor 488-conjugated Hb in a range of concentrations (0.6 – 20 µM) as indicated in 50uL DMEM/F12 medium with 25 mM HEPES for 2 h at 37°C.

To quantify the uptake of fluorescent ligands, filters were washed five times with cold PBS containing Ca^{2+} and Mg^{2+}, solubilized in 150 µl 20 mM MOPS, pH 7.4/0.1% Triton X-100 for 30 min shaking at 4°C, and fluorescence of each protein was quantified sequentially using the GloMax Multi-Detection System (Promega).

2.2.3 Measurement of protein uptake after changes in $1,25(OH)_2D$ exposure

LLC-PK1 (5×10^5) or OK (4×10^5) cells were plated in triplicate samples on 12-mm Transwell (0.4 µm pore) polycarbonate membrane inserts (Corning) in a 12-well plate, with 0.5 ml apical medium and 1.5 ml basolateral medium. The following day, cells were transferred to an orbital shaker set at 146 rpm in the incubator and allowed to grow for an additional 3-4 days with daily medium changes. On the final culture day, cells were incubated in serum-free medium with or without $1,25(OH)_2D$ (Tocris) present. After 24 h of $1,25(OH)_2D$ exposure, cells were incubated with fluorescently-labeled proteins and protein uptake was quantified as described above in section 2.2.1.

2.3 Hemoglobin Preparation and Quantitation

Hemoglobin A (HbA) was isolated from expired RBC units as described [151, 152]. Sickle hemoglobin (HbS) was obtained from Sigma. Hb concentration and oxidation state was determined by spectral deconvolution using HbA standard spectra for met, oxy, and deoxy species as previously reported [151, 152]. Hb concentrations were calculated per mole of heme. Hb was conjugated to Alexa Fluor 568 or Alexa Fluor 488 using the Protein Labeling Kits (Thermo Fisher Scientific) according to the manufacturer's instructions.

2.4 Sequence and Structure Analysis

Sequences of human Hbα, Hbβ, and albumin were retrieved from UniProt (Hb α P69905, Hb β P68871, Albumin P02768). We compared the solvent accessible surfaces of the Hb dimer in the absence and in the presence of Hpt as observed in the Hpt-Hb complex (PDB: 4F4O) [153]. The sequences for the individual helices that form the main interactions with Hpt (Hb α helices G and H, and Hb β helices G and H) were aligned against the sequence of human albumin using the BLAST and CLUSTAL W software [154, 155]. The sequences identified in human albumin were compared with the available structure of human albumin (PDB: 3SQJ) [156] to evaluate secondary structure conservation. Protein structures and electrostatic surface potentials were generated with PyMOL Molecular Graphics System (2002) (DeLano Scientific, San Carlos, CA).

2.5 Aconitase Activity

LLC-PK1 (2×10^6), or OK (1.6×10^6) cells were plated in singlet to duplicate samples on 24-mm Transwell (0.4 µm pore) polycarbonate membrane inserts (Corning) in a 6-well plate, with 1.5 ml apical and 2.5 ml basolateral medium. The following day, cells were transferred to an orbital shaker set at 146 rpm in the incubator and allowed to grow for an additional 3-4 days with daily medium changes. During this time cells were exposed to Hb (oxyHb or metHb) at concentrations and time periods as indicated.

Cells were washed twice with ice-cold PBS, scraped off filters, and pelleted. Cell pellets were then lysed in 150 µL assay buffer by passage through a 22-gage needle 10 times. Aconitase was collected by sequential centrifugation at 3,000 rpm (2 × 10 min) and 12,000 rpm (1 × 10 min) and collection of supernatant. Aconitase activity was measured using the Aconitase Activity Colorimetric Assay Kit (BioVision) according to the manufacturer's instructions. Aconitase activity was normalized to total protein within each sample.

2.6 Quantitative PCR (qPCR) Analysis

OK (4×10^5) cells or LLC-PK1 (5×10^5) cells cultured as above (section 2.2.1) in the presence of Hb (oxyHb or metHb) or $1,25(OH)_2D$ at concentrations and time periods as indicated. Cells were collected using Accutase (Sigma) and RNA was extracted using the Ambion PureLink RNA mini kit (ThermoFisher) according to the manufacturer's protocol. LLC-PK1 cell total RNA was treated with RQ1 Rnase-Free Dnase (Promega) according to the manufacturer's protocol.

cDNA was synthesized from 1 µg total RNA using Reverse Transcriptase, High Capacity cDNA Kit (Life Technologies).

Gene expression was measured by qPCR using the iTaq Universal SYBR Green Supermix 500 (Bio-Rad) on a CFX ConnectTM Real-Time PCR Detection System (Bio-Rad). Gene primers used in experiments are listed below in Table 1. The expression of each gene was normalized to *ACTB* expression and relative fold change (RFC) was calculated using the equation $FC = 2^{\delta\delta Cq}$, where $\delta\delta Cq = treatment\ \delta Cq - control\ \delta Cq$ and $\delta Cq = target\ gene\ Cq - ACTN\ Cq$.

Table 1. qPCR primers used in experiments.

Cell line	Gene	Forward primer (5'→3')	Reverse primer (5'→3')
OK	*CUBN*	AAGAAGGAAAGGTCCTGCATGT	GTTCAGGAGGGTGACTAGAGC
	LRP2	AGGCTCCCTTCTGCCATCTCTTC	GCAGAATCTGGTCCAAAACCTGACAC
	CYP24A1	CCCCAGTGGAGCTTCACAAA	TTCTTCTGCACCCGTGGATT
	CYP27B1	ACGGTCTCCAACACACTGTC	TGACGTAATCACCCACACGG
	ACTB	AGTACCCCATTGAACACGGT	GTCTCAAACATGATCTGTGTCATCT
LLC-PK1	*CUBN*	CCGGAGAGTGTGTCCAGAAC	GCCCAGGTCAAGCGGAG
	LRP2	CTGCTCTTGTAGACCTGGGTTC	TCGGCACAGGTACACTCATAAC
	CYP24A1	ATGAGAAGAGATTTGGGCTCC	GTCACAGACGCATACAATTCC
	CYP27B1	CAGTGTGGTTGGCCAGTTTC	GCCTCTGCCATTCTTCACCT
	ACTB	CCAGATCATGTTCGAGACCTTC	TCTTCATGAGGTAGTCGGTCAG

2.7 Western Blot Analysis

2.7.1 Heme oxygenase 1 expression

HK-2 (5×10^5) cells were cultured as above (section 2.2.1) in the presence of 50 µM OxyHb for the indicated periods, then washed, solubilized, and equivalent amounts of total protein were separated by SDS-PAGE on 4–15% Criterion TGX gels (Bio-Rad). Samples were blotted

using rabbit polyclonal anti HO-1 antibody (1:1,500; Abcam ab137749) and mouse monoclonal β-actin antibody (1:5,000; Sigma A1978).

2.7.2 CYP24A1 and CYP27B1 expression

OK (4×10^5) cells were cultured as above (section 2.2.1) for 24 h or 72 h in the presence of Hb (oxyHb or metHb) at the indicated concentration and time periods. Cells were then washed, solubilized, and lysates were normalized by total protein. Equivalent amounts of total protein were separated by SDS-PAGE on 4–15% Criterion TGX Stain-Free™ gels (Bio-Rad). Samples were blotted using rabbit polyclonal anti CYP24A1 antibody (1:1,000; LifeSpan BioSciences, Inc. LS-C407760) and rabbit polyclonal anti CYP27B1 antibody (1:700; LifeSpan BioSciences, Inc. LS-C407761).

2.7.3 Megalin and cubilin expression

OK (4×10^5) cells or LLC-PK1 (5×10^5) cells were cultured as above (section 2.2.3). Cells were then washed, solubilized, and lysates were normalized by total protein. Equivalent amounts of total protein were separated by SDS-PAGE on 3–8% Criterion XT Tris-Acetate gels (Bio-Rad). Samples were blotted using rabbit polyclonal anti-megalin antibody (1:5,000; MC-220, gift from Dan Biemesderfer). OK cells were blotted using rabbit polyclonal anti-cubilin antibody (1:1,000; designed against opossum epitope in collaboration with Lampire Biological Products). LLC-PK1 cells were blotted using rabbit polyclonal anti-cubilin antibody (1:1,000; Biorbyt orb4997).

2.8 Statistical Analysis and Graphical Representation

Statistical analysis was completed using StataSE 15 (StataCorp. 2017. *Stata Statistical Software: Release 15*. College Station, TX: StataCorp LLC). Experiment-to-experiment variability was assessed as a possible confounder in all experiments. If this variability was significant, it was factored in as a covariate when determining significance of experimental conditions via ANCOVA analysis followed by pairwise comparison. Additionally, in these experiments graphed data were normalized by dividing each data point by its experimental mean to allow a clearer view of data trends. All graphics were generated using GraphPad Prism version 7.03 (GraphPad Software, La Jolla California USA).

3.0 Hemoglobin Inhibits Albumin Uptake by Proximal Tubule Cells: Implications for Sickle Cell Disease

Reprinted with minor edits from American Journal of Physiology – Cell Physiology, vol. 312 (6), Megan L. Eshbach, Amandeep Kaur, Youssef Rbaibi, Jesús Tejero, and Ora A. Weisz, Hemoglobin inhibits albumin uptake by proximal tubule cells: implications for sickle cell disease, C733-C740, Copyright (2017), with permission from American Physiological Society.

3.1 Introduction

SCD is a devastating disease resulting from a single mutation (Glu7Val) in Hb that causes RBCs to assume a rigid curved shape that blocks their passage through the vasculature. Obstruction of capillaries by sickled RBCs results in ischemia, severe pain, and necrosis. Additionally, RBCs in SCD patients are susceptible to hemolysis, resulting in chronically elevated plasma levels of free Hb that can skyrocket during hemolytic crises [30]. Free Hb in the circulation can scavenge NO produced by endothelial cells, leading to vasoconstriction that compounds vaso-occlusion [157]. Exposure of cells to heme proteins also triggers the production of cytotoxic ROS [157].

With the development of treatment regimens to increase life expectancy, kidney manifestations of SCD have become increasingly appreciated. There are numerous renal complications in SCD, including glomerulopathy, acute kidney injury, CKD, impaired urinary concentrating ability, and distal nephron dysfunction. Kidney disease currently accounts for >15% of mortality in SCD patients [6]. These complications are due in part to the propensity of RBCs to

sickle in the hypoxic renal medulla. However, exposure of kidney cells to Hb liberated during hemolysis also plays an important role in the progression of renal disease. Released Hb dimers (consisting of α- and β-globin chains, each with molecular mass ~16 kDa) are readily filtered into the tubule lumen with a fractional filtration coefficient of 0.03 [59]. At the normal plasma level of Hb of 3 mg/dl (2 μM), the concentration in the glomerular ultrafiltrate entering the kidney tubule lumen is very low, ~60 nM. However, plasma concentrations of Hb are chronically about tenfold higher in SCD patients, and during hemolytic crisis, the concentration of plasma Hb can approach 1 g/dl, resulting in tubular concentrations above 15 μM [158].

Filtered Hb is taken up by the multiligand receptors megalin and cubilin, which are abundantly expressed in the S1 segment of the kidney PT [96]. Previous studies show that Hb binds to megalin and cubilin with relatively high affinity (1.7 μM and 4.1 μM, respectively [60]). Megalin and cubilin also bind with comparable affinities to a large number of other filtered low-molecular-weight (LMW) proteins and other ligands, including DBP, intrinsic factor-cobalamine (vitamin B12), and parathyroid hormone [159]. In addition, megalin and cubilin take up the low level of albumin that normally escapes the glomerular filtration barrier. Disruption of the apical endocytic pathway leads to tubular proteinuria, that if left unchecked can trigger inflammation and fibrosis resulting in end-stage renal disease [13].

The PT is known to be especially sensitive to heme toxicity, and cytoprotective responses (upregulated expression of ferritin, ferroportin, heme oxygenase-I, heme oxygenase-II, Hpt, and hemopexin) have been well characterized in response to heme-induced injury [56, 57]. Consistent with this, tubular proteinuria has been reported in a significant fraction of SCD patients, and particularly in younger patients [10-12]. These patients also exhibit increased excretion of urinary biomarkers characteristic of tubular injury [160]. Tubular proteinuria in these patients frequently

occurred independently of glomerular dysfunction, suggesting that PT injury is an initiating step in the cascade leading to CKD in SCD patients.

PT function, including the uptake of filtered megalin/cubilin ligands, is highly responsive to changes in fluid shear stress that accompany tubular flow [161, 162]. Because NO mediates mechanosensitive responses in endothelial cells, we wondered whether Hb released into the tubule lumen during hemolytic crises might scavenge NO to impair apical endocytosis. To test this, we assessed whether exposing PT cells to levels of Hb expected during SCD crisis affects uptake of albumin. We found that Hb inhibits albumin uptake by PT cells in a dose-dependent manner. Surprisingly, the effect of Hb is independent of any effect on NO and instead results from direct competition for uptake by megalin/cubilin receptors. Impaired uptake of normally filtered megalin/cubilin ligands uptake during hemolytic crisis may explain clinical manifestations of SCD of unknown etiology.

3.2 Results

3.2.1 Hemoglobin inhibits receptor-mediated albumin uptake by proximal tubule cells.

To test whether the NO scavenging by Hb affects PT endocytosis, we incubated polarized OK cells for 1 h with apically added 0.6 μM Alexa Fluor 647-albumin in the presence or absence of 50 μM OxyHb, MetHb, or CNMetHb. These three forms of Hb have different NO scavenging potential, with OxyHb being significantly more potent [163]. As an additional control, we also pretreated cells for 30 min with the NOS inhibitor L-NAME (L-NG-nitroarginine methyl ester, 100 μM) before adding fluorescent albumin. Cells were then washed extensively, and cell-

associated albumin was visualized in fixed cells by confocal microscopy (Fig. 5A) or quantified by spectrofluorimetry (Fig. 5B). As we previously demonstrated, Alexa Fluor 647-albumin readily accumulated in intracellular vesicular compartments in OK cells [161]. Addition of any of the three forms of Hb during the albumin incubation profoundly inhibited the uptake of albumin by PT cells. In contrast, L-NAME had no apparent effect on albumin uptake. Quantitation of albumin uptake by spectrofluorimetry in multiple experiments confirmed these qualitative observations (Fig. 5B). OxyHb also inhibited albumin uptake in human proximal tubule HK-2 cells, which also express megalin/cubilin but have a markedly lower endocytic capacity than OK cells (Fig. 5C).

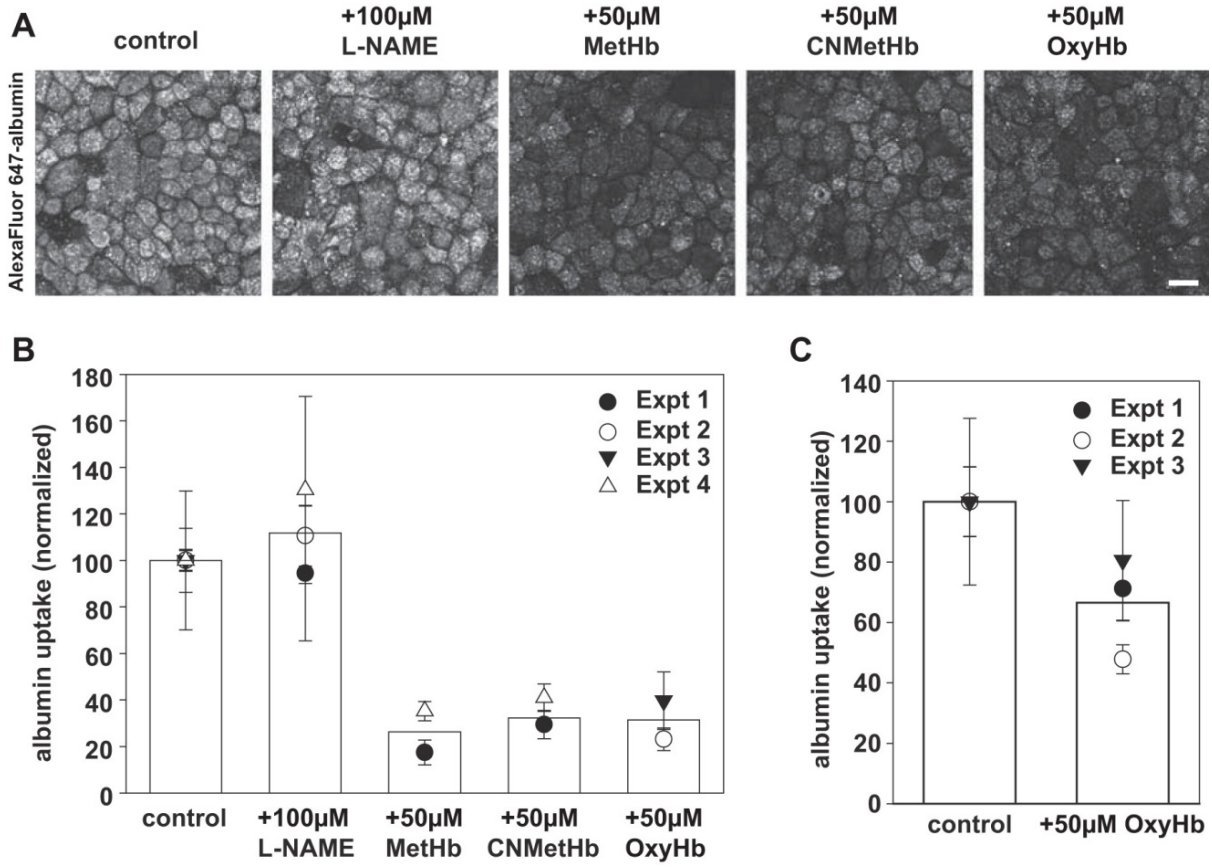

Figure 5. Hemoglobin inhibits apical uptake of albumin by proximal tubule cells.

A: filter-grown OK cells were preincubated for 30 min at 37°C with L-NAME (100 μM) where indicated and then exposed to 0.6 μM apically added Alexa Fluor 647-albumin in the presence or absence of 50 μM MetHb, CNMet-Hb, or OxyHb for 1 h at 37°C. After extensive washing, cells were fixed and processed for immunofluorescence to visualize cell-associated albumin. Representative fields are shown. Scale bar, 25 μm. B: cells incubated as above were

solubilized, and cell-associated albumin was quantified by spectrofluorimetry. Mean albumin uptake in control cells was set at 100 to facilitate comparison between experiments. The results from several independent experiments (means ± SD of triplicate samples) are plotted, with each experiment represented by a different symbol. The mean uptake for a given condition is represented by the bar. C: filter-grown human HK-2 cells were incubated for 1 h at 37°C with 0.6 μM Alexa Fluor 647-albumin in the presence or absence of 50 μM OxyHb. Cell-associated albumin was quantified as above, and the mean ± SD of three independent experiments each performed in triplicate is plotted.

The insensitivity of albumin uptake to L-NAME and the equivalently robust inhibition we observed using Hb forms with different NO scavenging capabilities suggest that the effect of Hb on albumin uptake is independent of NO and independent of the heme reduction state. We hypothesized that Hb may be directly competing with albumin for binding to megalin/cubilin. Hb has been demonstrated using surface plasmon-reference analysis to bind to megalin and cubilin with affinities of 1.7 μM and 4.1 μM, respectively [60]. In comparison, albumin binds to OK apical membranes with a K_d of 0.3 μM [164].

Normalized data from multiple experiments demonstrated a dose-dependent effect of OxyHb on albumin uptake with an estimated half-maximal inhibitory concentration of ~5 μM (Fig. 6). OxyHbS containing the SCD-causing mutation Glu7Val inhibited with a similar dose response. However, we still observed ~15% residual albumin uptake even when high concentrations of OxyHb (up to 250 μM) were added.

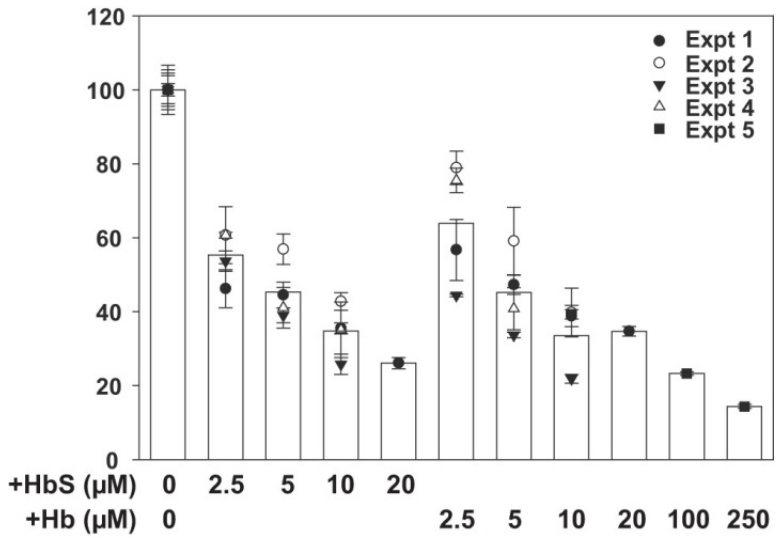

Figure 6. Dose response of hemoglobin and sickle cell hemoglobin S inhibition of albumin uptake.

Triplicate filters of cells were preincubated with the indicated concentration of OxyHb or OxyHbS prior to addition of Alexa Fluor 647-albumin for 1 h and quantitation of albumin uptake. Cell-associated albumin in control untreated cells was normalized to 100 to enable combining data from multiple independent experiments, each represented by a distinct symbol. Based on this dose response, the half-maximal concentration at which OxyHb inhibits uptake of albumin is ~5 μM.

Western blotting confirmed that prolonged exposure of human PT cells to Hb caused a dramatic elevation in heme oxygenase-1 as previously reported; however little if any upregulation was observed within 4 h of incubation (Fig. 7A). To confirm that the inhibitory effect of Hb on albumin endocytosis was not due to cellular toxicity, we preincubated cells with OxyHb for up to 5 days with 10–50 μM OxyHb, then washed the cells and examined the effect on endocytosis of Alexa Fluor 647-albumin in the absence of competing Hb. As shown in Fig. 7B, preincubation with Hb had no effect on albumin uptake. Consistent with our previous results above, inclusion of 10 μM OxyHb in the apical medium during the 1 h uptake period reduced albumin endocytosis by >60%. In contrast, when OxyHb was added to the basolateral medium of the Transwell filter supports, it had no effect on albumin uptake (not shown).

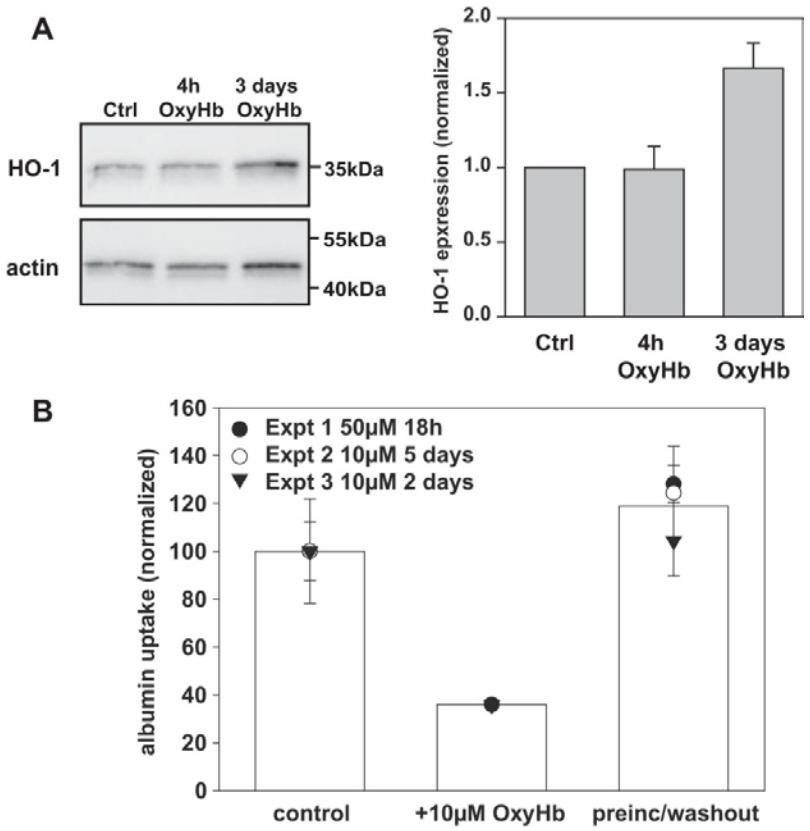

Figure 7. Hemoglobin acutely inhibits receptor-mediated endocytosis in proximal tubule cells.

A: HK-2 cells were incubated with 50 μM OxyHb for 4 h or 3 days as indicated, then solubilized and blotted to detect heme oxygenase-1 (HO-1) and β-actin (as a loading control). Quantitation of HO-1 expression (avg ± range) relative to control and normalized to β-actin in two independent experiments is shown next to the blot. B: filter-grown OK cells were preincubated at 37°C with apically added OxyHb (10–50 μM) for 18 h to 5 days as indicated prior to extensive washout and subsequent addition of Alexa Fluor 647-albumin for 1 h at 37°C in the absence of OxyHb. As a positive control, OxyHb (10 μM) was included during the albumin uptake period; untreated cells incubated with Alexa Fluor 647-albumin were used as a negative control. Fluorescent cell-associated albumin was quantified by spectrofluorimetry. Data (means ± SD) from three independent experiments each performed in triplicate are shown.

3.2.2 Albumin inhibits hemoglobin uptake by proximal tubule cells.

Hb has previously been shown to be internalized by cells in the PT via a megalin-dependent pathway [60]. In those studies, addition of BSA did not inhibit Hb binding, suggesting that albumin and Hb may interact with distinct sites on megalin/cubilin. To examine this in OK cells, we

incubated OK cells with 1 µM apically added Alexa Fluor 568-OxyHb for 1 h, then fixed and imaged the cells. As shown in Fig. 8A, Hb was internalized into vesicular compartments similar to those observed with fluorescent albumin (Fig. 5A). As expected for a receptor-mediated event, uptake was abolished by inclusion of excess unlabeled Hb during the incubation period (Fig. 8A). We also observed significant inhibition of Hb uptake upon inclusion of 30 µM albumin (Fig. 8A). To test this further, we examined the dose dependence of albumin inhibition of Hb uptake using our spectrofluorimetry assay. In these experiments we found that 50 µM unlabeled Hb inhibited the uptake of fluorescently conjugated Hb by ~75% and 30 µM albumin inhibited Hb uptake by ~50% (Fig. 8B).

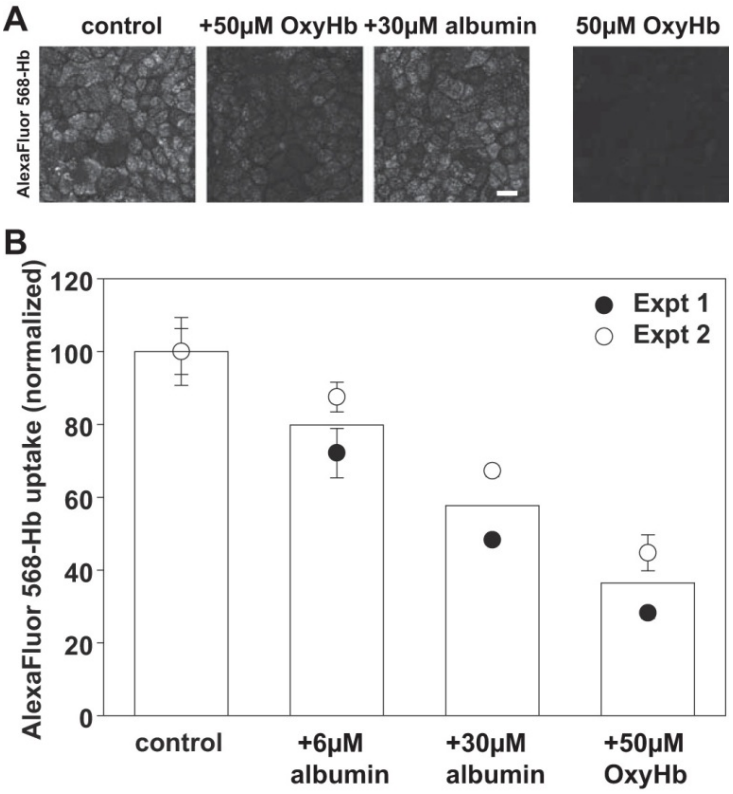

Figure 8. Albumin inhibits endocytosis of hemoglobin by OK cells.

A: OK cells were incubated with apically added 2 µM Alexa Fluor 568-Hb in the presence or absence of 50 µM unlabeled OxyHb or 30 µM albumin for 1 h at 37°C, then fixed and processed for immunofluorescence. As a control to confirm that OxyHb fluorescence is not detected in our studies, cells were incubated for 1 h with 50 µM unlabeled OxyHb (right-hand panel) Scale bar, 25 µm. B: OK cells were incubated with apically added 2 µM Alexa Fluor 568-

Hb in the presence or absence of the incubated concentrations of albumin or unlabeled Hb for 1 h at 37°C prior to quantitation of cell-associated Hb fluorescence. Data from two experiments performed in triplicate are shown. Background fluorescence in cells incubated only with 50 µM unlabeled OxyHb was <10% that of the control values.

3.2.3 Haptoglobin inhibits Hb uptake by proximal tubule cells and restores albumin endocytosis.

Hpt is a large (unfiltered) protein in serum that binds with very high affinity (estimated K_d > 10^{-12} M) to the dimer-dimer interface of Hb [153, 165, 166]. We found that 10 µM Hpt inhibited uptake of Alexa Fluor 568-OxyHb by OK cells (Fig. 9A). We used our spectrofluorimetry assay to confirm this quantitatively. However, because of the prohibitive cost of Hpt, we performed these assays with low concentrations of OxyHb (7.5 µM) and stoichiometric amounts of Hpt. As shown in Fig. 9B, addition of 7.5 µM OxyHb to OK cells inhibited the uptake of Alexa Fluor 647-albumin by ~30%. Preincubation of 7.5 µM OxyHb for 30 min with 7.5 µM Hpt restored albumin uptake to nearly control levels (Fig. 9B). Hpt also reversed the inhibitory effect of HbS on albumin uptake with comparable efficacy (not shown). Addition of 7.5 µM Hpt without Hb resulted in a minor but not statistically significant reduction in albumin uptake, suggesting that Hpt itself may weakly inhibit albumin uptake as well.

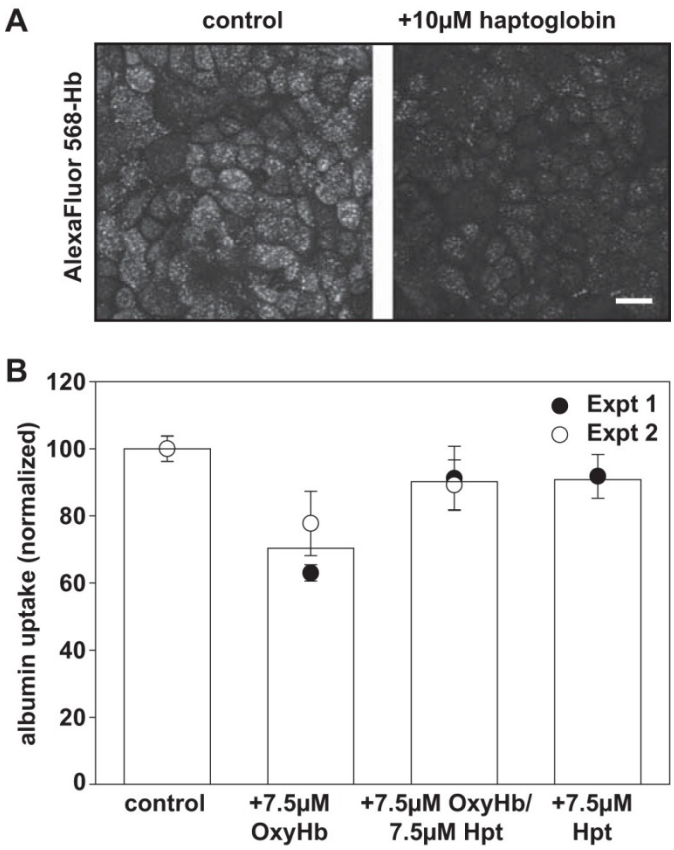

Figure 9. Haptoglobin inhibits hemoglobin uptake and restores albumin endocytosis by OK cells.

A: OK cells were incubated with 2 μM Alexa Fluor 568-OxyHb for 1 h at 37°C in the presence or absence of 10 μM haptoglobin (Hpt), then washed, fixed, and processed for immunofluorescence to visualize cell-associated Hb. Scale bar, 25 μm. B: filter-grown OK cells were incubated with 40 μg/ml Alexa Fluor 647-albumin in the presence of OxyHb (7.5 μM) and/or 7.5 μM Hpt as indicated. After extensive washing, cells were solubilized and fluorescent cell-associated albumin was quantified. Data (means ± SD) from two independent experiments each performed in triplicate are shown.

3.2.4 Modeling the hemoglobin interaction site with megalin.

As shown above, our results indicate that low concentrations of Hb (<10 μM) can impair albumin uptake. In addition, stoichiometric amounts of Hpt prevent this inhibition. The structure of the Hb-Hpt complex is known, involving two Hpt molecules and a Hb dimer [153]. Thus, it is reasonable to hypothesize that the binding site of Hb to megalin/cubilin may no longer be exposed

upon the formation of the Hb-Hpt complex. In addition, the competitive effect of albumin suggests that the binding sites used by albumin and Hb may share similar properties. Based on these premises we searched for Hb motifs that met the following conditions: 1) are solvent-exposed in the dimer Hb structure, 2) are involved in the Hb-Hpt interface, 3) share sequence and structural similarity to motifs in albumin, 4) share electrostatic surface similarities to motifs in albumin.

The interaction of Hb and Hpt covers a large (2,954 $Å^2$) surface with a number of Hb motifs involved [153]. The regions of Hb involved in the interface include the helices G and H in Hb α and the helices C, G, and H of Hb β [153]. As albumin and Hb are all-α-helical proteins, we used individual Hb α-helices as our search motif.

The Hb helical fragments involved in Hpt binding were aligned to human albumin sequence to search for comparable albumin motifs. Portions of albumin showing sequence homology to the Hb sequences were inspected for similar secondary structure. Three regions of albumin with sequence homology and similar secondary structure were identified (Fig. 10). Based on these results we conclude that helices G and H in Hb may be involved in the interaction with megalin/cubilin.

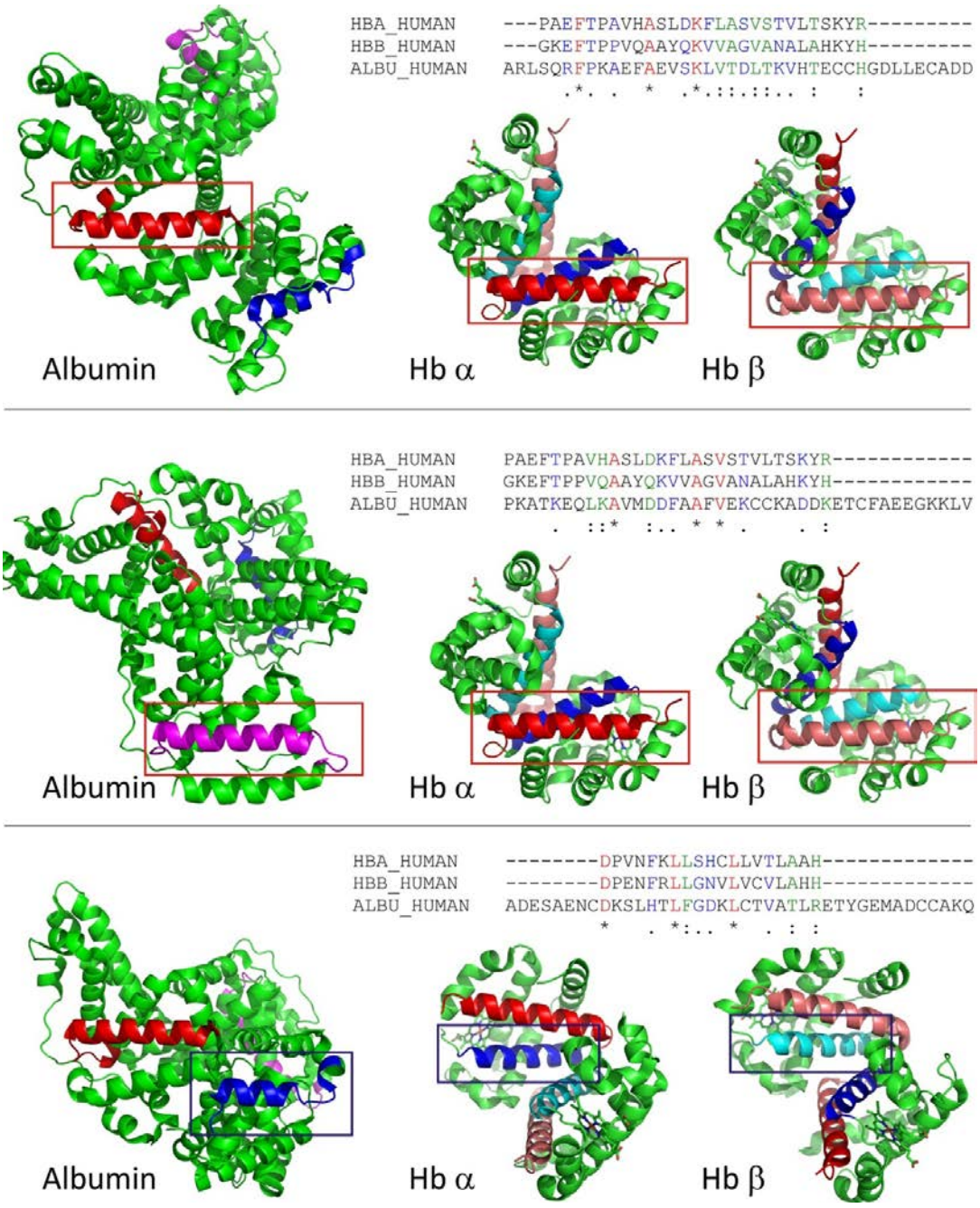

Figure 10. Sequence and structure comparison of potential megalin/cubilin binding regions in hemoglobin and albumin.

Hb helical fragments involved in Hpt binding were aligned to human albumin sequence to search for comparable albumin motifs (see materials and methods for details). Three sequences in albumin were identified that have sequence and structural similarity to Hb. Top: alignment of Hb α- and β-helix H to albumin residues 244–271. The sequence alignment is shown on top. Aligned sequences are shown in the structures of albumin and Hb αβ-dimer and indicated by a red box. Helical elements are shown in red (albumin, hemoglobin α) and salmon (hemoglobin β); Middle:

alignment of Hb α- and β-helix H to albumin residues 561–588. The sequence alignment is shown on top. Aligned sequences are shown in the structures of albumin and Hb αβ-dimer and indicated by a red box. Helical elements are shown in pink (albumin) red (hemoglobin α), and salmon (hemoglobin β) Bottom: alignment of Hb α- and β-helix G to albumin residues 87–105. The sequence alignment is shown on top. Aligned sequences are shown in the structures of albumin and Hb αβ-dimer and indicated by a blue box. Helical elements are shown in dark blue (albumin, hemoglobin α) and cyan (hemoglobin β).

3.3 Discussion

Our results demonstrate that binding of Hb to megalin/cubilin competes directly for the uptake of albumin by PT cells. We observed potent inhibition of albumin uptake by concentrations of Hb predicted to enter the tubule lumen in patients during hemolytic crisis. We hypothesize that competition for ligand binding by excess Hb in the tubule lumen, rather than cytotoxic responses to heme, are the cause of tubular proteinuria frequently observed in SCD patients. Additionally, loss of these ligands may contribute to impaired vitamin homeostasis in SCD patients.

We found that 5 μM Hb and HbS inhibited albumin uptake by ~50%; however, we were unable to fully prevent uptake even at much higher concentrations of Hb. This suggests that albumin binds to multiple sites on megalin/cubilin, only some of which are inhibited by Hb. This is likely given that these receptors contain multiple ligand binding domains to engage a broad array of filtered ligands [159]. Additionally, non-receptor-mediated mechanisms may contribute to the small amount of residual albumin uptake at high Hb concentrations.

Our data suggest that the interaction site for Hb with megalin/cubilin overlaps the Hpt binding site within the dimer-dimer interface. Based on this finding and on BLAST searches for regions of homology between albumin and Hb that map to this interface, we identified three

sequences in albumin as putative binding motifs for megalin/cubilin, due to their sequence and structure similarities with Hb domains that are involved in Hpt binding.

A surprising finding is that whereas PT cells are highly sensitive to Hb, we did not observe any apparent toxicity in OK or HK-2 cells even after prolonged exposure to OxyHb. Control studies confirmed upregulation of heme oxygenase 1 in HK-2 cells exposed to OxyHb as previously reported [167]. However, preincubation of OK cells with 50 μM OxyHb for up to 5 days did not impair subsequent albumin uptake. It is possible that other functions of our cells are compromised by exposure to Hb.

Our findings have potential implications for our understanding the pathogenesis of SCD. Hb αβ-dimers in the plasma are readily filtered into the tubule lumen in the absence of glomerular injury and reach concentrations during hemolytic crisis that would significantly impair the reabsorption of albumin and other megalin/cubilin ligands. Thus, our finding may explain why a significant fraction of young SCD patients exhibit tubular proteinuria independent of glomerular damage [10, 12]. Prolonged exposure of PT cells to Hb is likely to overwhelm protective responses and lead to tubular injury that may initiate and/or contribute to the progression of CKD/end-stage renal disease in SCD patients.

Our results suggest a possible explanation for why children with severe manifestations of SCD have abnormally low levels of 25(OH)D [17] and low bone mineral density [168]. Defective uptake of filtered ligands by megalin/cubilin in the PT is known to affect serum vitamin levels. This is especially evident in the case of vitamin D_3, which is taken up by megalin/cubilin in its inactive, insoluble form [25(OH)D] bound to DBP, converted to the active $1,25(OH)_2D$ form, and released from the basolateral surface of PT cells into the bloodstream [169]. For example, patients with Dent disease, caused by mutations in a PT hydrogen-chloride antiporter that plays a role in

apical endocytosis, have low levels of vitamin D3 and frequently develop osteomalacia and hypophosphatemic rickets [129]. Cubilin-deficient dogs also have lower serum levels of mono- and dihydroxylated vitamin D3 metabolites [128]. Although we did not test whether Hb competes for uptake of DBP, it is notable that DBP is highly homologous to albumin [170]. Our studies provide a potential mechanism to explain the early steps in the development of kidney disease and suggest the possibility that selectively targeting the interaction of Hb with megalin/cubilin may have therapeutic value beyond simply preserving PT function in SCD patients.

4.0 Hemoglobin Alters Vitamin Carrier Uptake and Mitochondrial Dynamics in Proximal Tubule Cells: Implications for Vitamin D Metabolism in Sickle Cell Disease Patients

4.1 Introduction

SCD is one of the most prevalent monogenic disorders and is caused by autosomal recessive inheritance of pathogenic mutations in the β-globin subunit of Hb. These mutations increase Hb polymerization in RBCs, forcing them into a sickled shape, and lead to increased vascular blockage and hemolytic crisis in SCD patients [38]. In recent years, therapeutic advances have significantly extended SCD patient lifespan, causing a rise in the prevalence of severe comorbidities, including SCN. SCN currently accounts for up to 18% of SCD patient mortality and is thought to arise in consequence of both recurring hemolytic crisis in the hypoxic renal medulla and increased exposure to cell-free Hb released in RBC hemolysis [6].

Compared to healthy individuals, SCD patients chronically have approximately 10 times higher concentrations of circulating cell-free Hb, and serum concentrations can reach up to 1 g/dl (620 μM) during times of hemolytic crisis [158]. Hb circulates primarily as dimers (~32 kDa), which can escape the glomerular barrier and enter the PT lumen. Reabsorption of filtered proteins by PT epithelial cells is accomplished through apical endocytosis mediated by megalin and cubilin receptors [96]. Megalin and cubilin each possess multiple interaction sites that enable the binding and internalization of numerous filtered proteins, including Hb [60, 159]. Incomplete reabsorption can cause tubular proteinuria, defined as urinary loss of proteins normally reabsorbed by the PT. Importantly, many young SCD patients develop tubular proteinuria [10-12], suggesting that PT dysfunction occurs early in the progression of kidney disease.

Prolonged PT dysfunction and tubular proteinuria have been linked to kidney inflammation and fibrosis, which can eventually lead to glomerular dysfunction, frank proteinuria, and renal failure [13, 14]. Additionally, PT dysfunction can prevent normal uptake of vitamin carrier proteins that bind to megalin and cubilin, including DBP and RBP, and failure to reclaim these carrier proteins can lead to vitamin deficiencies [129, 159, 171, 172]. This is particularly true for vitamin D, as the PT is the primary site for vitamin D reclamation and activation [16]. There is a high prevalence of vitamin D deficiency in SCD patients [17, 18], although the contribution of PT dysfunction is unknown.

We previously reported that excess Hb can inhibit albumin endocytic uptake by PT cells [173]. Because albumin and DBP have similar secondary structures, we hypothesized that Hb may also inhibit DBP uptake by PT cells. Additionally, Hb-induced cytotoxicity in PT cells could affect vitamin D metabolism, as oxidative stress has been linked to altered PT vitamin D hydroxylase expression and activity [174-176]. Reduced DBP uptake and impaired vitamin D metabolism in the PT could play a significant role in the development of vitamin D deficiency in SCD patients. Thus, we set out to assess how exposure to cell-free Hb affects the uptake of vitamin carriers DBP and RBP, and vitamin D hydroxylase expression in PT cells. We found that Hb significantly inhibits DBP uptake, similarly to what we reported for albumin. However, uptake of RBP was considerably less sensitive to Hb, suggesting that Hb binding competition is selective for a subset of megalin/cubilin ligands. Additionally, we observed that prolonged exposure to Hb led to increased oxidative stress at the mitochondrial level in PT cells and to discordant changes in *CYP27B1* mRNA and protein levels. Together, our data suggests that increased cell-free Hb levels in SCD patients may impair vitamin D reclamation and activation by PT cells, which could contribute to vitamin D deficiency commonly observed in patients.

4.2 Results

4.2.1 Hemoglobin inhibits DBP uptake similarly to previously reported inhibition of albumin uptake in proximal tubule cells

To assess any inhibitory effect of Hb on DBP uptake, we incubated polarized, filter-grown OK cells with 25 nM Alexa Fluor 647-labeled DBP (comparable to the estimated tubular concentration) in the presence or absence of unlabeled oxyHb at concentrations estimated to enter the kidney tubule lumen chronically (0.6 μM) or during hemolytic crisis (≤20 μM) in SCD patients. Cells were incubated under these conditions for 1 h to allow for significant endocytic uptake, washed extensively, solubilized, and cell-associated DBP was quantified by spectrofluorimetry. DBP uptake was significantly inhibited in a dose dependent manner by all concentrations of Hb tested (Fig. 11A). Half-maximal inhibition of DBP was observed at ~0.8 μM Hb, close to the estimated chronic tubular concentration in SCD. At the highest Hb concentration tested (20 μM) DBP uptake was inhibited by 87% (Fig. 11A). OxyHb also significantly inhibited DBP uptake in a porcine PT cell line (LLC-PK1) that expresses megalin and cubilin receptors but has substantially lower endocytic capacity in comparison to OK cells (Fig. 11B).

To further elucidate whether reduced DBP uptake is due to competitive inhibition by Hb, we differentially labeled Hb with Alexa Fluor 488 and measured DBP and Hb uptake simultaneously in PT cells. These dual fluorescence assays were scaled down to a 96-well plate format to enable incubation with high concentrations of Alexa Fluor 488-Hb. After incubation with fluorescently-labeled proteins for 2 h, cells were solubilized, and cell-associated fluorescence quantified. In agreement with our hypothesis, DBP uptake decreased while Hb uptake increased

with increasing concentrations of Hb (Fig. 11C). Of note, the estimated half-maximal inhibition of DBP in these experiments (~0.9 µM Hb) is similar to that observed in cells grown on filters.

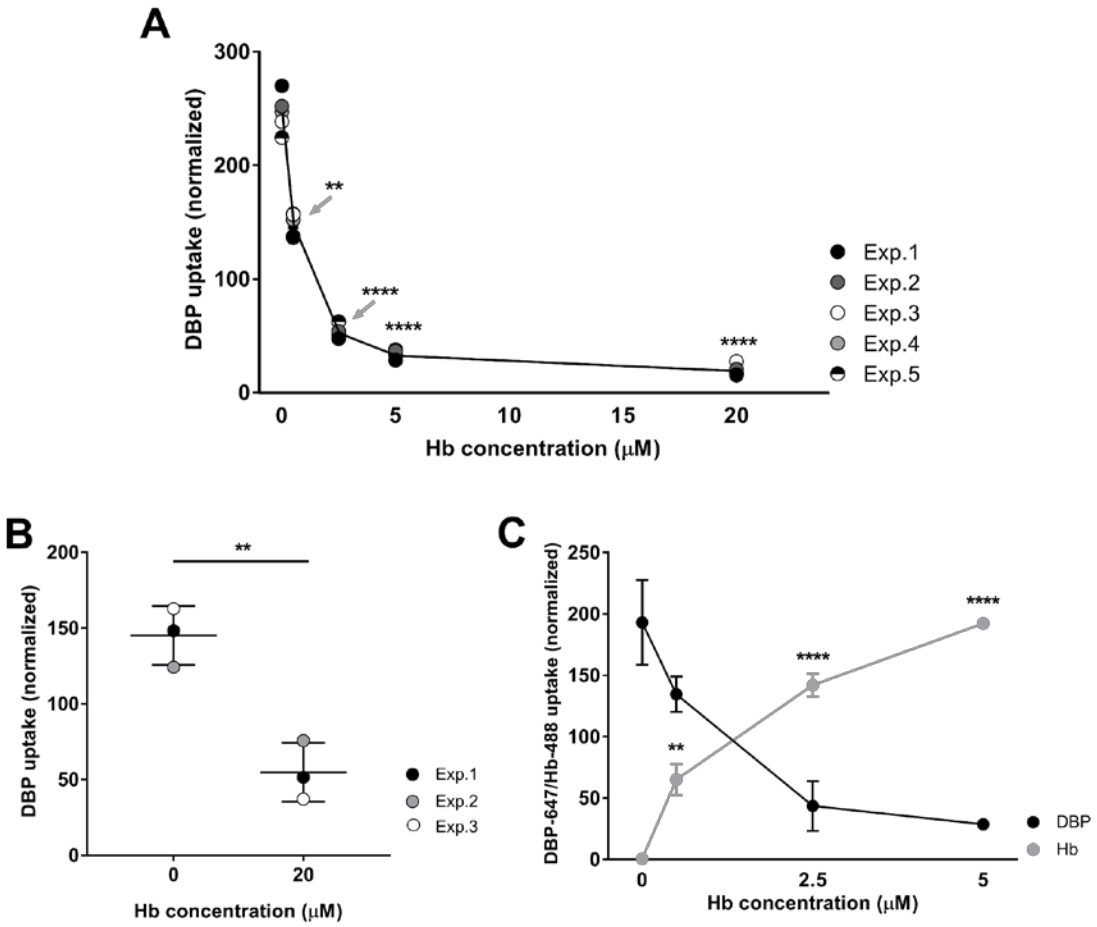

Figure 11. Hb inhibits DBP uptake in proximal tubule cells via direct competition.

A: Filter-grown OK cells were incubated with 25 nM apically-added Alexa Fluor 647-DBP in the presence of a range of oxyHb concentrations (0-20 µM) for 1 h at 37°C. Cells were then solubilized, and cell-associated DBP was quantified by spectrofluorimetry. Data from five experiments done in duplicate are plotted, with each experiment represented by a different symbol. B: Filter-grown LLC-PK1 cells were incubated with 0.5 µM Alexa Fluor 647-DBP in the presence or absence of 20 µM oxyHb and cell-associated DBP was quantified as in (A). Data from three experiments (mean ± SD and individual points) performed in duplicate were plotted. C: OK cells grown in a 96-well plate were incubated with 25 nM Alexa Fluor 647-DBP and a range of Alexa Fluor-488 Hb concentrations (0-20 µM) for 2 h at 37°C. Cell-associated DBP and Hb fluorescence were quantified by spectrofluorimetry. Data (mean ± SD) from four experiments performed in sextuplicate are shown. Graphed uptake values were normalized by dividing each point by their respective experimental mean. **p≤0.01, ****p≤0.0001 by one-way ANCOVA Dunnett's multiple comparisons (A), two sample t-test (B), or two-way ANOVA Dunnett's multiple comparisons (C).

Because DBP and albumin are comparable in size and secondary structure, we posited that Hb would compete for PT cell uptake with both proteins similarly. To test this, we measured uptake of 0.6 μM Alexa Fluor 647-albumin and Alexa Fluor 488-Hb in the same manner as described above. As expected, Hb inhibits albumin uptake in a very similar dose-dependent manner to DBP (Appendix B Fig. 20). Interestingly, the estimated half-maximal inhibition of albumin (~0.6 μM Hb) was similar to that observed for DBP (~0.8-0.9 μM Hb). We also observed equivalent PT cell Hb uptake after incubation with albumin and DBP (Fig. 11C and Appendix B Fig. 20, gray line). Together, these data suggest that Hb similarly competes with predicted tubular concentrations of albumin and DBP.

4.2.2 Hemoglobin marginally inhibits RBP uptake by proximal tubule cells.

Because we found Hb similarly inhibits uptake of albumin and DBP, we hypothesized Hb binding inhibition may be selective for proteins highly alpha helical in structure. To test this, we measured the uptake of RBP, a smaller filtrate protein (~21 kDa) comprised primarily of β-sheets, in the presence or absence of oxyHb at the same concentrations as above. While oxyHb significantly inhibited uptake of 0.1 μM Alexa Fluor 647-RBP in both OK cells and LLC-PK1 cells (Fig. 12), the effect size of this inhibition was smaller in comparison to observed albumin and DBP inhibition. In OK cells, RBP uptake was inhibited by 27% at the highest Hb concentration tested (20 μM) (Fig. 12A), which is much less than the observed ~87-93% inhibition of albumin/DBP uptake. This suggests that Hb does not compete with RBP for receptor binding in the same manner it does with albumin and DBP. However, it is important to note that Hb inhibition of RBP, albeit marginal, was present in PT cells.

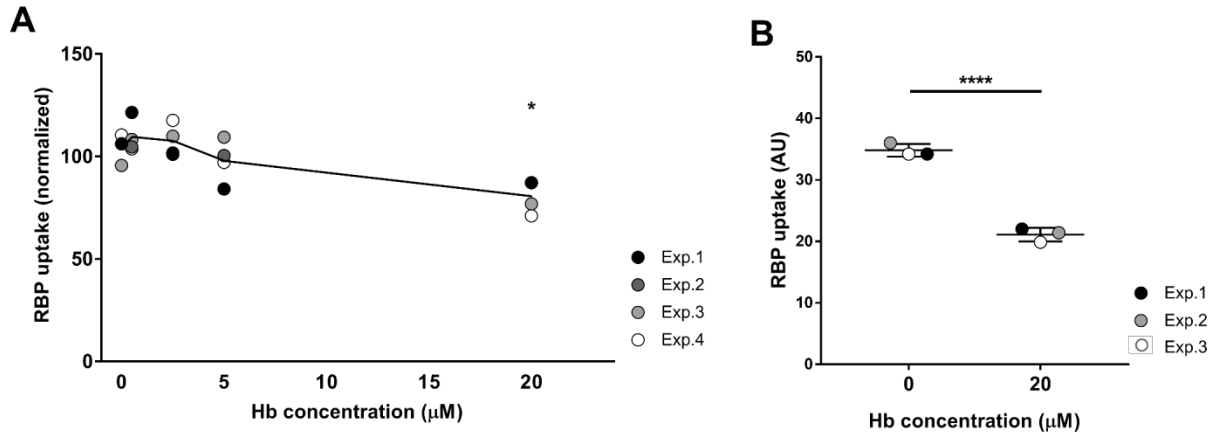

Figure 12. Hb inhibits RBP uptake by proximal tubule cells.

A: Filter-grown OK cells were incubated with 0.1 μM apically-added Alexa Fluor 647-RBP in the presence of a range of Hb concentrations (0-20 μM) and cell-associated RBP was quantified as above. Data from four experiments done in duplicate are plotted, with each experiment represented by a different symbol. Graphed uptake values were normalized by dividing each point by their respective experimental mean. B: Filter-grown LLC-PK1 cells were incubated with 0.5 μM RBP in the presence or absence of 20 μM Hb and cell-associated RBP was quantified. Data (mean ± SD and individual points) from three experiments performed in duplicate are plotted. *$p \leq 0.05$, ****$p \leq 0.0001$ by one-way ANCOVA Dunnett's multiple comparisons (A) or two sample t-test (B).

4.2.3 Chronic exposure to hemoglobin increases mitochondrial oxidative stress in proximal tubule cells and alters vitamin D hydroxylase expression

After observing that Hb outcompetes DBP for PT cell uptake we began to consider the effects of increased concentrations of Hb entering PT cells. Hb exposure can lead to increased oxidative stress through increased ROS production and lipid peroxidation [36]. These same forms of oxidative stress have been shown to altered hydroxylase expression and activity [175, 176], suggesting Hb-induced oxidative stress could limit vitamin D metabolism in the PT through manipulation of vitamin D hydroxylases CYP27B1 and CYP24A1. As vitamin D hydroxylases are localized within the mitochondria of PT cells, we first set out to assess oxidative stress at the

mitochondrial level in our culture model. To do this, we measured the enzymatic activity of aconitase, an enzyme in the citric acid cycle that converts citrate to isocitrate and is localized primarily to mitochondria. Oxidation of the iron cluster within aconitase's active site results in ablation of the enzyme's catalytic activity. As a result, reduced aconitase activity is a sensitive indicator of mitochondrial-specific oxidative stress [177]. Filter-grown PT cells were incubated in the presence or absence of Hb (oxyHb and metHb) at different concentrations for 24-72 h. Cells were then washed, lysed, and equal volumes of lysate were incubated with substrate (citrate) for 1 h. Aconitase activity was then quantified by colorimetric development of produced isocitrate and normalized to sample total protein. Exposure to metHb alone led to a significant decrease in aconitase activity in OK cells, suggesting increased oxidative stress (Fig. 13). Although metHb is reportedly more toxic [32, 36], it was surprising that chronic oxyHb exposure did not also affect mitochondrial oxidative stress. LLC-PK1 cells exhibited similar trends in oxidative stress to OK cells (Appendix B Fig. 21), but to a lesser magnitude. This is likely due to reduce Hb endocytic uptake.

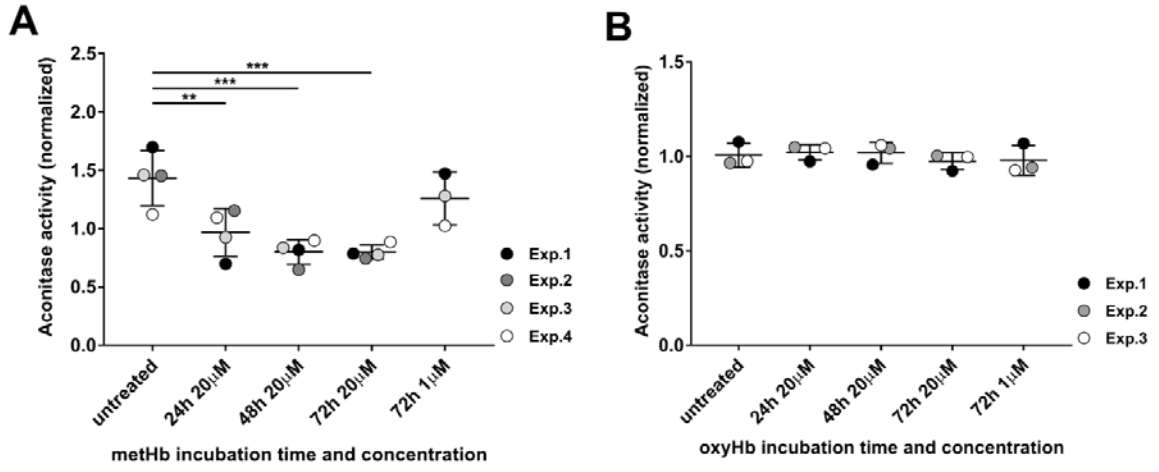

Figure 13. Chronic metHb, but not oxyHb, exposure decreases aconitase activity in proximal tubule cells.

Filter-grown OK cells were incubated with metHb (A) or oxyHb (B) for 24-72 h at the concentrations indicated. Cells were then washed, lysed, and equal lysate volumes were incubated with aconitase substrate for 1 h. Colorimetric

measurement of isocitrate production was used to quantify sample aconitase activity and normalized to total protein. Data (mean ± SD and individual points) from 3-4 experiments are plotted. Graphed values were normalized by dividing each point by their respective experimental mean. **$p \leq 0.01$, ***$p \leq 0.001$ by one-way ANCOVA Dunnett's multiple comparisons.

After confirming increased oxidative stress in our PT cell culture model, we next set out to measure any effects this had on vitamin D hydroxylase expression. To do so, we treated filter-grown OK cells chronically (72 h) with either high or low concentrations of oxyHb or metHb as indicated. Cells were then lysed, and total RNA and protein were collected. Quantitative PCR (qPCR) and western blotting were performed to measure CYP24A1 and CYP27B1 mRNA and protein expression, respectively. Sample mRNA expression was normalized to *ACTB* mRNA levels, while protein expression was normalized to total loaded protein. Interestingly, we observed a selective increase in *CYP27B1* transcript expression after exposure to both metHb and oxyHb (Fig. 14). This increase in transcript level was not mirrored by increased CYP27B1 protein as both vitamin D hydroxylase proteins' expression were unchanged with Hb treatment (Fig. 14, C and D).

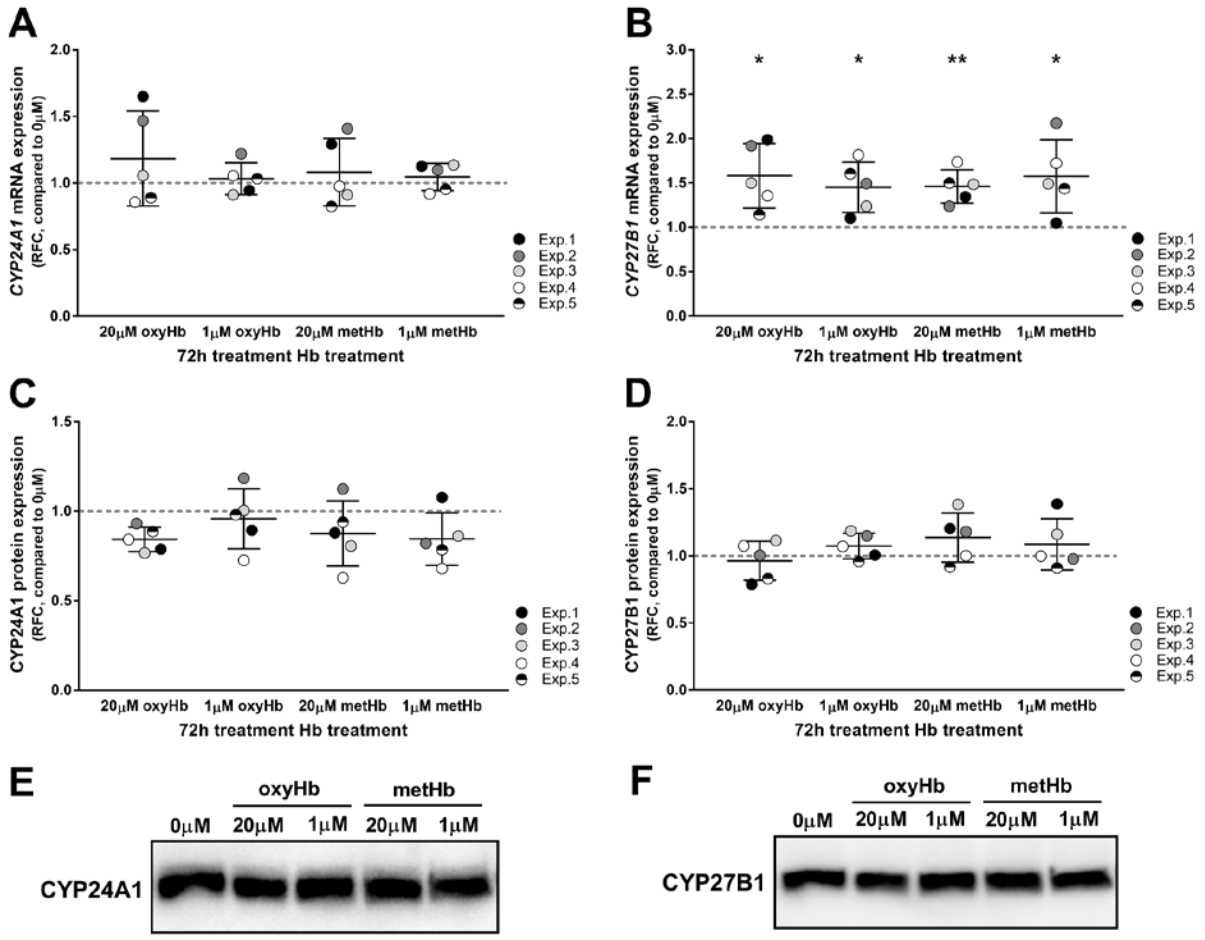

Figure 14. Prolonged Hb exposure selectively increases *CYP27B1* transcript levels in proximal tubule cells.

Filter-grown OK cells were incubated with oxyHb or metHb for 72 h at concentrations indicated. Cells were then washed, lysed, and total RNA and protein were collected. Expressional changes of *CYP24A1* and *CYP27B1* transcripts (A and B, respectively) were quantified by qPCR and normalized to *ACTB* transcript levels. Changes in protein expression of CYP24A1 and CYP27B1 (C and D, respectively) were quantified via western blotting of equal total protein. Representative western blot data for CYP24A1 (E) and CYP27B1 (F) expression are shown. Relative fold change (RFC) in treatment conditions compared to an untreated control (not shown) from five experiments are plotted (mean ± SD and individual points). *p≤0.05, **p≤0.01, by one-sample t-test.

Because oxidative damage to proteins can affect degradation rates [178], we hypothesized that the observed disconnect between increased mRNA and unchanged protein levels of CYP27B1 may be due to increased protein degradation. However, cycloheximide chase experiments

suggested that CYP24A1 and CYP27B1 half-lives are long (>8 h) and not appreciably altered by Hb exposure (data not shown).

4.3 Discussion

Our results demonstrate that Hb at concentrations estimated to be present within the kidney tubule lumen of SCD patients profoundly inhibits DBP uptake by PT cells. The concentration of Hb that half-maximally inhibits DBP uptake is close to its estimated tubular concentration in patients. Thus, Hb competition for DBP uptake may result in chronic loss of filtered DBP into the urine, which could contribute to the development of vitamin D deficiency commonly observed in SCD. Additionally, impaired DBP uptake by the PT may hamper the effectiveness of vitamin D supplementation. Indeed, vitamin D supplementation is more difficult in SCD patients compared with otherwise healthy, vitamin D-deficient individuals. Because of this, SCD patients generally need a higher dose to reach sufficiency [179, 180].

In addition to inhibiting DBP uptake, we found that prolonged metHb exposure led to increased mitochondrial-associated oxidative stress in PT cells. Because oxidative stress has been associated with changes in vitamin D hydroxylase expression and function [174-176], we next assessed CYP24A1 and CYP27B1 expression in PT cells after prolonged Hb exposure. Interestingly, both metHb and oxyHb exposure led to a differential increase in *CYP27B1* mRNA expression with unchanged protein expression. Upon finding this discordant change in CYP27B1 expression with Hb exposure, we speculated CYP27B1 protein may be degrading at an enhanced rate, which could balance any increased transcription and translation to result in the appearance of unchanged protein levels. However, we were unable to measure an appreciable difference in

protein degradation with Hb treatment. This suggests that the observed discordant changes in CYP27B1 mRNA and protein levels could be caused by alteration of translational or post-translational regulation rather than protein degradation. Additionally, the effect on *CYP27B1* mRNA expression may not directly depend on oxidation levels as oxyHb did not increase mitochondrial oxidative stress, but increased *CYP27B1* expression similarly to metHb.

An important extension of our results would be to measure the effects of prolonged exposure to Hb on the enzymatic activity of CYP27B1 and CYP24A1, which could also affect vitamin D metabolism in PT cells. Interestingly, HO-1 induction can lead to degradation of heme groups in the active site of CYP family proteins, causing decreased activity [174, 181], and a previous study reported decreased vitamin D hydroxylase activity under conditions of oxidative stress [175]. Consistent with this possibility, we have reported increased HO-1 expression in human PT cells after prolonged exposure to Hb [173]. Further studies are needed to truly assess the impact of prolonged Hb exposure on PT vitamin D metabolism, including evaluation of vitamin D metabolite production in both *in vitro* and *in vivo* models of SCD. Nevertheless, we have provided the first implications that SCD-related PT dysfunction may contribute to vitamin D deficiency to our knowledge. This suggests the PT as a crucial target for therapeutic intervention to maintain vitamin D levels in SCD patients.

Our studies indicate that impeding the interaction of Hb with megalin/cubilin receptors may be a useful therapeutic approach in the prevention of both vitamin D deficiency and tubular proteinuria in SCD patients. Hb differentially inhibited the uptake of normally filtered proteins, suggesting specificity in Hb-receptor binding. We observed similar degrees of Hb inhibition on albumin and DBP uptake, suggesting that Hb, albumin, and DBP bind to common sites in megalin and cubilin receptors. RBP uptake was inhibited by Hb to a lesser degree. As the secondary

structure of RBP is unlike that of Hb, albumin, and DBP it likely binds to different sites to megalin/cubilin receptors. The difference in competition could also be related to receptor-specific binding as Hb [60], albumin [98, 182], and DBP [128] are reported to bind to both megalin and cubilin, and RBP [183] is only reported to bind to megalin. However, it should be noted that inhibition of all tested proteins by Hb remained incomplete even at high concentrations of Hb. This suggests that there may be some difference between binding sites specific to Hb, albumin, and DBP. There may also be some endocytosis via nonspecific binding or fluid phase uptake in PT cells. Understanding the molecular basis of Hb competition would help identify therapeutic compounds that selectively target the interaction of Hb with megalin/cubilin receptors. Further, recognizing differences in Hb competition with specific proteins may provide useful information for the selection of early biomarkers of tubular proteinuria in SCD patients. Urinary excretion of RBP has been previously used in the diagnosis of tubular proteinuria in the pediatric SCD population [12]. However, our data suggest that RBP may not be an ideal biomarker of tubular proteinuria in SCD patients, as its uptake is not inhibited as profoundly as other proteins such as DBP. Therefore, we propose measurement of urinary DBP excretion as a biomarker since it may allow for diagnosis of tubular proteinuria earlier and/or with greater sensitivity. Future studies assessing patterns of urinary protein excretion early in life may help to better understand how to best characterize the progression of tubular proteinuria and its relation to kidney disease in SCD patients.

4.4 Future Directions

Further studies, including additional assessment of vitamin D hydroxylase enzyme activity after Hb exposure, are needed to determine a link between our observed change in *CYP27B1* mRNA expression and alteration of vitamin D metabolism. We have set up a collaboration with Dr. Thomas Nolin at the University of Pittsburgh School of Pharmacy, to measure vitamin D metabolite production. Dr. Nolin has previously measured vitamin D metabolites in human serum using ultra high performance liquid chromatography-tandem mass spectrometry (UHPLC-MS/MS) [184]. We plan to expand this technique to measure vitamin D metabolites in our LLC-PK1 cell model as these cells have been previously reported to metabolize 25(OH)D to $1,25(OH)_2D$ and $24,25(OH)_2D$ [185-187]. UHPLC-MS/MS can measure all metabolites pertinent to this study [25(OH)D, $1,25(OH)_2D$, $24,25(OH)_2D$] and has the sensitivity to read levels as low as 5 ng/ml 25(OH)D and 10 pg/ml $1,25(OH)_2D$. We have treated LLC-PK1 cells with 25(OH)D in various culture conditions, including free or DBP-bound incubation in the presence or absence of Hb, and have collected cell lysates and culture medium for analysis. Dr. Nolin is currently improving his vitamin D metabolite assay, and, upon proper optimization, we will run these samples to assess any changes in metabolism.

Our measurement of vitamin D metabolites will also be extended beyond *in vitro* cell culture to assess vitamin D status in the Townes SCD mouse model. We are currently collecting serum from SCD mice with matched controls to assess any differences in circulating vitamin D metabolites. There are some caveats of measuring mouse serum which may make interpretation of these data difficult. This includes the amount of serum needed to measure vitamin D metabolites. Dr. Nolin's assay requires a minimum of 0.5 mL serum volume, which necessitates complete exsanguination of the experimental mice. This means we will not be able to conduct repeated

measures and any variation in sample collection may have a large effect on differences in vitamin D metabolites collected. Additionally, pushing the metabolite assay to its lower volume limit may hinder the discernment of subtle changes in vitamin D metabolites. Nevertheless, these data could help to demonstrate possible clinical relevance of our *in vitro* studies as it would extend our profiling of SCD-related vitamin D deficiency beyond a single cell environment.

If either *in vitro* or *in vivo* models provide promising results, we would likely consider assessment of serum vitamin D metabolite status in humans. Measuring vitamin D metabolite levels in humans would be more complicated by environmental confounders, such as sun exposure and dietary intake of vitamin D. However, assessing vitamin D metabolism in a human SCD cohort should be possible if recruitment accounted for these environmental confounders as well as differences in disease state, such as frequency of hemolytic crises and Hb serum concentration at time of sample collection.

In addition to assessment of vitamin D metabolism, we may use our PT cell model to screen for therapeutic compounds. We have developed a scalable, dual fluorescent screen that measures simultaneous PT cell uptake of albumin/DBP and Hb. This assay could be used to find compounds that selectively inhibit Hb interaction with megalin and cubilin. Because we have observed differential binding inhibition by Hb on the uptake of albumin and DBP vs. RBP, structural analysis looking at similarities and differences between these proteins may help to refine compounds to use in a targeted drug screen. It will be difficult to find compounds that only inhibit Hb uptake, as Hb likely contains multiple low affinity binding sites similar to other filtered proteins. However, global inhibition of PT endocytic uptake may still be useful in preventing uptake of large amounts of Hb filtered during hemolytic crisis, which could help to preserve kidney function in patients.

5.0 Vitamin D Alters Protein Endocytosis by Proximal Tubule Cells

5.1 Introduction

Hormonally active vitamin D [1,25$(OH)_2$D] regulates a multitude of cellular processes through binding to VDR. Regulation by 1,25$(OH)_2$D-VDR is cell-type specific and primarily mediates changes in gene transcription to alter biological activity [119]. 1,25$(OH)_2$D-VDR is involved in regulating calcium homeostasis, cellular proliferation and differentiation, hormone secretion, and immune function [123]. Because of its involvement in a variety of cellular processes, sustaining appropriate levels of active vitamin D is critical.

PT cells are among the few cell types that express CYP27B1, which converts 25(OH)D to 1,25$(OH)_2$D and are generally considered the primary site for vitamin D activation in the body [16]. PT cells also express VDR, and 1,25$(OH)_2$D-mediated regulation of several genes in in these cells has been reported [125, 131]. Overall, the transcriptional regulation in PT cells functions as a negative feedback loop to suppress vitamin D activation once sufficient levels are available. For example, 1,25$(OH)_2$D-VDR signaling can reduce PT expression of CYP27B1 and concomitantly increase levels of CYP24A1, a hydroxylase involved in vitamin D degradation, to limit total 1,25$(OH)_2$D levels [123].

1,25$(OH)_2$D is also reported to regulate PT cell expression of multiligand receptors megalin and cubilin [132, 133]. Megalin and cubilin bind to many proteins in the kidney ultrafiltrate, including vitamin D carrier proteins albumin and DBP, and are critical for robust protein reabsorption [159]. Changes in protein uptake driven by vitamin D regulation could have implications for kidney function and health. Incomplete reabsorption of protein by the PT can

cause urinary excretion of unabsorbed protein, termed tubular proteinuria. Tubular proteinuria has been linked to deterioration of kidney function and progression of disease [13, 14]. Additionally, incomplete vitamin carrier reclamation could affect vitamin status. Reported $1,25(OH)_2D$-mediated changes in receptor expression are discordant as expression of megalin increases and cubilin decreases [132, 133]. Thus, it is difficult to postulate the effect of $1,25(OH)_2D$ regulation on endocytic uptake.

Because PT cell protein reabsorption plays a critical role in the maintenance of vitamin homeostasis as well as a protein-free urine, it is important to understand any correlation between $1,25(OH)_2D$ regulation of megalin and cubilin expression and endocytic uptake. Therefore, we set out to assess PT cell uptake of several megalin/cubilin ligands under conditions simulating $1,25(OH)_2D$ supplementation. We measured albumin, DBP, and RBP uptake as well as changes in megalin and cubilin mRNA and protein expression in two PT cell lines treated with $1,25(OH)_2D$. We observed increased RBP uptake in both cell lines upon exposure to $1,25(OH)_2D$. However, only one of the two tested cell lines (LLC-PK1) exhibited $1,25(OH)_2D$-driven changes in receptor expression. This cell line also exhibited increased DBP uptake after $1,25(OH)_2D$ exposure. While the observed changes in endocytosis were different between cell lines and of relatively small magnitude, our results suggest that active vitamin D status and signaling may influence protein reabsorption by the PT.

5.2 Results

5.2.1 1,25(OH)$_2$D supplementation increases RBP endocytic uptake in proximal tubule cells

To investigate the effect of 1,25(OH)$_2$D supplementation on endocytic capacity, we conducted our experiments in opossum OK and porcine LLC-PK1 cells, two PT cell lines that are commonly used to study endocytosis and vitamin D signaling/metabolism. Polarized, filter-grown PT cells were cultured in the presence or absence of 1,25(OH)$_2$D for 24 h. After exposure to 1,25(OH)$_2$D, OK cells were incubated with 0.6 µM Alexa Fluor 647-albumin, 0.1 µM Alexa Fluor 647-DBP, or 0.1 µM Alexa Fluor 647-RBP for 1 h at 37°C. Cells were then washed, solubilized, and cell-associated fluorescent protein was quantified via spectrofluorimetry. Experiments using LLC-PK1 cells were conducted in the same manner, except concentrations of DBP and RBP were increased to 0.5 µM to increase the sensitivity of our uptake assay as LLC-PK1 cells have markedly lower endocytic capacity compared with OK cells. Treatment with 1,25(OH)$_2$D increased RBP uptake in both OK and LLC-PK1 cells (Fig. 15 A and B). While the effect size was small (1.2-fold in OK cells and 1.5-fold in LLC-PK1 cells), this increase in uptake was significant in OK cells and congruent between both cell lines. Exposure to 1,25(OH)$_2$D also led to apparently increased DBP uptake in LLC-PK1 cells (Fig. 15 C and D), but no effect on albumin uptake was observed (Fig. 15 E and F). This was surprising as albumin and DBP likely bind to megalin and cubilin similarly since they have comparable secondary structures. To add to the complexity of this observation, the change in DBP uptake after 1,25(OH)$_2$D exposure appeared to be biphasic, with 100 nM treatment causing the greatest increase in uptake (Fig. 15C).

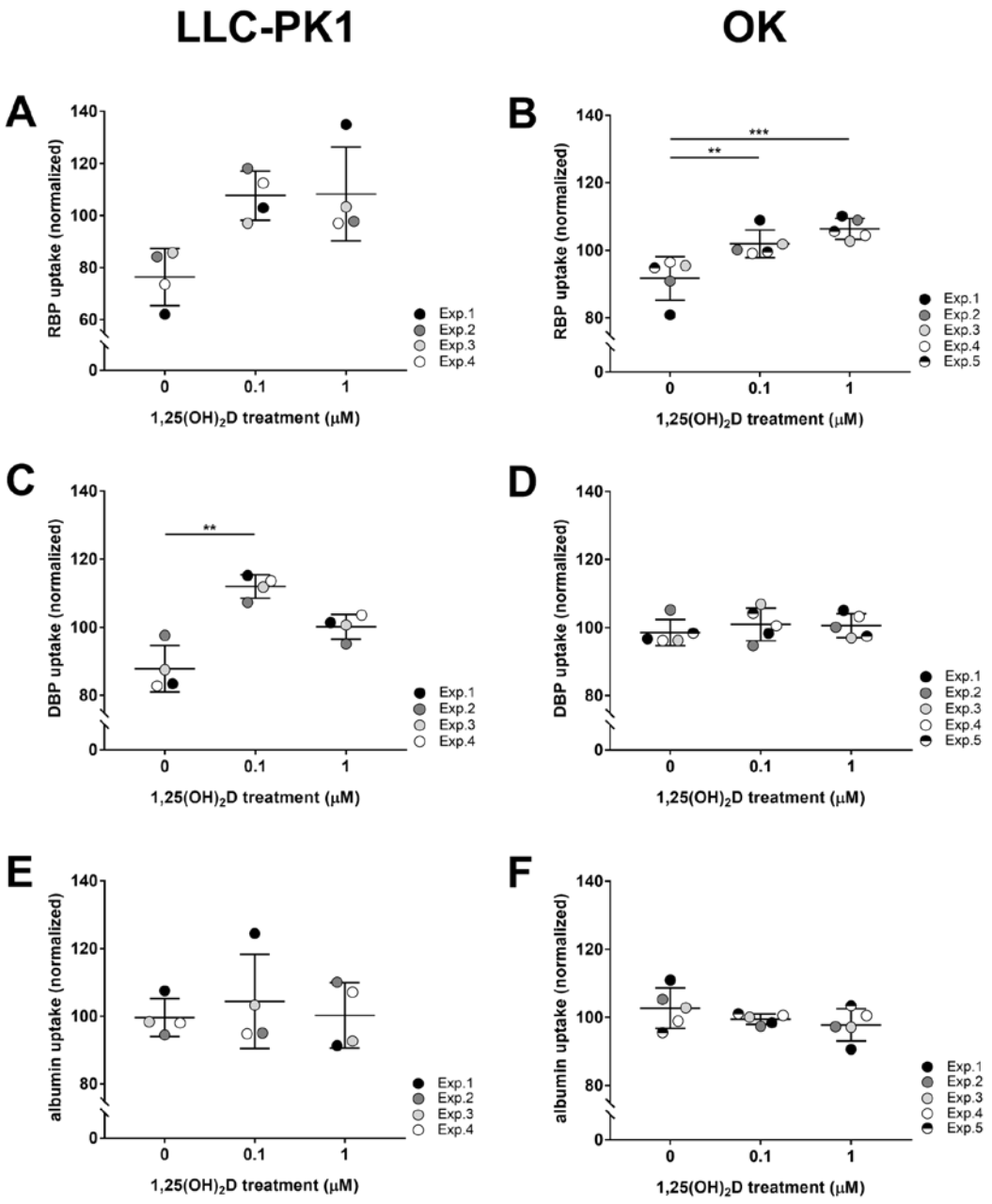

Figure 15. Changes in 1,25(OH)$_2$D treatment alter DBP and RBP uptake in in proximal tubule cells.

Filter-grown proximal tubule cells were incubated with 1,25(OH)$_2$D for 24 h at concentrations indicated. After treatment, cells were incubated with apically added Alexa Fluor 647-RBP (A and B), Alexa Fluor 647-DBP (C and D), or Alexa Fluor 647-albumin (E and F) for 1 h at 37°C. Cells were then solubilized, and cell-associated fluorescence was quantified by spectrofluorimetry. While 0.6 μM albumin was used to measure both LLC-PK1 (E) and OK (F) cell uptake, concentrations of RBP and DBP were different between cell lines: 0.5 μM RBP (A) and 0.5 μM DBP (C) in LLC-PK1 cells vs. 0.1 μM RBP (B) and 0.1 μM DBP (D) in OK cells. Data (mean ± SD and individual points) from

4-5 experiments done in triplicate are plotted. Graphed uptake values were normalized by dividing each point by their respective experimental mean. **p≤0.01, ***p≤0.001 by one-way ANCOVA Dunnett's multiple comparisons.

5.2.2 1,25(OH)$_2$D regulation of megalin and cubilin receptor expression varies in proximal tubule cell lines

While both cell lines are known to express megalin, cubilin, and VDR, 1,25(OH)$_2$D-VDR regulation of megalin and cubilin expression has not been reported. Thus, we set out to measure megalin and cubilin expression after 1,25(OH)$_2$D treatment to see if the observed changes in endocytosis could be correlated to changes in megalin/cubilin expression. Filter-grown PT cells were treated with the same concentrations of 1,25(OH)$_2$D for 24 h as above. Cells were then were washed, lysed, and total RNA and protein collected and quantified. Quantitative PCR (qPCR) and western blotting were performed to analyze *LRP2*/megalin and *CUBN*/cubilin mRNA and protein expression, respectively. We observed a significant decrease in cubilin, but not megalin, expression with 1,25(OH)$_2$D treatment in LLC-PK1 cells (Fig. 16).

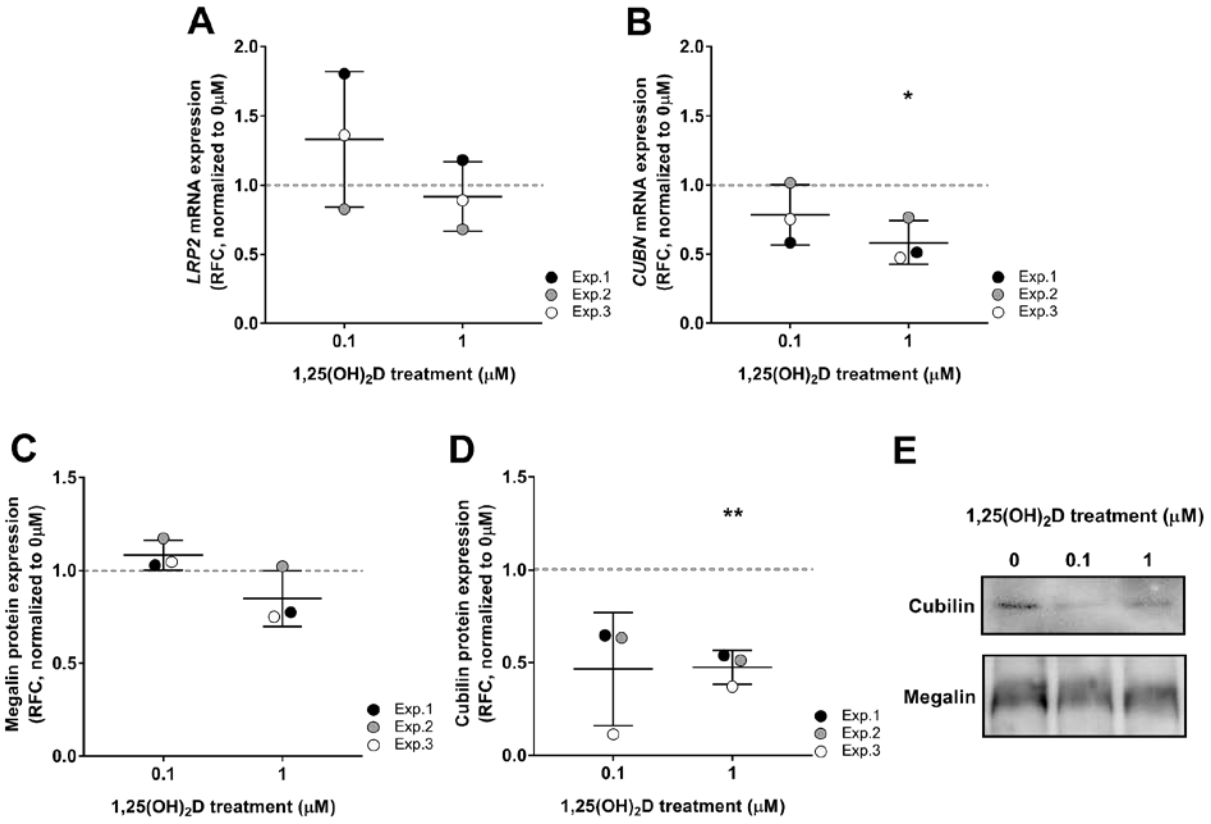

Figure 16. Cubilin expression is significantly downregulated by 1,25(OH)$_2$D in LLC-PK1 cells.

Filter-grown LLC-PK1 cells were incubated with 1,25(OH)$_2$D for 24 h at concentrations indicated. Cells were then washed, lysed, and total RNA and protein were collected. Expressional changes of *LRP2* and *CUBN* transcripts (A and B, respectively) were quantified by qPCR and normalized to *ACTB* transcript levels. Changes in protein expression of megalin and cubilin (C and D, respectively) were quantified via western blotting of equivalent loaded protein. Relative fold change (RFC) in treatment conditions compared to an untreated control (not shown) from three experiments are plotted (mean ± SD and individual points). Representative western blot data for megalin and cubilin expression are shown (E). *p≤0.05, **p≤0.01, by one-sample t-test.

Surprisingly, OK cells did not exhibit a significant change in either megalin or cubilin expression with 1,25(OH)$_2$D exposure (Fig. 17). However, we observed increased *CYP24A1* mRNA expression after treatment with 1,25(OH)$_2$D in both cell lines (Fig. 22 in Appendix B), verifying that VDR signaling occurred at concentrations of 1,25(OH)$_2$D tested. Together, our data

suggest that 1,25(OH)$_2$D regulation of megalin and cubilin receptors is cell-line dependent and possibly species-specific.

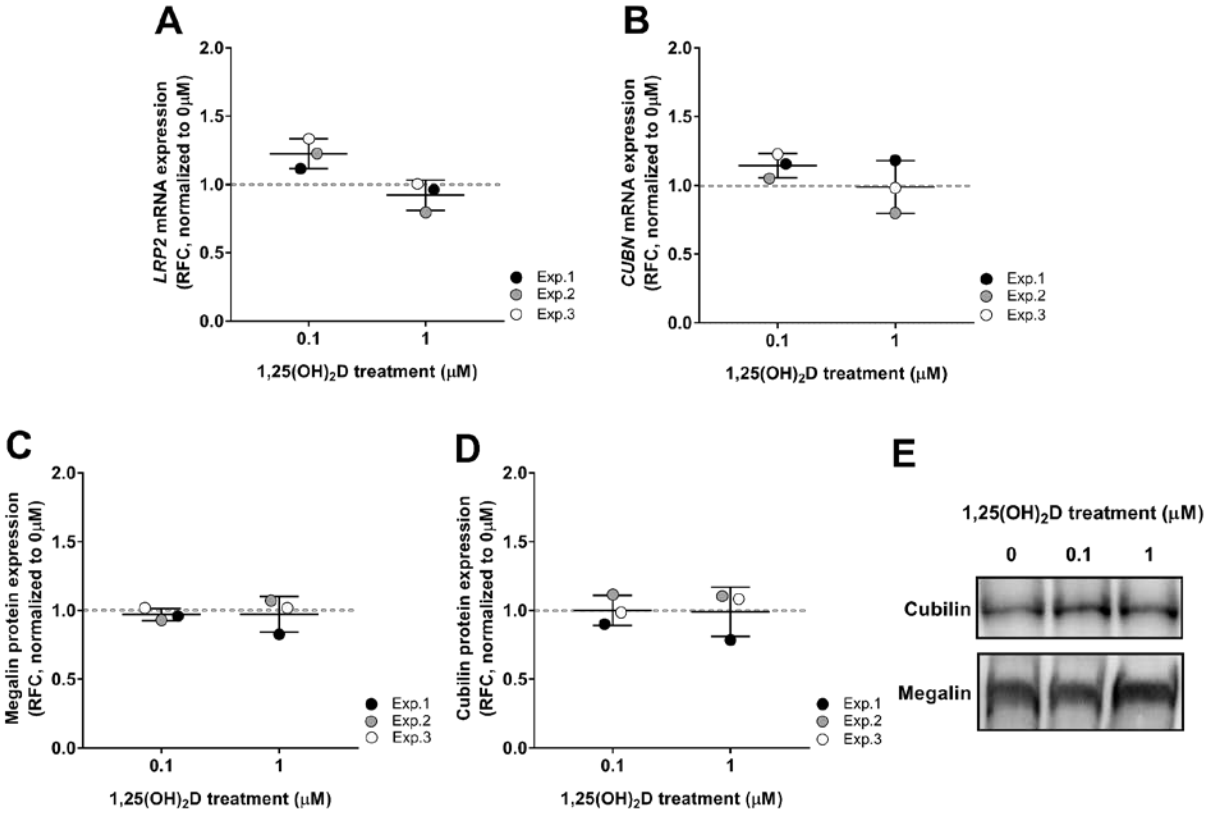

Figure 17. Megalin and cubilin expression is not regulated by 1,25(OH)$_2$D in OK cells.

Filter-grown OK cells were incubated with 1,25(OH)$_2$D for 24 h at concentrations indicated. Cells were then washed, lysed, and total RNA and protein were collected. Expressional changes of *LRP2* and *CUBN* transcripts (A and B, respectively) were quantified by qPCR and normalized to *ACTB* transcript levels. Changes in protein expression of megalin and cubilin (C and D, respectively) were quantified via western blotting of equivalent loaded protein. Relative fold change (RFC) in treatment conditions compared to an untreated control (not shown) from three experiments are plotted (mean ± SD and individual points). Representative western blot data for megalin and cubilin expression are shown (E).

5.3 Discussion

Although $1,25(OH)_2D$ supplementation has been reported to alter both megalin and cubilin expression previously [132, 133], we observed no regulation of megalin and decreased cubilin expression only in LLC-PK1 cells after 24 h of supplementation. Our inability to replicate changes in megalin expression in either cell line could be due to cell culture model differences. As $1,25(OH)_2D$ is known to regulate cell differentiation, the previous report of increased megalin expression with $1,25(OH)_2D$ exposure conducted under static conditions [132] may be an effect of increased PT cell differentiation rather than direct VDR regulation of megalin. We may have missed this change with supplementation in our cells as they were cultured under fluid shear stress prior to $1,25(OH)_2D$ supplementation, which we have demonstrated to increase PT cell differentiation and metabolic function [150, 188]. Conversely, we expect observed differences in $1,25(OH)_2D$ effects on cubilin expression between LLC-PK1 and OK cells to be species specific. While LLC-PK1 cells are derived from porcine origin and have been demonstrated to metabolize vitamin D similarly to humans, OK cells reportedly metabolize vitamin D differently. They have not been observed to produce $1,25(OH)_2D$ and possess an evolutionary modification in CYP24A1 that leads to alternative metabolite production [186, 189, 190]. This deviation in vitamin D metabolism may imply divergence in $1,25(OH)_2D$-VDR regulation as well. However, we found that $1,25(OH)_2D$ treatment created a dramatic increase in *CYP24A1* expression, suggesting that both LLC-PK1 and OK cells can respond to $1,25(OH)_2D$.

Despite conflicting effects of $1,25(OH)_2D$ on receptor expression, both OK and LLC-PK1 cells had increased RBP uptake with $1,25(OH)_2D$ treatment. It is difficult to understand how RBP uptake is increased in OK cells as there was no change in total megalin or cubilin expression with $1,25(OH)_2D$ treatment. However, $1,25(OH)_2D$ treatment could possibly alter apical surface

expression of megalin/cubilin receptors, which may change endocytic dynamics. In fact, cubilin relies on another protein amnionless for trafficking to the apical surface of cells [105]. Because of this, it may be of interest to assess amnionless expression after 1,25$(OH)_2$D treatment. Additionally, studies evaluating megalin and cubilin receptor localization after 1,25$(OH)_2$D exposure are needed to determine any significant differences in apical surface expression. A change in nonspecific endocytosis or other possible RBP receptors expression may also explain increased RBP uptake in OK cells. Indeed, we have observed expression of the STRA6 receptor in OK cells [191], which can bind to RBP. STRA6 has only been reported to bind rather than internalize RBP and its localization in PT cells is not characterized, making it unclear if 1,25$(OH)_2$D regulation of STRA6 could cause the observed increase in cell-associated RBP.

While we found no change in receptor expression in OK cells treated with 1,25$(OH)_2$D, LLC-PK1 cells responded to treatment with a decrease in cubilin expression. We believe that this decreased cubilin expression is likely responsible for the observed increase in RBP uptake in LLC-PK1 cells. Cubilin relies on interaction with other membrane proteins, such as megalin, for cell surface localization as it does not contain a membrane tether [159, 192]. While interaction between megalin and cubilin at the cell surface is not thought to alter either receptor's binding specificity, we hypothesize that decreased megalin-cubilin interaction due to decreased cubilin expression may change megalin's binding capacity. As RBP is only reported to bind to megalin, an increase in megalin binding capacity could result in increased RBP uptake.

It is unlikely that the proposed change in megalin binding capacity with decreased cubilin expression would also explain the observed increased DBP uptake in LLC-PK1 cells. DBP binds to both megalin and cubilin receptors with reportedly similar affinities [128], making it difficult to believe a decrease in cubilin would increase uptake. Additionally, the size and secondary protein

structure of DBP is very similar to albumin, which did not change in uptake with $1,25(OH)_2D$ treatment. To further complicate matters, the increase in DBP with different doses of $1,25(OH)_2D$ appeared to be biphasic, suggesting more than one type of interaction. Other receptors for DBP are not reported, implying the biphasic nature of its uptake is dependent on megalin/cubilin receptors or changes in fluid phase uptake in PT cells. However, it is unlikely that changes in fluid phase uptake would selectively increase protein uptake as it is nonspecific in nature. More experiments using a wider range of $1,25(OH)_2D$ concentrations are needed to determine any dose dependent effects on DBP uptake and to better characterize possible differences between DBP and albumin uptake.

While further studies are needed to understand the exact mechanism of $1,25(OH)_2D$-related effects on PT cell protein endocytosis, we have found differential uptake of specific proteins by two PT cell lines with changes in $1,25(OH)_2D$ supplementation. Interestingly, the two vitamin carriers tested, DBP and RBP, had increased uptake with $1,25(OH)_2D$ supplementation, suggesting a role for active vitamin D signaling in vitamin reabsorption by the PT. An increased uptake of DBP with $1,25(OH)_2D$ signaling could indicate an added effort for internalization and degradation of excess vitamin D as *CYP24A1* expression is also amplified. However, it is difficult to understand the clinical significance of observed effects on endocytosis reported here as $1,25(OH)_2D$ concentrations used, while common in cell culture experimentation, are supraphysiologic in humans and measured effect sizes were rather small. Nevertheless, we report the first evidence of changes in endocytosis with varying $1,25(OH)_2D$ levels, which may indicate PT cell protein reabsorption is connected to vitamin D status.

5.4 Future Directions

In order to connect the changes in cubilin expression with direct $1,25(OH)_2D$-VDR regulation, *in silico* analysis of the *CUBN* gene promoter region in the *Sus scrofa* genome is needed to identify possible VDRE regions. In addition to confirming transcriptional regulation by $1,25(OH)_2D$, this information may provide sequence information that could help identify other VDREs within the porcine genome and possibly other species.

We hypothesize that decreased cubilin expression is linked to increased RBP uptake in LLC-PK1 cells. To directly test this, we plan to conduct experiments using siRNA knockdown of cubilin in PT cells without alteration of $1,25(OH)_2D$ supplementation. Increased RBP uptake with specific cubilin knockdown would suggest effects observed with $1,25(OH)_2D$ treatment were specific to the downregulation of cubilin expression. However, if no increase in RBP uptake occurs with cubilin knockdown $1,25(OH)_2D$ may be causing alternative changes to the endocytic pathway to change in RBP uptake.

We would also like to assess any differences in surface expression of both megalin and cubilin after $1,25(OH)_2D$ treatment as this may have an impact on endocytosis. To do this, we will biotinylate the apical surface of cells before lysis and protein collection. We can then selectively pool surface proteins using streptavidin pull down. Western blotting of this surface pool for megalin and cubilin expression could then provide an assessment of surface-specific megalin and cubilin. This data could also be confirmed using immunofluorescence analysis of megalin/cubilin localization in cells. While we have previously used this method to assess megalin expression in OK cells (data not published), its use in LLC-PK1 cells will be difficult as expression of each receptor is lower. However, we are currently optimizing an enzyme-linked immunosorbent assay

(ELISA) protocol to assess megalin/cubilin expression, which may have the added sensitivity needed to probe LLC-PK1 cells.

Because LLC-PK1 cells reportedly metabolize vitamin D in the same manner as humans it is likely $1,25(OH)_2D$ signaling effects on endocytic uptake would also be similar. However, as there may be notable differences between species in $1,25(OH)_2D$-VDR regulation of megalin and cubilin expression and endocytosis, it would be advantageous to replicate our studies in human PT cells to confirm similar changes in protein uptake. This will likely be difficult as current human PT cell lines as well as primary cell cultures generally have poor endocytic capacity. Thus, additional efforts will likely be necessary to improve the sensitivity of our assay to allow for differential measurement. This could involve measurement of radiolabeled, rather than fluorescently-tagged, protein uptake. Additionally, biochemical analyses, such as western blotting or ELISA, of protein lysate could provide more sensitive measurement compared to spectrofluorimetry.

6.0 Conclusions

As kidney disease becomes an increasing concern for SCD patients, understanding the pathophysiology and progression of disease is critical to better develop targeted treatments. Tubular proteinuria commonly occurs early in SCD patients before the onset of many other clinical symptoms of renal dysfunction, suggesting the PT as an excellent target for therapeutic intervention. Over the course of my studies, I have worked to characterize how PT function is affected by exposure to the increased cell-free Hb levels expected to be present in SCD. Through measurement of endocytic uptake of fluorescently-labeled proteins, I found that Hb selectively competes for megalin/cubilin receptor binding and internalization in PT cells. This binding competition may be selective based on protein secondary structure as Hb dramatically inhibited highly alpha helical proteins albumin and DBP, but only marginally inhibited RBP, which is comprised primarily of β-sheets. Inhibition of normally filtered protein uptake by increased concentrations of Hb may be the primary cause of tubular proteinuria.

Because the PT is the primary site of vitamin D activation, megalin/cubilin receptor-mediated endocytosis of DBP is critical for vitamin D retention and homeostasis. In these studies, I demonstrated that DBP is dramatically inhibited by Hb not just at high concentrations expected during hemolytic crisis but also at expected chronic levels. This suggests SCD patients could be losing DBP-associated vitamin D in their urine regularly. The urinary loss of vitamin D could contribute to vitamin D deficiency in patients, especially if these patients aren't properly supplemented. In addition to inhibition of vitamin D internalization, I found that prolonged Hb exposure caused alteration of expression of vitamin D activating enzyme CYP27B1 in PT cells, suggesting vitamin D metabolism may be affected by Hb exposure. Changes to CYP27B1 could

be driven by increased oxidative stress, which have been reported previously to affect hydroxylase expression and activity [175, 176]. In fact, I have found evidence of increased oxidative stress, through measurement of decreased aconitase activity and increased cytoprotective HO-1 expression, in my PT culture model. However, further studies are needed to understand the effect of prolonged Hb exposure on hydroxylase activity in order to assess any remarkable change in vitamin D metabolism. I am currently generating samples from both cell culture and Townes SCD mouse models to profile vitamin D metabolites and describe any alteration in metabolism.

Changes in PT vitamin D metabolism in the context of SCD could affect levels of active $1,25(OH)_2D$. Because $1,25(OH)_2D$-VDR signaling in the PT is reported to alter expression of megalin and cubilin, I looked to understand any effects it may have on endocytic uptake. I found that changes in $1,25(OH)_2D$ availability led to differential changes in cubilin expression as well as increased DBP and RBP uptake. Although observed increases in endocytic uptake were rather small with $1,25(OH)_2D$ treatment, this may indicate SCD patients could have further difficulty in protein reabsorption if deficient in $1,25(OH)_2D$ levels. This could further contribute to the progression of vitamin deficiency observed in patients.

Although my analysis was limited to the cellular level, I have provided evidence that may link increased cell-free Hb exposure to the development of tubular proteinuria and vitamin D deficiency in SCD patients. As many of the effects of Hb on PT cell function reported here rely on endocytic uptake of Hb, there may be therapeutic potential in compounds that could selectively inhibit Hb's interaction with megalin and cubilin receptors. Selective inhibition of Hb uptake could allow PT cell reabsorption of normally filtered proteins to prevent tubular proteinuria and reduce Hb-induced toxicity to preserve PT function. Additionally, the prevention of Hb internalization at the expense of DBP could have therapeutic value in preserving vitamin D reclamation and

activation by the PT. Although it may be difficult to selectively inhibit Hb uptake by cells due to likely similarity in binding domains with proteins like albumin and DBP, compounds that could inhibit all endocytosis may still be useful to preserve PT cell health during hemolytic crisis when high concentrations of Hb are entering the tubule lumen.

Appendix A. Introductory Tables and Figures

Table 2. Reported forms of sickle cell disease.

Genotype	β-globin mutation
Severe disease	
HbS/S	p.6Glu>Val/p.6Glu>Val
HbS/β^0 thalassaemia	p.6Glu>Val/various
HbS/β^+ thalassaemia	p.6Glu>Val/various
HbS/O Arab	p.6Glu>Val/p.121Glu>Lys
HbS/D Punjab	p.6Glu>Val/p.121Glu>Gln
HbS/C Harlem	p.6Glu>Val/p.6Glu>Val, p.73Asp>Asn
HbC/S Antilles	p.Glu>Lys/p.6Glu<Val, p.23Val>Ile
HbS/Quebec-CHORI	p.6Glu>Val/p.87Thr>Ile
Moderate disease	
HbS/C	p.6Glu>Val/p.6Glu>Lys
HbS/β^+ thalassaemia	p.6Glu>Val/various
HbA/S Oman	unchanged/p.6Glu>Val, β121Glu>Lys
Mild disease	
HbS/β^{++} thalassaemia	p.6Glu>Val/various
HbS/E	p.6Glu>Val/p.26Glu>Lys
HbA/S Jamaica Plain	unchanged/p.6Glu>Val, p.68Leu/Phe
Very mild disease	
HbS/HPFH	p.6Glu>Val/various
HbS/other variants	p.6Glu>Val/various

All genotypes known to cause SCD include at least one copy of the HbS variant. Some variants listed include two mutations to one allele and are denoted by a comma between mutations listed. β-thalassaemia alleles are variable and are characterized by their resulting reduction in Hb expression (β^0 = complete loss of expression, β^+ = residual expression remaining (~10%), β^{++} = mild reduction in expression) [25]. HPFH = hereditary persistence of fetal haemoglobin, is caused by large deletions within the β-globin gene cluster [193].

Table 3. Physiologic concentrations and binding affinities of proteins relevant to this study.

Protein	Size (kDa)	Glomerular sieving coefficient (GSC)	Megalin binding affinity (K_d)	Cubilin binding affinity (K_d)	Serum Level	Tubular level (estimated)
Albumin	65.5	6.2×10^{-4}	Not reported	0.63μM	4.5g/dL (687μM)	2.8mg/dL (427nM)
Hemoglobin (Hb) *Normal* *SCD chronic* *SCD hemolytic crisis*	16.125	0.03	1.7μM	4.1μM	 3mg/dl (1.9μM) ~30mg/dl (20μM) ≤1g/dl (620μM)	 90μg/dl (55.8nM) ~900μg/dl (558nM) ≤ 30mg/dl (20μM)
Retinol-binding protein (RBP)	21	0.38	12.0-36.2μM	Not reported	580μg/dL (276.2nM)	220μg/dL (105nM)
Vitamin D-binding protein (DBP)	51.3	1.6×10^{-3}	120nM	110nM	40mg/dL (7.8μM)	64ng/dL (12.5nM)

Serum levels of albumin, RBP, and DBP were reported in Norden [194].The glomerular sieving coefficient (GSC) found in rats by Tojo [195] was used to estimate tubular levels of albumin. We believe this is a more accurate estimate than the human albumin sieving coefficient calculated by Norden based on measurements of urinary albumin in Dent disease patients [194] because that study assumed no albumin is reabsorbed by the PT. The difference between reported albumin GSCs found in Tojo and Norden was applied to approximate the GSC and tubular levels of DBP as it is comparable to albumin in size and should be filtered similarly. Because of the large difference in size of RBP from albumin, the GSC found in Norden was used to estimate tubular levels. Hb tubular levels were estimated based on GSC found in Monke [59] and serum concentrations reported in Naumann [158]. Binding affinities for albumin [182], Hb [60], RBP [183], and DBP [128] were previously reported in citations listed. Albumin has been shown to bind to megalin [98], but its binding affinity has not been reported. Albumin's affinity to megalin is thought to be comparable to its affinity to cubilin. Ability of RBP to bind to cubilin has not been tested.

Table 4. Common complications of sickle cell disease.

Clinical complication	Brief description
Cardiothoracic system	
Cardiomegaly	Enlargement of the heart
Chronic restrictive lung disease	Restricted lung expansion, resulting in decreased lung volume and inadequate oxygenation
Pulmonary hypertension	High blood pressure in pulmonary arteries
Diastolic heart failure	Left ventricle inability to fill during diastolic phase, reducing the amount of blood pumped by the heart
Acute chest syndrome	Vaso-occlusive crisis of the pulmonary vasculature
Dysrhythmias	Abnormal rhythm of the heart
Nervous system	
Hemorrhagic stroke	Arterial bleeding into the brain
Venous sinus thrombosis	Blood clotting within the dural venous sinuses of the brain
Acute ischemic stroke	Sudden loss of blood flow to the brain
Silent cerebral infarction	Abnormal magnetic resonance imaging (MRI) of the brain without history or physical findings of a stroke
Proliferative retinopathy	Development of new, fragile blood vessels in the retina
Chronic pain	Any pain lasting more than 12 weeks
Orbital infarction	Ischemia of all intraorbital and intraocular structures due to occlusion of the ophthalmic artery and its branches
Cognitive impairment	Trouble remembering, learning, concentrating, and/or making decisions
Immune system	
Leukocytosis	Abnormally high white blood cell count
Septicemia	Bacterial infection of the blood
Splenic sequestration	Trapped blood in the spleen; can lead to enlargement/damage to the spleen
Functional hyposplenism	Reduced splenic function characterized by defective immune response against infection
Anemia	Red blood cell deficiency
Hemolysis	Rupture of red blood cells
Musculoskeletal system	
Avascular necrosis	Death of bone tissue due to inadequate blood flow
Skin ulceration	Open sores on the skin, commonly found on legs
Urogenital System	
Papillary necrosis	Tissue death in renal papillae
Proteinuria	Excretion of protein in the urine; can manifest as tubular proteinuria or frank proteinuria
Renal failure	Loss of kidney function
Hematuria	Presence of blood in the urine
Hyposthenuria	Secretion of low specific gravity urine due to concentrating defect
Priapism	Persistent/painful erection of the penis
Gastrointestinal system	
Cholelithiasis	Gallstone formation
Ischemic cholangiopathy	Bile duct damage caused by inadequate blood flow
Hepatopathy	Liver damage caused by venous congestion
Mesenteric vaso-occlusion/ischemia	Arterial blockage/ischemia of the intestine, commonly the small intestine

Table 5. Megalin and cubilin ligands that are filtered through the glomerular barrier.

Protein	Megalin ligand	Cubilin ligand
Vitamin carrier proteins		
Vitamin D–binding protein	Yes	Yes
Folate–binding protein	Yes	
Retinol–binding protein	Yes	
Transcobalamin, Transcobamalin II	Yes	
Intrinsic factor		Yes
Other carrier proteins		
Albumin	Yes	Yes
Hemoglobin	Yes	Yes
Myoglobin	Yes	Yes
Lactoferrin	Yes	
Liver-type fatty acid–binding protein	Yes	
Metallothionein	Yes	
Neutrophil gelatinase-associated lipocalin	Yes	
Odorant–binding protein	Yes	
Selenoprotein P	Yes	
Sex hormone–binding globulin	Yes	
Transthyretin	Yes	
Transferrin		Yes
Lipoproteins		
Apolipoprotein B	Yes	
Apolipoprotein E	Yes	
Apolipoprotein J/clusterin	Yes	
Apolipoprotein H	Yes	
Apolipoprotein M	Yes	
Apolipoprotein A-I		Yes
High-density lipoprotein		Yes
Hormones and signaling proteins		
Angiotensin II	Yes	
Bone morphogenic protein 4	Yes	
Connective tissue growth factor	Yes	
Epidermal growth factor	Yes	
Insulin	Yes	
Insulin-like growth factor	Yes	
Leptin	Yes	
Parathyroid hormone	Yes	
Prolactin	Yes	
Sonic hedgehog protein	Yes	
Survivin	Yes	
Thyroglobulin	Yes	
Fibroblast growth factor		Yes

Table 5 Continued

Enzymes and enzyme inhibitors		
Recombinant activated factor VIIa	Yes	Yes
α-amylase	Yes	
α-galactosidase A	Yes	
Cathepsin B	Yes	
Cystatin C	Yes	
Lysozyme	Yes	
Plasminogen	Yes	
Plasminogen activator inhibitor type I	Yes	
Tissue plasminogen activator	Yes	
Urokinase	Yes	
Lipoprotein lipase	Yes	
Immune- and stress-related proteins		
Immunoglobulin light chains	Yes	Yes
α_1-microglobulin	Yes	Yes
β_2-microglobulin, Pancreatitis-associated protein	Yes	
Clara cell secretory protein		Yes
Drugs and toxins		
Aminoglycosides	Yes	Yes
Aprotinin	Yes	
Colistin	Yes	
Gentamicin	Yes	
Polymyxin B	Yes	
Trichosanthin	Yes	
Others		
Ca^{2+}	Yes	Yes
Receptor-associated protein	Yes	Yes
Coagulation factor VII	Yes	Yes
Coagulation factor VIII	Yes	
Cytochrome C	Yes	
Seminal vesicle secretory protein II	Yes	
Advanced glycation end products	Yes	

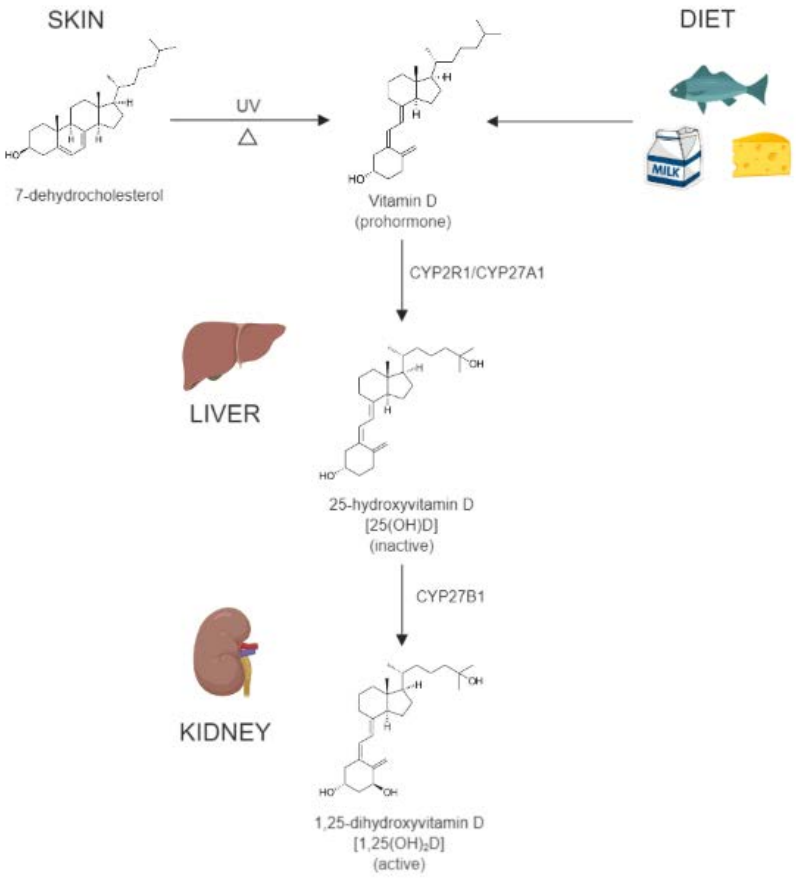

Figure 18. Vitamin D activation in the body.

Prohormone vitamin D enters the body system in one of two ways: (1) UV irradiation and thermal rearrangement of 7-dehydrocholesterol in the skin or (2) dietary intake. This prohormone vitamin D is then transported to the liver where enzymes CYP2R1 and (possibly) CYP27A1 convert it to 25-dihydroxyvitamin D [25(OH)D], an inactive form of vitamin D primed for activation. Once primed in the liver, 25(OH)D is transported to the kidney PT where it is converted to its active form $1,25(OH)_2D$ by CYP27B1. Note: Structures of vitamin D_3 (cholecalciferol) form are shown here. Plant based vitamin D_2 (ergocalciferol) would enter the system only through dietary uptake but otherwise would be processed identically to vitamin D_3.

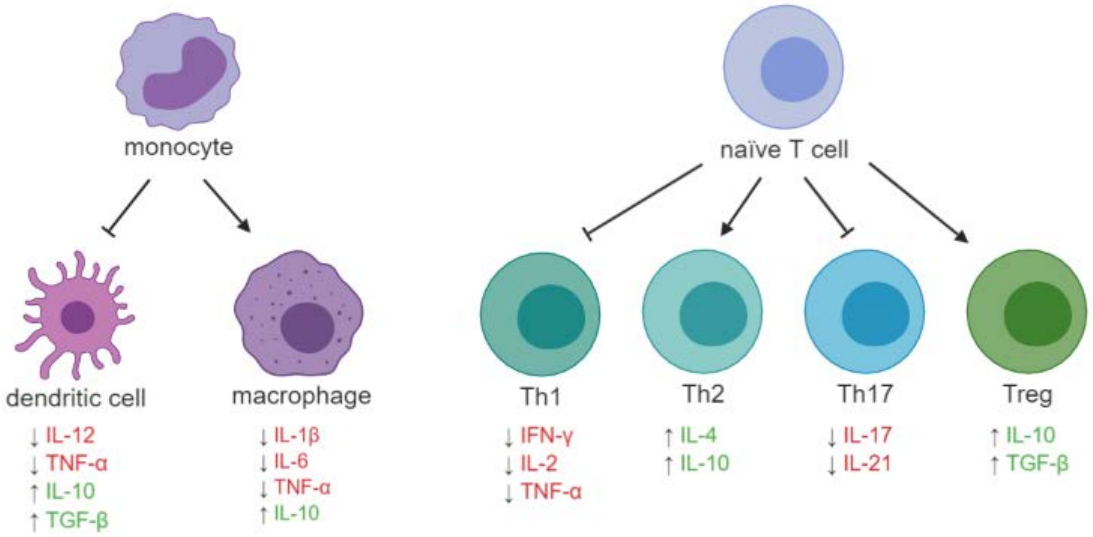

Figure 19. Effects of vitamin D signaling on immune cell maturation and corresponding cytokine expression.

Active vitamin D [1,25$(OH)_2$D] regulates immune cell maturation and cytokine expression to reduce inflammation overall. 1,25$(OH)_2$D signaling promotes monocyte maturation into macrophages over dendritic cells and shifts T cell maturation toward Th2 and Treg cells. Correspondingly, this shift in maturation alters production key cytokines with decreased pro-inflammatory (red) and increased anti-inflammatory (green) cytokine expression. Abbreviations: Th1, T helper cell type 1; Th2, T helper cell type 2; Th17, T helper cell type 17; Treg, regulatory T cell; IFN, interferon; IL, interleukin; TNF, tumor necrosis factor; TGF, transforming growth factor.

Appendix B. Supplementary Data

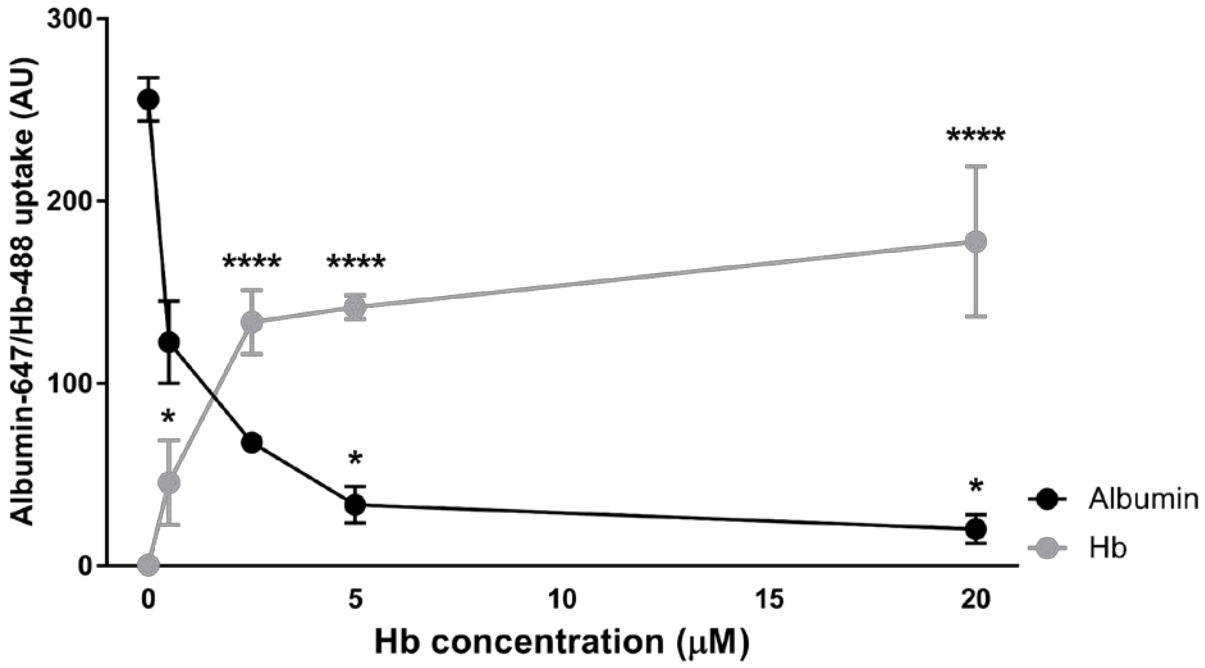

Figure 20. Hb and albumin compete for proximal tubule cell uptake.

OK cells grown in a 96-well plate format were incubated with 0.6 μM Alexa Fluor 647-albumin and a range of Alexa Fluor-488 Hb concentrations (0-20 μM) for 2 h at 37°C. Cells were then solubilized and cell-associated albumin and Hb fluorescence were quantified by spectrofluorimetry. Data (mean ± SD) from three experiments performed in sextuplicate are shown. Graphed uptake values were normalized by dividing each point by their respective experimental mean. *$p \leq 0.05$, ****$p \leq 0.0001$ by two-way ANOVA Dunnett's multiple comparisons.

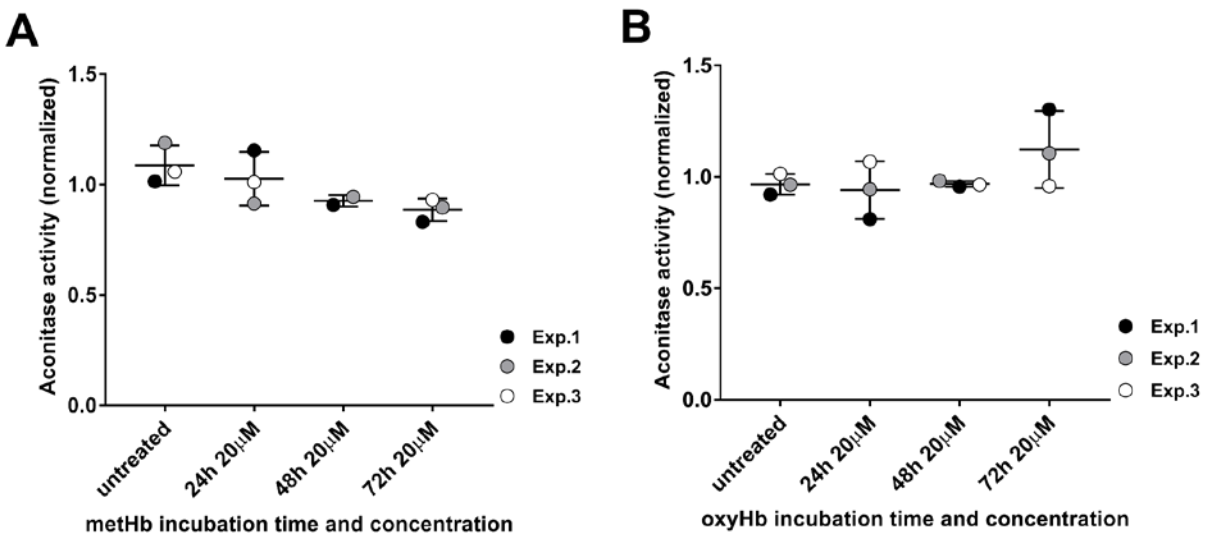

Figure 21.Chronic metHb, but not oxyHb, exposure decreases aconitase activity in LLC-PK1 cells.

Filter-grown LLC-PK1 cells were incubated with metHb (A) or oxyHb (B) for 24-72 h at concentrations indicated. Cells were then washed, lysed, and equal lysate volumes were incubated with aconitase substrate for 1 h. Colorimetric measurement of isocitrate production was used to quantify aconitase activity and normalized to total protein. Data (mean ± SD and individual points) from three experiments are plotted. Graphed values were normalized by dividing each point by their respective experimental mean. These results are similar to experiments done is OK cells (Fig. 13).

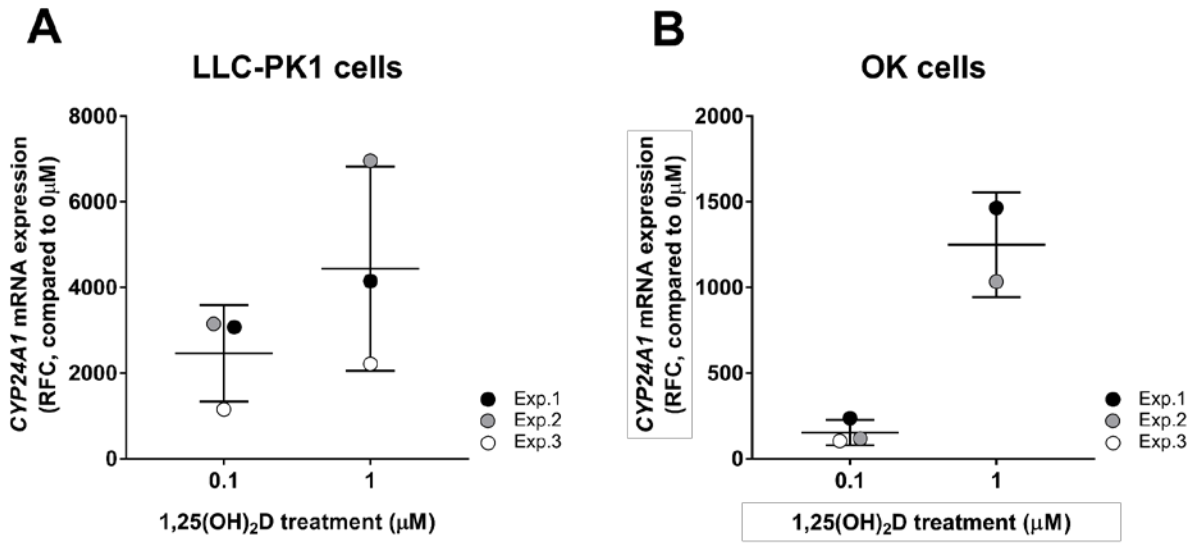

Figure 22. *CYP24A1* mRNA expression is upregulated by 1,25(OH)$_2$D in proximal tubule cells.

Filter-grown LLC-PK1 (A) and OK (B) cells were incubated with 1,25(OH)$_2$D for 24 h at concentrations indicated. Cells were then washed, lysed, and total RNA was collected. Expressional changes of *CYP24A1* transcript were quantified by qPCR and normalized to *ACTB* transcript levels. Relative fold change (RFC) in treatment conditions compared to an untreated control (not shown) from 2-3 experiments are plotted (mean ± SD and individual points).

Appendix C. List of Abbreviations

$1,25(OH)_2D$ – 1,25-dihydroxyvitamin D; calcitriol
$1,24,25(OH)_3D$ – 1,24,25-trihydroxyvitamin D
$24,25(OH)_2D$ – 24,25-dihydroxyvitamin D; dihydroxycholecalciferol
25(OH)D – 25-hydroxyvitamin D; calcifediol
2,3-DPG – 2,3-diphosphoglycerate
ACE – angiotensin converting enzyme
ARB – angiotensin receptor type II blocker
BSA – bovine serum albumin
CKD – chronic kidney disease
CO_2 – carbon dioxide
CUB – complement C1r/C1s, Uegf, Bmp1
DBP – vitamin D binding protein
EGF – epidermal growth factor
ESRD – end-stage renal failure
ETA – endothelin type A receptor
FcRN – MHC-related Fc receptor for IgG
Fe^{2+} – iron, ferrous state
Fe^{3+} – iron, ferric state
GSC – glomerular sieving coefficient
H^+ – hydrogen atom
Hb – hemoglobin
HbA – hemoglobin A
HBB –hemoglobin β-globin subunit gene
HbC – hemoglobin C
HbF – hemoglobin F
HbS – hemoglobin S
HO-1 – heme oxygenase-1
Hpt – haptoglobin
IFN-γ – interferon gamma
IL-1β – interleukin 1 beta
IL-10 – interleukin 10
IL-12 – interleukin 12
IL-17 – interleukin 17
IL-2 – interleukin 2
IL-21 – interleukin 21
IL-4 – interleukin 4
IL-6 – interleukin 6
LDLR – low-density lipoprotein receptor
LMW – low molecular weight
L-NAME – L-NG-nitroarginine methyl ester
O_2 – oxygen molecule

OK – opossum kidney
oxyHb – oxyhemoglobin
MDCK – Madin-Darby canine kidney
metHb – methemoglobin
CNmetHb – cyanmethemoglobin
NO – nitric oxide
NOS – nitric oxide synthase
NSAIDs – nonsteroidal anti-inflammatory drugs
PT – proximal tubule
RAP – receptor-associated protein
RBCs – red blood cells
RBP – retinol binding protein
ROS – reactive oxygen species
SCD – sickle cell disease
SCN – sickle cell nephropathy
TGF-β – transforming growth factor beta
Th1 – T helper cell type 1
Th17 – T helper cell type 17
Th2 – T helper cell type 2
TNF-α – tumor necrosis factor alpha
Treg – regulatory t cell
VDR – vitamin D receptor
VDRE – vitamin D response element

Bibliography

1. Rees, D.C., T.N. Williams, and M.T. Gladwin, *Sickle-cell disease.* The Lancet, 2010. **376**(9757): p. 2018-2031.
2. Piel, F.B., et al., *Global epidemiology of sickle haemoglobin in neonates: a contemporary geostatistical model-based map and population estimates.* Lancet, 2013. **381**(9861): p. 142-51.
3. Hassell, K.L., *Population estimates of sickle cell disease in the U.S.* Am J Prev Med, 2010. **38**(4 Suppl): p. S512-21.
4. DAVIS, J.R., *Sickle Cell Disease: Diagnosis, Management, Education and Research.* American Journal of Diseases of Children, 1974. **128**(2): p. 261-261.
5. Elmariah, H., et al., *Factors associated with survival in a contemporary adult sickle cell disease cohort.* American journal of hematology, 2014. **89**(5): p. 530-535.
6. Nath, K.A. and R.P. Hebbel, *Sickle cell disease: renal manifestations and mechanisms.* Nat Rev Nephrol, 2015. **11**(3): p. 161-71.
7. Thomas, A.N., C. Pattison, and G.R. Serjeant, *Causes of death in sickle-cell disease in Jamaica.* British Medical Journal (Clinical research ed.), 1982. **285**(6342): p. 633-635.
8. Powars, D.R., et al., *Outcome of sickle cell anemia: a 4-decade observational study of 1056 patients.* Medicine (Baltimore), 2005. **84**(6): p. 363-76.
9. Hariri, E., et al., *Sickle cell nephropathy: an update on pathophysiology, diagnosis, and treatment.* Int Urol Nephrol, 2018. **50**(6): p. 1075-1083.
10. Alvarez, O., et al., *Early blood transfusions protect against microalbuminuria in children with sickle cell disease.* Pediatr Blood Cancer, 2006. **47**(1): p. 71-6.
11. Lonsdorfer, A., et al., *Proteinuria in sickle cell trait and disease: an electrophoretic analysis.* Clin Chim Acta, 1989. **181**(3): p. 239-47.
12. Marsenic, O., K.G. Couloures, and J.M. Wiley, *Proteinuria in children with sickle cell disease.* Nephrol Dial Transplant, 2008. **23**(2): p. 715-20.
13. Nielsen, R. and E.I. Christensen, *Proteinuria and events beyond the slit.* Pediatr Nephrol, 2010. **25**(5): p. 813-22.
14. Chevalier, R.L., *The proximal tubule is the primary target of injury and progression of kidney disease: role of the glomerulotubular junction.* Am J Physiol Renal Physiol, 2016. **311**(1): p. F145-61.
15. Eshbach, M.L. and O.A. Weisz, *Receptor-Mediated Endocytosis in the Proximal Tubule.* Annual Review of Physiology, 2017. **79**(1): p. 425-448.
16. Chun, R.F., et al., *Vitamin D and DBP: the free hormone hypothesis revisited.* J Steroid Biochem Mol Biol, 2014. **144 Pt A**: p. 132-7.
17. Nolan, V.G., et al., *Prevalence of Vitamin D Deficiency in Sickle Cell Disease: A Systematic Review.* PLoS ONE, 2015. **10**(3): p. e0119908.
18. de Oliveira, J.F., et al., *[Vitamin D in children and adolescents with sickle cell disease: an integrative review]*. Rev Paul Pediatr, 2015. **33**(3): p. 350-5.
19. Adegoke, S.A., et al., *Relationship between serum 25-hydroxyvitamin D and inflammatory cytokines in paediatric sickle cell disease.* Cytokine, 2017. **96**: p. 87-93.

20. Herrick, J.B., *Peculiar elongated and sickle-shaped red blood corpuscles in a case of severe anemia. 1910.* Yale J Biol Med, 2001. **74**(3): p. 179-84.
21. Piel, F.B., et al., *Global distribution of the sickle cell gene and geographical confirmation of the malaria hypothesis.* Nat Commun, 2010. **1**: p. 104.
22. Piel, F.B., et al., *Global migration and the changing distribution of sickle haemoglobin: a quantitative study of temporal trends between 1960 and 2000.* The Lancet Global Health, 2014. **2**(2): p. e80-e89.
23. Bunn, H.F., *Pathogenesis and treatment of sickle cell disease.* N Engl J Med, 1997. **337**(11): p. 762-9.
24. Nagel, R.L., M.E. Fabry, and M.H. Steinberg, *The paradox of hemoglobin SC disease.* Blood Rev, 2003. **17**(3): p. 167-78.
25. Galanello, R. and R. Origa, *Beta-thalassemia.* Orphanet J Rare Dis, 2010. **5**: p. 11.
26. Farid, Y. and P. Lecat, *Biochemistry, Hemoglobin Synthesis*, in *StatPearls*. 2019, StatPearls Publishing LLC.:Treasure Island (FL).
27. Schechter, A.N., *Hemoglobin research and the origins of molecular medicine.* Blood, 2008. **112**(10): p. 3927-3938.
28. Huehns, E.R., et al., *Human Embryonic Hemoglobins.* Cold Spring Harb Symp Quant Biol, 1964. **29**: p. 327-31.
29. Sankaran, V.G. and S.H. Orkin, *The switch from fetal to adult hemoglobin.* Cold Spring Harbor perspectives in medicine. **3**(1): p. a011643-a011643.
30. Serjeant, G.R., *The natural history of sickle cell disease.* Cold Spring Harb Perspect Med, 2013. **3**(10): p. a011783.
31. Wienert, B., et al., *Wake-up Sleepy Gene: Reactivating Fetal Globin for beta-Hemoglobinopathies.* Trends Genet, 2018. **34**(12): p. 927-940.
32. Thom, C.S., et al., *Hemoglobin variants: biochemical properties and clinical correlates.* Cold Spring Harbor perspectives in medicine. **3**(3): p. a011858-a011858.
33. Perutz, M.F., G. Fermi, and T.B. Shih, *Structure of deoxyhemoglobin Cowtown [His HC3(146) beta----Leu]: origin of the alkaline Bohr effect and electrostatic interactions in hemoglobin.* Proc Natl Acad Sci U S A, 1984. **81**(15): p. 4781-4.
34. Brewer, G.J., *2,3-DPG and Erythrocyte Oxygen Affinity.* Annual Review of Medicine, 1974. **25**(1): p. 29-38.
35. Bonaventura, C., et al., *Molecular Controls of the Oxygenation and Redox Reactions of Hemoglobin.* Antioxidants & Redox Signaling, 2013. **18**(17): p. 2298-2313.
36. Reeder, B.J. and M.T. Wilson, *Hemoglobin and myoglobin associated oxidative stress: from molecular mechanisms to disease States.* Curr Med Chem, 2005. **12**(23): p. 2741-51.
37. Mansouri, A. and A.A. Lurie, *Concise review: methemoglobinemia.* Am J Hematol, 1993. **42**(1): p. 7-12.
38. Kato, G.J., et al., *Sickle cell disease.* Nat Rev Dis Primers, 2018. **4**: p. 18010.
39. Connes, P., et al., *The role of blood rheology in sickle cell disease.* Blood Rev, 2016. **30**(2): p. 111-8.
40. Kuypers, F.A., *Hemoglobin s polymerization and red cell membrane changes.* Hematol Oncol Clin North Am, 2014. **28**(2): p. 155-79.
41. Kuypers, F.A., *Membrane lipid alterations in hemoglobinopathies.* Hematology Am Soc Hematol Educ Program, 2007: p. 68-73.

42. Balandya, E., et al., *Alteration of lymphocyte phenotype and function in sickle cell anemia: Implications for vaccine responses.* American journal of hematology, 2016. **91**(9): p. 938-946.
43. Quinn, C.T., et al., *Biochemical surrogate markers of hemolysis do not correlate with directly measured erythrocyte survival in sickle cell anemia.* American journal of hematology, 2016. **91**(12): p. 1195-1201.
44. Alayash, A.I., *Oxidative pathways in the sickle cell and beyond.* Blood Cells Mol Dis, 2018. **70**: p. 78-86.
45. Crosby, W.H., *The metabolism of hemoglobin and bile pigment in hemolytic disease.* The American Journal of Medicine, 1955. **18**(1): p. 112-122.
46. Reiter, C.D., et al., *Cell-free hemoglobin limits nitric oxide bioavailability in sickle-cell disease.* Nat Med, 2002. **8**(12): p. 1383-9.
47. Steinberg, M.H. and G.P. Rodgers, *Pathophysiology of sickle cell disease: role of cellular and genetic modifiers.* Semin Hematol, 2001. **38**(4): p. 299-306.
48. Conran, N., C.F. Franco-Penteado, and F.F. Costa, *Newer aspects of the pathophysiology of sickle cell disease vaso-occlusion.* Hemoglobin, 2009. **33**(1): p. 1-16.
49. Frenette, P.S. and G.F. Atweh, *Sickle cell disease: old discoveries, new concepts, and future promise.* The Journal of clinical investigation, 2007. **117**(4): p. 850-858.
50. Hebbel, R.P., *Ischemia-reperfusion injury in sickle cell anemia: relationship to acute chest syndrome, endothelial dysfunction, arterial vasculopathy, and inflammatory pain.* Hematol Oncol Clin North Am, 2014. **28**(2): p. 181-98.
51. Francis, Y.F. and H.G. Worthen, *Hyposthenuria in sickle cell disease.* J Natl Med Assoc, 1968. **60**(4): p. 266-70.
52. Scheinman, J.I., *Sickle cell disease and the kidney.* Nat Clin Pract Nephrol, 2009. **5**(2): p. 78-88.
53. Becker, A.M., *Sickle cell nephropathy: challenging the conventional wisdom.* Pediatr Nephrol, 2011. **26**(12): p. 2099-109.
54. Nath, K.A., Z.S. Katusic, and M.T. Gladwin, *The perfusion paradox and vascular instability in sickle cell disease.* Microcirculation, 2004. **11**(2): p. 179-93.
55. Nath, K.A., et al., *Role of cellular metabolites in progressive renal injury.* Kidney Int Suppl, 1992. **38**: p. S109-13.
56. Nath, K.A., et al., *Age sensitizes the kidney to heme protein-induced acute kidney injury.* Am J Physiol Renal Physiol, 2013. **304**(3): p. F317-25.
57. Tracz, M.J., J. Alam, and K.A. Nath, *Physiology and pathophysiology of heme: implications for kidney disease.* J Am Soc Nephrol, 2007. **18**(2): p. 414-20.
58. Zager, R.A., A. Vijayan, and A.C. Johnson, *Proximal tubule haptoglobin gene activation is an integral component of the acute kidney injury "stress response".* Am J Physiol Renal Physiol, 2012. **303**(1): p. F139-48.
59. Monke, J.V. and C.L. Yuile, *The Renal Clearance of Hemoglobin in the Dog.* J Exp Med, 1940. **72**(2): p. 149-65.
60. Gburek, J., et al., *Megalin and cubilin are endocytic receptors involved in renal clearance of hemoglobin.* J Am Soc Nephrol, 2002. **13**(2): p. 423-30.
61. Rubio-Navarro, A., et al., *Podocytes are new cellular targets of haemoglobin-mediated renal damage.* J Pathol, 2018. **244**(3): p. 296-310.
62. De Miguel, C., et al., *Endothelin-1 and the kidney: new perspectives and recent findings.* Curr Opin Nephrol Hypertens, 2016. **25**(1): p. 35-41.

63. Gaston, M.H., et al., *Prophylaxis with oral penicillin in children with sickle cell anemia. A randomized trial.* N Engl J Med, 1986. **314**(25): p. 1593-9.
64. Benson, J.M. and B.L. Therrell, Jr., *History and current status of newborn screening for hemoglobinopathies.* Semin Perinatol, 2010. **34**(2): p. 134-44.
65. McGann, P.T. and R.E. Ware, *Hydroxyurea therapy for sickle cell anemia.* Expert Opin Drug Saf, 2015. **14**(11): p. 1749-58.
66. Husain, M., A.D. Hartman, and P. Desai, *Pharmacogenomics of sickle cell disease: steps toward personalized medicine.* Pharmgenomics Pers Med, 2017. **10**: p. 261-265.
67. Walsh, K.E., et al., *Medication adherence among pediatric patients with sickle cell disease: a systematic review.* Pediatrics, 2014. **134**(6): p. 1175-83.
68. Minniti, C.P., *l-Glutamine and the Dawn of Combination Therapy for Sickle Cell Disease.* N Engl J Med, 2018. **379**(3): p. 292-294.
69. Wilmore, D.W., *Food and Drug Administration Approval of Glutamine for Sickle Cell Disease: Success and Precautions in Glutamine Research.* JPEN J Parenter Enteral Nutr, 2017. **41**(6): p. 912-917.
70. Bhatia, M. and M.C. Walters, *Hematopoietic cell transplantation for thalassemia and sickle cell disease: past, present and future.* Bone Marrow Transplantation, 2007. **41**: p. 109.
71. Esrick, E.B. and D.E. Bauer, *Genetic therapies for sickle cell disease.* Semin Hematol, 2018. **55**(2): p. 76-86.
72. Hoban, M.D., S.H. Orkin, and D.E. Bauer, *Genetic treatment of a molecular disorder: gene therapy approaches to sickle cell disease.* Blood, 2016. **127**(7): p. 839-48.
73. Quinn, C.T., et al., *Losartan for the nephropathy of sickle cell anemia: A phase-2, multicenter trial.* Am J Hematol, 2017. **92**(9): p. E520-e528.
74. Sharpe, C.C. and S.L. Thein, *Sickle cell nephropathy - a practical approach.* Br J Haematol, 2011. **155**(3): p. 287-97.
75. Sabaa, N., et al., *Endothelin receptor antagonism prevents hypoxia-induced mortality and morbidity in a mouse model of sickle-cell disease.* J Clin Invest, 2008. **118**(5): p. 1924-33.
76. Kasztan, M., et al., *Long-Term Endothelin-A Receptor Antagonism Provides Robust Renal Protection in Humanized Sickle Cell Disease Mice.* J Am Soc Nephrol, 2017. **28**(8): p. 2443-2458.
77. Taylor, C., et al., *Combined hydroxyurea and ETA receptor blockade reduces renal injury in the humanized sickle cell mouse.* Acta Physiol (Oxf), 2019. **225**(2): p. e13178.
78. Abbott, K.C., I.O. Hypolite, and L.Y. Agodoa, *Sickle cell nephropathy at end-stage renal disease in the United States: patient characteristics and survival.* Clin Nephrol, 2002. **58**(1): p. 9-15.
79. Nielsen, L., et al., *Morbidity and mortality of sickle cell disease patients starting intermittent haemodialysis: a comparative cohort study with non- Sickle dialysis patients.* Br J Haematol, 2016. **174**(1): p. 148-52.
80. McClellan, A.C., et al., *High one year mortality in adults with sickle cell disease and end-stage renal disease.* Br J Haematol, 2012. **159**(3): p. 360-7.
81. Vinge, L., et al., *The effect of progressive glomerular disease on megalin-mediated endocytosis in the kidney.* Nephrology Dialysis Transplantation, 2010. **25**(8): p. 2458-2467.

82. Kerjaschki, D. and M.G. Farquhar, *The pathogenic antigen of Heymann nephritis is a membrane glycoprotein of the renal proximal tubule brush border.* Proc Natl Acad Sci U S A, 1982. **79**(18): p. 5557-61.
83. Ozawa, M., et al., *A new glycoprotein antigen common to teratocarcinoma, visceral endoderm, and renal tubular brush border.* Dev Biol, 1982. **91**(2): p. 351-9.
84. Farquhar, M.G., et al., *The Heymann nephritis antigenic complex: megalin (gp330) and RAP.* J Am Soc Nephrol, 1995. **6**(1): p. 35-47.
85. Saito, A., et al., *Complete cloning and sequencing of rat gp330/"megalin," a distinctive member of the low density lipoprotein receptor gene family.* Proc Natl Acad Sci U S A, 1994. **91**(21): p. 9725-9.
86. Hjälm, G., et al., *Cloning and Sequencing of Human gp330, a Ca2+-Binding Receptor with Potential Intracellular Signaling Properties.* European Journal of Biochemistry, 1996. **239**(1): p. 132-137.
87. Jeon, H. and S.C. Blacklow, *Structure and physiologic function of the low-density lipoprotein receptor.* Annu Rev Biochem, 2005. **74**: p. 535-62.
88. Takeda, T., H. Yamazaki, and M.G. Farquhar, *Identification of an apical sorting determinant in the cytoplasmic tail of megalin.* American Journal of Physiology-Cell Physiology, 2003. **284**(5): p. C1105-C1113.
89. Bachinsky, D.R., et al., *Detection of two forms of GP330. Their role in Heymann nephritis.* Am J Pathol, 1993. **143**(2): p. 598-611.
90. Zou, Z., et al., *Linking receptor-mediated endocytosis and cell signaling: evidence for regulated intramembrane proteolysis of megalin in proximal tubule.* J Biol Chem, 2004. **279**(33): p. 34302-10.
91. Christ, A., et al., *The soluble intracellular domain of megalin does not affect renal proximal tubular function in vivo.* Kidney International, 2010. **78**(5): p. 473-477.
92. Li, Y., R. Cong, and D. Biemesderfer, *The COOH terminus of megalin regulates gene expression in opossum kidney proximal tubule cells.* Am J Physiol Cell Physiol, 2008. **295**(2): p. C529-37.
93. Birn, H., et al., *Receptor-associated protein is important for normal processing of megalin in kidney proximal tubules.* J Am Soc Nephrol, 2000. **11**(2): p. 191-202.
94. Willnow, T.E., et al., *RAP, a specialized chaperone, prevents ligand-induced ER retention and degradation of LDL receptor-related endocytic receptors.* Embo j, 1996. **15**(11): p. 2632-9.
95. Czekay, R.P., et al., *Endocytic trafficking of megalin/RAP complexes: dissociation of the complexes in late endosomes.* Mol Biol Cell, 1997. **8**(3): p. 517-32.
96. Christensen, E.I., et al., *Endocytic receptors in the renal proximal tubule.* Physiology (Bethesda), 2012. **27**(4): p. 223-36.
97. Leheste, J.R., et al., *Megalin knockout mice as an animal model of low molecular weight proteinuria.* Am J Pathol, 1999. **155**(4): p. 1361-70.
98. Cui, S., et al., *Megalin/gp330 mediates uptake of albumin in renal proximal tubule.* Am J Physiol, 1996. **271**(4 Pt 2): p. F900-7.
99. Seetharam, B., D.H. Alpers, and R.H. Allen, *Isolation and characterization of the ileal receptor for intrinsic factor-cobalamin.* J Biol Chem, 1981. **256**(8): p. 3785-90.
100. Seetharam, B., et al., *Identification of rat yolk sac target protein of teratogenic antibodies, gp280, as intrinsic factor-cobalamin receptor.* J Clin Invest, 1997. **99**(10): p. 2317-22.

101. Sahali, D., et al., *Characterization of a 280-kD protein restricted to the coated pits of the renal brush border and the epithelial cells of the yolk sac. Teratogenic effect of the specific monoclonal antibodies.* J Exp Med, 1988. **167**(1): p. 213-8.
102. Moestrup, S.K., et al., *The intrinsic factor-vitamin B12 receptor and target of teratogenic antibodies is a megalin-binding peripheral membrane protein with homology to developmental proteins.* J Biol Chem, 1998. **273**(9): p. 5235-42.
103. Amsellem, S., et al., *Cubilin is essential for albumin reabsorption in the renal proximal tubule.* J Am Soc Nephrol, 2010. **21**(11): p. 1859-67.
104. Kozyraki, R., et al., *Megalin-dependent cubilin-mediated endocytosis is a major pathway for the apical uptake of transferrin in polarized epithelia.* Proc Natl Acad Sci U S A, 2001. **98**(22): p. 12491-6.
105. Strope, S., et al., *Mouse amnionless, which is required for primitive streak assembly, mediates cell-surface localization and endocytic function of cubilin on visceral endoderm and kidney proximal tubules.* Development, 2004. **131**(19): p. 4787-95.
106. He, Q., et al., *Amnionless function is required for cubilin brush-border expression and intrinsic factor-cobalamin (vitamin B12) absorption in vivo.* Blood, 2005. **106**(4): p. 1447-53.
107. Ahuja, R., et al., *Interactions of cubilin with megalin and the product of the amnionless gene (AMN): effect on its stability.* Biochem J, 2008. **410**(2): p. 301-8.
108. Anderson, C.L., et al., *Perspective-- FcRn transports albumin: relevance to immunology and medicine.* Trends Immunol, 2006. **27**(7): p. 343-8.
109. Chaudhury, C., et al., *The major histocompatibility complex-related Fc receptor for IgG (FcRn) binds albumin and prolongs its lifespan.* J Exp Med, 2003. **197**(3): p. 315-22.
110. Akilesh, S., et al., *Podocytes use FcRn to clear IgG from the glomerular basement membrane.* Proc Natl Acad Sci U S A, 2008. **105**(3): p. 967-72.
111. Tenten, V., et al., *Albumin is recycled from the primary urine by tubular transcytosis.* J Am Soc Nephrol, 2013. **24**(12): p. 1966-80.
112. Gekle, M., *Renal albumin handling: a look at the dark side of the filter.* Kidney Int, 2007. **71**(6): p. 479-81.
113. Park, C.H. and T. Maack, *Albumin absorption and catabolism by isolated perfused proximal convoluted tubules of the rabbit.* J Clin Invest, 1984. **73**(3): p. 767-77.
114. Gudehithlu, K.P., et al., *Degradation of albumin by the renal proximal tubule cells and the subsequent fate of its fragments.* Kidney Int, 2004. **65**(6): p. 2113-22.
115. Hatae, T., et al., *Formation of apical tubules from large endocytic vacuoles in kidney proximal tubule cells during absorption of horseradish peroxidase.* Cell Tissue Res, 1986. **246**(2): p. 271-8.
116. Rabito, C.A., *Phosphate uptake by a kidney cell line (LLC-PK1).* Am J Physiol, 1983. **245**(1): p. F22-31.
117. Ryan, M.J., et al., *HK-2: an immortalized proximal tubule epithelial cell line from normal adult human kidney.* Kidney Int, 1994. **45**(1): p. 48-57.
118. Mattila, P.E., et al., *Rab11a-positive compartments in proximal tubule cells sort fluid-phase and membrane cargo.* Am J Physiol Cell Physiol, 2014. **306**(5): p. C441-9.
119. Christakos, S., et al., *Vitamin D: Metabolism, Molecular Mechanism of Action, and Pleiotropic Effects.* Physiol Rev, 2016. **96**(1): p. 365-408.
120. Holick, M.F., *Vitamin D deficiency.* N Engl J Med, 2007. **357**(3): p. 266-81.

121. Heaney, R.P., et al., *Vitamin D3 distribution and status in the body.* J Am Coll Nutr, 2009. **28**(3): p. 252-6.
122. Clements, M.R., et al., *Metabolic inactivation of vitamin D is enhanced in primary hyperparathyroidism.* Clin Sci (Lond), 1987. **73**(6): p. 659-64.
123. Bikle, D., *Vitamin D: Production, Metabolism, and Mechanisms of Action,* in *Endotext,* K.R. Feingold, et al., Editors. 2000, MDText.com, Inc.: South Dartmouth (MA).
124. Canoa, P., et al., *Use of surface plasmon resonance in the binding study of vitamin D, metabolites and analogues with vitamin D binding protein.* Anal Bioanal Chem, 2017. **409**(10): p. 2547-2558.
125. Chesney, R.W., *Interactions of vitamin D and the proximal tubule.* Pediatr Nephrol, 2016. **31**(1): p. 7-14.
126. Gray, R.W., et al., *The metabolism of vitamin D3 and 25-hydroxyvitamin D3 in normal and anephric humans.* J Clin Endocrinol Metab, 1974. **39**(6): p. 1045-56.
127. Nykjaer, A., et al., *An endocytic pathway essential for renal uptake and activation of the steroid 25-(OH) vitamin D3.* Cell, 1999. **96**(4): p. 507-15.
128. Nykjaer, A., et al., *Cubilin dysfunction causes abnormal metabolism of the steroid hormone 25(OH) vitamin D(3).* Proc Natl Acad Sci U S A, 2001. **98**(24): p. 13895-900.
129. Szczepanska, M., et al., *Dent disease in children: diagnostic and therapeutic considerations.* Clin Nephrol, 2015. **84**(4): p. 222-30.
130. Bikle, D.D., *Vitamin D metabolism, mechanism of action, and clinical applications.* Chem Biol, 2014. **21**(3): p. 319-29.
131. Wang, Y., J. Zhu, and H.F. DeLuca, *The vitamin D receptor in the proximal renal tubule is a key regulator of serum 1alpha,25-dihydroxyvitamin D(3).* Am J Physiol Endocrinol Metab, 2015. **308**(3): p. E201-5.
132. Liu, W., et al., *Regulation of gp330/megalin expression by vitamins A and D.* Eur J Clin Invest, 1998. **28**(2): p. 100-7.
133. Bonnet, L., et al., *Gene expression pattern in response to cholecalciferol supplementation highlights cubilin as a major protein of 25(OH)D uptake in adipocytes and male mice white adipose tissue.* Endocrinology, 2017.
134. Overbergh, L., et al., *Identification and immune regulation of 25-hydroxyvitamin D-1-alpha-hydroxylase in murine macrophages.* Clin Exp Immunol, 2000. **120**(1): p. 139-46.
135. Korf, H., et al., *1,25-Dihydroxyvitamin D3 curtails the inflammatory and T cell stimulatory capacity of macrophages through an IL-10-dependent mechanism.* Immunobiology, 2012. **217**(12): p. 1292-300.
136. Gauzzi, M.C., et al., *Suppressive effect of 1alpha,25-dihydroxyvitamin D3 on type I IFN-mediated monocyte differentiation into dendritic cells: impairment of functional activities and chemotaxis.* J Immunol, 2005. **174**(1): p. 270-6.
137. Piemonti, L., et al., *Vitamin D3 affects differentiation, maturation, and function of human monocyte-derived dendritic cells.* J Immunol, 2000. **164**(9): p. 4443-51.
138. Tian, Y., et al., *Effect of 1,25-dihydroxyvitamin D3 on Th17 and Th1 response in patients with Behcet's disease.* Invest Ophthalmol Vis Sci, 2012. **53**(10): p. 6434-41.
139. Colin, E.M., et al., *1,25-dihydroxyvitamin D3 modulates Th17 polarization and interleukin-22 expression by memory T cells from patients with early rheumatoid arthritis.* Arthritis Rheum, 2010. **62**(1): p. 132-42.

140. Jeffery, L.E., et al., *1,25-Dihydroxyvitamin D3 and IL-2 combine to inhibit T cell production of inflammatory cytokines and promote development of regulatory T cells expressing CTLA-4 and FoxP3.* J Immunol, 2009. **183**(9): p. 5458-67.
141. Rak, K. and M. Bronkowska, *Immunomodulatory Effect of Vitamin D and Its Potential Role in the Prevention and Treatment of Type 1 Diabetes Mellitus-A Narrative Review.* Molecules, 2018. **24**(1).
142. Yamamoto, E. and T.N. Jorgensen, *Immunological effects of vitamin D and their relations to autoimmunity.* J Autoimmun, 2019.
143. Sassi, F., C. Tamone, and P. D'Amelio, *Vitamin D: Nutrient, Hormone, and Immunomodulator.* Nutrients, 2018. **10**(11).
144. Bandeira, I.C., et al., *Chronic inflammatory state in sickle cell anemia patients is associated with HBB(*)S haplotype.* Cytokine, 2014. **65**(2): p. 217-21.
145. Keikhaei, B., et al., *Altered levels of pro-inflammatory cytokines in sickle cell disease patients during vaso-occlusive crises and the steady state condition.* Eur Cytokine Netw, 2013. **24**(1): p. 45-52.
146. Musa, B.O., et al., *Pattern of serum cytokine expression and T-cell subsets in sickle cell disease patients in vaso-occlusive crisis.* Clin Vaccine Immunol, 2010. **17**(4): p. 602-8.
147. Osunkwo, I., et al., *Vitamin D deficiency and chronic pain in sickle cell disease.* Br J Haematol, 2011. **153**(4): p. 538-40.
148. Fattizzo, B., et al., *Reduced 25-OH vitamin D in patients with autoimmune cytopenias, clinical correlations and literature review.* Autoimmun Rev, 2016. **15**(7): p. 770-5.
149. Schleithoff, S.S., et al., *Vitamin D supplementation improves cytokine profiles in patients with congestive heart failure: a double-blind, randomized, placebo-controlled trial.* Am J Clin Nutr, 2006. **83**(4): p. 754-9.
150. Long, K.R., et al., *Proximal tubule apical endocytosis is modulated by fluid shear stress via an mTOR-dependent pathway.* Mol Biol Cell, 2017. **28**(19): p. 2508-2517.
151. Tejero, J., et al., *Low NO concentration dependence of reductive nitrosylation reaction of hemoglobin.* J Biol Chem, 2012. **287**(22): p. 18262-74.
152. Huang, Z., et al., *Enzymatic function of hemoglobin as a nitrite reductase that produces NO under allosteric control.* J Clin Invest, 2005. **115**(8): p. 2099-107.
153. Andersen, C.B., et al., *Structure of the haptoglobin-haemoglobin complex.* Nature, 2012. **489**(7416): p. 456-9.
154. Altschul, S.F., et al., *Gapped BLAST and PSI-BLAST: a new generation of protein database search programs.* Nucleic Acids Res, 1997. **25**(17): p. 3389-402.
155. Thompson, J.D., D.G. Higgins, and T.J. Gibson, *CLUSTAL W: improving the sensitivity of progressive multiple sequence alignment through sequence weighting, position-specific gap penalties and weight matrix choice.* Nucleic Acids Res, 1994. **22**(22): p. 4673-80.
156. He, Y., et al., *Large-scale production of functional human serum albumin from transgenic rice seeds.* Proc Natl Acad Sci U S A, 2011. **108**(47): p. 19078-83.
157. Wood, K.C., L.L. Hsu, and M.T. Gladwin, *Sickle cell disease vasculopathy: a state of nitric oxide resistance.* Free Radic Biol Med, 2008. **44**(8): p. 1506-28.
158. Naumann, H.N., et al., *Plasma hemoglobin and hemoglobin fractions in sickle cell crisis.* Am J Clin Pathol, 1971. **56**(2): p. 137-47.
159. Eshbach, M.L. and O.A. Weisz, *Receptor-Mediated Endocytosis in the Proximal Tubule.* Annu Rev Physiol, 2017. **79**: p. 425-448.

160. Sundaram, N., et al., *Biomarkers for early detection of sickle nephropathy.* Am J Hematol, 2011. **86**(7): p. 559-66.
161. Raghavan, V., et al., *Shear stress-dependent regulation of apical endocytosis in renal proximal tubule cells mediated by primary cilia.* Proc Natl Acad Sci U S A, 2014. **111**(23): p. 8506-11.
162. Weinbaum, S., et al., *Mechanotransduction in the renal tubule.* Am J Physiol Renal Physiol, 2010. **299**(6): p. F1220-36.
163. Donadee, C., et al., *Nitric oxide scavenging by red blood cell microparticles and cell-free hemoglobin as a mechanism for the red cell storage lesion.* Circulation, 2011. **124**(4): p. 465-76.
164. Gekle, M., et al., *Functional characterization of albumin binding to the apical membrane of OK cells.* Am J Physiol, 1996. **271**(2 Pt 2): p. F286-91.
165. Alayash, A.I., *Haptoglobin: old protein with new functions.* Clin Chim Acta, 2011. **412**(7-8): p. 493-8.
166. Chiancone, E., et al., *Studies on the reaction of haptoglobin with haemoglobin and haemoglobin chains. I. Stoichiometry and affinity.* J Mol Biol, 1968. **34**(2): p. 347-56.
167. Chintagari, N.R., et al., *Haptoglobin attenuates hemoglobin-induced heme oxygenase-1 in renal proximal tubule cells and kidneys of a mouse model of sickle cell disease.* Blood Cells Mol Dis, 2015. **54**(3): p. 302-6.
168. Lal, A., et al., *Bone mineral density in children with sickle cell anemia.* Pediatr Blood Cancer, 2006. **47**(7): p. 901-6.
169. Willnow, T.E. and A. Nykjaer, *Pathways for kidney-specific uptake of the steroid hormone 25-hydroxyvitamin D3.* Curr Opin Lipidol, 2002. **13**(3): p. 255-60.
170. Cooke, N.E. and E.V. David, *Serum vitamin D-binding protein is a third member of the albumin and alpha fetoprotein gene family.* J Clin Invest, 1985. **76**(6): p. 2420-4.
171. Charlton, J.R., et al., *Immature megalin expression in the preterm neonatal kidney is associated with urinary loss of vitamin carrier proteins.* Pediatr Res, 2019. **85**(3): p. 405-411.
172. Becker-Cohen, R., et al., *Vitamin A deficiency associated with urinary retinol binding protein wasting in Dent's disease.* Pediatr Nephrol, 2012. **27**(7): p. 1097-102.
173. Eshbach, M.L., et al., *Hemoglobin inhibits albumin uptake by proximal tubule cells: implications for sickle cell disease.* Am J Physiol Cell Physiol, 2017. **312**(6): p. C733-c740.
174. Zordoky, B.N. and A.O. El-Kadi, *Role of NF-kappaB in the regulation of cytochrome P450 enzymes.* Curr Drug Metab, 2009. **10**(2): p. 164-78.
175. Crivello, J.F., *Oxidative stress limits vitamin D metabolism by bovine proximal tubule cells in vitro.* Arch Biochem Biophys, 1988. **262**(2): p. 471-80.
176. Wang, L., et al., *Upregulation of nuclear factor-kappaB activity mediates CYP24 expression and reactive oxygen species production in indoxyl sulfate-induced chronic kidney disease.* Nephrology (Carlton), 2016. **21**(9): p. 774-81.
177. Gardner, P.R., *Aconitase: Sensitive target and measure of superoxide*, in *Methods in Enzymology*. 2002, Academic Press. p. 9-23.
178. Breusing, N. and T. Grune, *Regulation of proteasome-mediated protein degradation during oxidative stress and aging.* Biol Chem, 2008. **389**(3): p. 203-9.
179. Bordbar, M.R., et al., *Evaluation of bone mineral density in children with sickle-cell anemia and its associated factors in the south of Iran: a case-control study.* Arch Osteoporos, 2017. **12**(1): p. 70.

180. Wykes, C., et al., *Vitamin D deficiency and its correction in children with sickle cell anaemia.* Ann Hematol, 2014. **93**(12): p. 2051-6.
181. Anwar-Mohamed, A., R.H. Elbekai, and A.O. El-Kadi, *MG-132 inhibits the TCDD-mediated induction of Cyp1a1 at the catalytic activity but not the mRNA or protein levels in Hepa 1c1c7 cells.* Toxicol Lett, 2008. **182**(1-3): p. 121-6.
182. Birn, H., et al., *Cubilin is an albumin binding protein important for renal tubular albumin reabsorption.* J Clin Invest, 2000. **105**(10): p. 1353-61.
183. Zhang, H., et al., *Core 2 GlcNAc modification and megalin ligand-binding activity.* Biochim Biophys Acta, 2008. **1780**(3): p. 479-85.
184. Stubbs, J.R., et al., *Decreased conversion of 25-hydroxyvitamin D3 to 24,25-dihydroxyvitamin D3 following cholecalciferol therapy in patients with CKD.* Clin J Am Soc Nephrol, 2014. **9**(11): p. 1965-73.
185. Keenan, M.J. and R.P. Holmes, *The uptake and metabolism of 25-hydroxyvitamin D3 and vitamin D binding protein by cultured porcine kidney cells (LLC-PK1).* Int J Biochem, 1991. **23**(11): p. 1225-30.
186. Condamine, L., et al., *Local action of phosphate depletion and insulin-like growth factor 1 on in vitro production of 1,25-dihydroxyvitamin D by cultured mammalian kidney cells.* J Clin Invest, 1994. **94**(4): p. 1673-9.
187. Colston, K. and D. Feldman, *1,25-Dihydroxyvitamin D3 receptors and functions in cultured pig kidney cells (LLC PK1). Regulation of 24,25-dihydroxyvitamin D3 production.* J Biol Chem, 1982. **257**(5): p. 2504-8.
188. Ren, Q., et al., *Shear stress and oxygen availability drive differential changes in OK proximal tubule cell metabolism and endocytosis.* Traffic, 2019.
189. Horiuchi, N., et al., *Synthesis of 25-hydroxyvitamin D3-26,23-lactone but not 24,25-dihydroxyvitamin D3 from 25-hydroxyvitamin D3 in opossum kidney cells treated with 1 alpha, 25-dihydroxyvitamin D3.* Horm Metab Res, 1995. **27**(2): p. 83-9.
190. Prosser, D.E., et al., *Single A326G mutation converts human CYP24A1 from 25-OH-D3-24-hydroxylase into -23-hydroxylase, generating 1alpha,25-(OH)2D3-26,23-lactone.* Proc Natl Acad Sci U S A, 2007. **104**(31): p. 12673-8.
191. Eshbach, M.L., et al., *The transcriptome of the Didelphis virginiana opossum kidney OK proximal tubule cell line.* Am J Physiol Renal Physiol, 2017. **313**(3): p. F585-f595.
192. Christensen, E.I. and H. Birn, *Megalin and cubilin: synergistic endocytic receptors in renal proximal tubule.* Am J Physiol Renal Physiol, 2001. **280**(4): p. F562-73.
193. Mayuranathan, T., et al., *Identification of rare and novel deletions that cause (δβ)0-thalassaemia and hereditary persistence of foetal haemoglobin in Indian population.* European Journal of Haematology, 2014. **92**(6): p. 514-520.
194. Norden, A.G., et al., *Glomerular protein sieving and implications for renal failure in Fanconi syndrome.* Kidney Int, 2001. **60**(5): p. 1885-92.
195. Tojo, A. and S. Kinugasa, *Mechanisms of glomerular albumin filtration and tubular reabsorption.* Int J Nephrol, 2012. **2012**: p. 481520.